Dark energy from generalized gravitational theories with a time-dependent Newton's constant(scalar tensor theories)

by
Lavrentios Kazantzidis

A thesis submitted in partial fulfillment
of the requirements for the degree of
Master of Science(M.Sc.)

University of Ioannina
Department of Physics
Division of Theoretical Physics

June 2017

Abstract

This work is focused on alternative forms of *Dark Energy*. The challenges that the ΛCDM model faces led to a variety of alternative models, such as extra dimensions, quintessence models, $f(R)$ extended gravity theories, scalar tensor quintessence models etc. The main goal of my master thesis is to investigate the cosmological dynamics for general scalar tensor quintessence field models. Firstly we introduce the reader to the mathematical formalism of Standard Cosmology and then we study alternative theories that can play the role of Dark Energy such as quintessence models based on linear-negative potentials of the form $V(\phi) = -s \cdot \phi$. In the second part of this work we review the scalar tensor quintessence field models and their theoretical background. We investigate the equation of state parameter $w(z)$ for these particular models and we use the Union2.1 dataset of 580 SnIa as a validity test and to explore the observational consistency of the theoretical model and its predictions for the fate of our Universe. Finally we study qualitatively different potentials of the form $V = s \cdot |\phi|^n$ and use, once again the Union2.1 dataset as a consistency test of our model.

Acknowledgements

First and foremost, I would like to express my gratitude to my supervisors, professor Panagiota Kanti and professor Leandros Perivolaropoulos for the opportunity they gave me to work with them and to touch on the latest results and challenges of Cosmology. Also I would like to thank them for their guidance and plenty advices. Without their help this thesis would be impossible to be accomplished.

Also I would like to thank all the department's theoretical division faculty members for their guidance, help and support throughout my undergraduate and my graduate years.

Finally many thanks to my family and friends for their unconditional love and support all these years.

Contents

Chapter 1

Introduction

Cosmology is undoubtedly one of the most intriguing chapters of physical science. Since human civilization began to deal with physical sciences, fundamental questions began to vex humanity, such as "Where do we come from?", "What are we?", "Where are we going?". Cosmology in general deals with this kind of questions by describing the past and predicting the future of our Universe. A more appropriate definition for Cosmology is that it is the branch of physics that studies the evolution and the creation of our Universe, as well as the scientific laws that governs it.

The development of cosmology can be considered as one of the scientific triumphs of the twentieth century and a tremendous step forward in understanding nature. For large scales Einstein gave a description of gravity by curved space-time in his theory of General Relativity (GR). Soon after his discovery Friedmann, Robertson and Walker accomplished a model of the evolution of the universe. At the other extreme for small scales Bohr, Einstein, Dirac, Heisenberg and others developed quantum mechanics at the beginning of the 20th century. By these findings it was possible for astrophysicists to understand the light emission of stars, which resulted in the measurability of the velocities of stars by the redshift.

At its beginning, cosmology hardly existed as a scientific discipline. Nowadays along with quantum field theory is considered to be one of the two cornerstones of modern physics. The progress in Physics and in particular the improved astrophysical observations of distant objects together with General Relativity (GR) and the Friedmann- Robertson-Walker (FRW) universe was a first step to model the evolution of the Universe. The *Big Bang* theory[1–3] was born. The *Big Bang* theory is the leading explanation about how the universe began. At its simplest, it talks about the universe as we know it starting with an energy denstiy singularity, then inflating over the next 13.8 billion years to the cosmos that we know today.

In the context of GR the Universe's composition as we know it today is roughly as follows:

- The first basic ingredient of the cosmos is the *Baryonic Matter* which accounts. This is the ordinary matter, i.e. atoms, that is composed of baryons (such as protons and neutrons) and leptons (such as electrons and neutrinos). It comprises in general gas, dust, stars, planets, people, etc. Another ingredient is the so-called *Radiation*, i.e particles that have zero mass such as photons. The *Baryonic Matter* and *Radiation* consist of 4% of our Universe.

- *Dark Matter*(DM) which accounts for an estimated 22%. This is the so-called "missing mass" of the Universe. Dynamical evidence[4–6] for the existence of dark matter comes from the motions of galaxies relative to one another and aids in the formation of structure in the universe. The dark matter is said to be "cold" because it is nonrelativistic (slow-

moving) during the era of structure formation. Dark matter is currently believed to be composed of some kind of new elementary particle.

- The remaining 74% of the universe is filled with an unknown component called *Dark Energy* which is a type of energy field that displays the properties of repulsive gravity and is responsible for the accelerating expansion of the Universe.

Finally it has to be mentioned that our Universe on scales greater than about 100 Mpc[1] appears to be isotropic and homogeneous as it is implied from the *cosmological principle* which is summarised in the following chapter.

The *Big Bang* theory describes how the universe expanded from a very high density and high temperature state. In the mid-1940s, after World War II, there were two distinct theories concerning the initial conditions of our Universe. One was Fred Hoyle's steady state model, whereby new matter would be created as the universe seemed to expand. In this model the universe is roughly the same at any point in time[7–10]. The other was Lemaitre's *Big Bang* theory[11, 12], advocated and developed by George Gamow, who introduced Big Bang Nucleosynthesis (BBN) and whose associates, Ralph Alpher and Robert Herman, predicted the cosmic microwave background radiation (CMB)[13], estimated at a temperature of 5K. Ironically, it was Hoyle who coined the phrase *Big Bang* that came to be applied to Lemaître's theory in an attempt to reduce the importance of theory. However an immediate confirmation of this theory emerged in 1965 from Penzias and Wilson, when they discovered by chance the CMB[14] and measured the temperature to be approximately 3K.

As with any theory, a number of mysteries and problems have arisen as a result of the development of the *Big Bang* theory. Some of these mysteries and problems have been resolved while others are still outstanding. Proposed solutions to some of the problems in the Big Bang model have revealed new mysteries of their own. For example, the horizon problem[15], which is the problem of determining why the Universe appears statistically homogeneous and isotropic in accordance with the *cosmological principle*[2], the magnetic monopole problem[16], which denotes that if the early universe were very hot, a large number of very heavy, stable magnetic monopoles would have been produced and the flatness problem[15], which says that a flat Universe is unstable towards increasing or decreasing curvature, therefore the contribution of spatial curvature to the expansion of the Universe could not be much greater than the contribution of matter. These problems were commonly resolved with inflationary theory, but the details of the inflationary universe are still left unresolved. Since 1998 many geometrical[17, 18] and dynamical[19, 20] cosmological observations indicate that the universe has recently entered a phase of accelerating expansion. In order to achieve such an expansion one should introduce an energy that works as repulsive gravity which have been attributed to *Dark Energy*(DE) or *Modify Gravity*. Determining the nature of DE and DM is one of the most crucial problems that modern cosmology faced up until now.

DM could interact through the *Weak interaction* and gravitationally with normal matter or electromagnetic radiation. This makes it very hard to detect it directly. While the search is still in progress[21–23], possible DM particles for consideration are axions[24], neutrinos[25], neutralinos[26] and so on. DM is important in the formation and continued growth of large scale structures, such as galaxies and galaxy clusters. Particle physics predicts the massive size of DM particles so that it can sustain structure forming properties. Weakly interacting particles, including DM and its candidate particles, are all classified as *Weakly Interacting Massive Particles*

[1] 1 parsec is a unit of length used to measure large distances to objects outside the Solar System. A parsec is approximately $3.09 \times 10^{16} m$

[2] See Chapter 2

(WIMPs). Another popular DM candidate is *MACHO*. *MACHO* is an acronym for massive (astrophysical) compact halo object. A *MACHO* is a body composed of normal baryonic matter that emits little or no radiation and drifts through interstellar space unassociated with any planetary movements. *MACHOs* include black holes or neutron stars as well as brown dwarfs[27].

The simplest candidate model for DE is none other than the cosmological constant which has constant in time energy density and pressure. This model is known as the ΛCDM model and is considered as the most widely accepted theory of Cosmology. To achieve a static universe Einstein introduced in 1917 this dark energy as a cosmological constant (Λ) in his equations. However due to Hubble's discovery of the expanding universe in 1927 the cosmological constant was abandoned. Nevertheless, after 1998 the cosmological constant was reintroduced to explain the observed accelerating expansion of the universe.

The ΛCDM model is based on a modified version of Einstein's equations[3]

$$G_{\mu\nu} - \Lambda g_{\mu\nu} = 8\pi T_{\mu\nu} \tag{1.1}$$

where Λ is the new free parameter, the cosmological constant. Indeed, the left-hand side of Eq.(1.1) is the most general local, coordinate-invariant, divergence-less, symmetric, two-index tensor we can construct solely from the metric and its first and second derivatives. Also this particular model has the additional advantage of simplicity due to a single free parameter.

However, it is somewhat problematic taking into account the fact that it faces two major issues/problems that have not been answered yet. These issues can be summarised in the following questions

- *The Cosmological Constant Problem*: Observationally, the cosmological constant density is 120 orders of magnitude smaller than the energy density associated with the Planck scale[4]. How could the cosmological constant have been so large during the inflation period and so small today?

- *The Cosmic Coincidence Problem*: Why is the energy density of DE comparable with the density of matter even though these densities evolve very differently with time?

Let us study each problem separately and focus at first in *the Cosmological Constant Problem*. From a particle point of view Λ identifies physically with the energy of zero-point quantum fluctuations in the vacuum and, with a constant equation of state, which can be defined as the fraction of pressure over density, of the form

$$w = \frac{p}{\rho} = -1 \tag{1.2}$$

This can also be seen clearly when the new term from Eq.(1.1) is placed on right hand side of this equation. In that case the cosmological constant is understood as a new contribution to the energy momentum tensor corresponding to dark energy with constant density and constant negative pressure. However the disagreement between the measured value of the cosmological constant and that predicted from the quantum field theory is 120 orders of magnitude[5]. This is the greatest discrepancy between measurement and theory known to man, and is known as the

[3]For an analytical derivation see the following chapter

[4]The Planck scale is lowest scale imaginable. Given a coordinate frame, we can reduce the coordinate distance between two events as much as we want however the proper distance between them will not decrease beyond Planck's length. In other words that the notions of distance, of causality and any other notion based on a metric structure lose their meaning at the Planck's scale

[5]This is expanded in detail in Subsection 2.8.1

cosmological constant problem and it remains unresolved until today as one of the most famous problems in modern physics. One could think that maybe our hypothesis is not correct, i.e. the dark energy is not due to vacuum energy (or Λ). In that case the problem remains but in a milder form: why is the vacuum energy zero (as opposed to huge value predicted by theory)?

Next we present *the Cosmic Coincidence Problem*[6]. Under the assumption that our Universe consists of matter, radiation and dark energy, we could define the corresponding energy densities. The fact that the energy densities of dark energy and cosmological matter are of the same order around the present time is very striking. In the standard ΛCDM model, the cosmological window during which these components have comparable density is short one must explain how we happen to live during the time when $\rho_m \simeq \rho_{DE}$.

In order to quantify the problem we can define the time-dependent energy densities of ρ_m and ρ_{DE} and based on them, define a new parameter, r, as the ratio of the two parameter as follows

$$r = \frac{\rho_m}{\rho_{DE}} \tag{1.3}$$

The ratio r ranges from $r \simeq 0$, when many orders of magnitude separate the two densities, to $r \simeq 1$, when the two densities are equal. Opinions on this problem are divided: some authors[28–30] think it is a problem, while others are not impressed, since it is hard to put a metric on being surprised by such an anomaly. What also complicates things is that baryonic matter is also comparable, while radiation is not that far off, being about two orders of magnitudes less important today.

On the other hand, one may wonder, why such coincidence is seen as a big problem. There are indeed some authors in the field who deny that the cosmic coincidence is actually a problem[31]. It appears to be a problem only if someone starts assuming that we could find ourselves with equal probability in any of the periods of the cosmic evolution. So, anthropic arguments[32, 33] necessarily enter the discussion.

Let us now be a little more explicit concerning the anthropic principle. In the literature there is a distinction between the weak[34–36] and the strong[37–39] version of the anthropic principle. In the first one, the relevant (anthropically weighted) a priori probability is supposed to concern only a particular given model of the universe, with which one may be concerned since the observed values of all physical and cosmological quantities are not equally probable. On the other hand the strong anthropic principle the relevant anthropic probability distribution is supposed to be extended over an ensemble of cosmological models that are set up with a range of different values of what, in a particular model are usually postulated to be fundamental constants. Therefore the observed values of these constants might have this particular value if it could be shown that all the other values were unfavourable to the existence of anthropic observers.

In the effort to address the problems of the ΛCDM model, several alternative theories have been proposed, such as extra dimensions[40–42], quintessence models[43], $f(R)$ extended gravity theories[44–46], scalar tensor quintessence models[47, 48], k-essence[49], Chaplygin gas[50–52] etc. Some of these models such as scalar tensor quintessence models have also had some success simultaneously tackling the coincidence problem, as the scalar field that plays the role of *Dark Energy* presents dynamics and in particular, is the dynamical "Newton's constant" ($F(\phi) = \frac{1}{8\pi G}$). In these models the dark energy is treated as a new matter field which is effectively homogenous, and evolves as the universe expands. Within the present work, we focus particularly on the scalar-tensor theory of graviation.

The thesis is organised as following:

[6]For more details see Subsection 2.8.2

- In chapter 2 we make a review of the standard cosmological case, where we derive the Friedmann's equations of motion for a Friedmann-Robertson-Walker (FRW) metric Universe by varying the Einstein-Hilbert action and also by following a more historical method. Following that, the cosmological constant and the solution of Friedmann equations is presented. Finally, in this chapter, we describe the basic challenges of the ΛCDM problem. During the calculations of this chapter we use the metric notation $g_{\mu\nu} = (+1, -1, -1, -1)$ together with the Planck units, where $c = \hbar = 1$.

- In chapter 3 we present an alternative theory for DE, i.e the *quintessence models* deriving Friedmann's equations of motion. For the calculations of this chapter and for the rest of the thesis we use once again the Planck units, but we change the metric notation to $g_{\mu\nu} = (-1, +1, +1, +1)$.[7]

- In chapter 4 we discuss modified gravity and the generalized background equations of the theory. We derive Friedmann's generalized equations from Lagrangian mechanics, together with the traditional variational method. This chapter concludes our theoretical framework.

- In chapter 5 we study the field dynamics of quintessence model with linear potential and then generalize it in scalar-tensor quintessence theory. We examine the evolution of the ϕ field (the candidate for dark energy) along with the scale factor and the equation of state parameter. In these sections we display numerically that Cosmic Doomsday can be prevented in such theories of gravity. Also we test our theory with the Union2.1 dataset. Finally, we study qualitative different potentials of the form $V = s \cdot |\phi|^n$ and use, once again, the Union2.1 dataset as a validity test of our theory constructing the 1σ and 2σ confidence level contours.

- In the final chapter we present our conclusions and future prospects.

[7] The different metric does not change the spacetime identities according to Sylvester's Law of Inertia(see following chapters).

Chapter 2

Standard Cosmology - ΛCDM Model

On an initial approach, we could say that General Relativity (GR) is the most fundamental theory of gravitation through which a physicist can study the Universe's spacetime. This particular theory is consistent with experimental data and the predictions of GR have been confirmed in all observations and experiments to date. With the term *Standard Cosmology* we are referring to the mathematical framework of GR and modern Cosmology, that describes our Universe. This includes Einstein's field equations and Friedmann's equations of motion in a homogeneous and isotropic Friedmann-Robertson-Walker (FRW) metric Universe, in the language of differential geometry.

In this chapter we will describe the necessary mathematical tools of GR, for the sections to follow and introduce the reader to the basic computations in Standard Cosmology.

2.1 Spacetime and Metric Tensor

In special relativity, space ($\vec{x}$) and time (t) can be regarded as interchangeable parts of a single entity, spacetime. Fundamental equations can be written only between physical quantities known as *4-vectors*. GR aims to include within the spacetime the effect of gravitational force on the particle motion. In that case we simply study particles that they move freely in a curved spacetime. Therefore, in GR we are interested in the distance between points in four dimensional spacetime, and we must also take into consideration the possibility that spacetime might be curved. The distance can be written as

$$ds^2 = \sum_{\mu,\nu=0}^{3} g_{\mu\nu} dx^\mu dx^\nu \tag{2.1}$$

In Eq.(2.1) the quantity $g_{\mu\nu}$ is called the *metric tensor* and is a function of the coordinates and contains all the information about the intrinsic geometry of the spacetime that we study, μ and ν are indices taking the values $0, 1, 2$ and 3, x^0 is the time coordinate and x^1, x^2 and x^3 are the three spatial coordinates. Fortunately, this complicated situation can be dramatically simplified by imposing the *cosmological principle*, which implies that at a given time, the Universe should not have any preferred locations and directions.

All the way through this thesis, the Universe is considered homogeneous, isotropic and spatially flat, known as the *Friedmann-Robertson-Walker(FRW)* Universe. This model can be described

by the non-flat line element[2, 53]

$$ds^2 = c^2dt^2 - \alpha^2(t)\left[\frac{dr^2}{1-kr^2} + r^2\left(d\theta^2 + sin^2\theta d\phi^2\right)\right] \tag{2.2}$$

where the quantity $\alpha(t)$ is the *scale factor*. This result is worth memorizing - after all, it is the metric of our Universe! The *scale factor* measures the universal expansion rate, it is a function of time alone, and it describes how physical separations are growing with time, since the coordinate distances are by definition fixed. The parameter k is called the *scalar curvature* and can take the values $k = +1, 0, -1$. The *scalar curvature* describes an open, a flat and a closed universe respectively. Each topological geometry can be seen in Fig.2.1

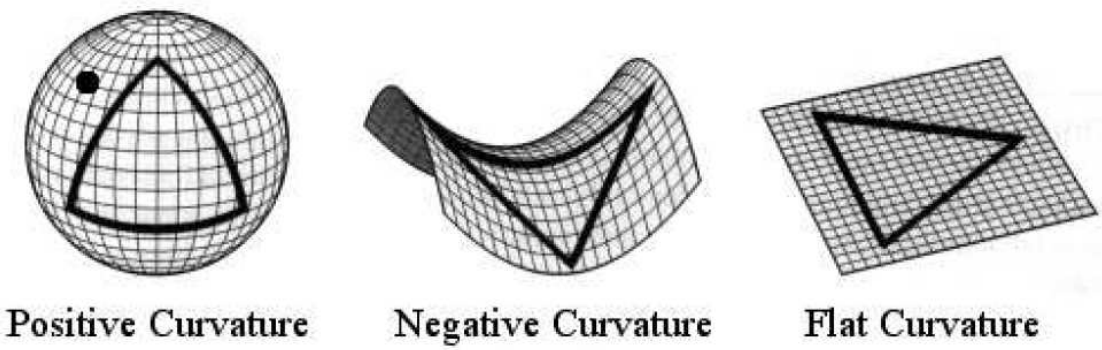

Figure 2.1: Examples of Curved Manifolds (The picture was obtained from Ref.[53] after permission of the author.)

2.2 Weyl's Hypothesis and the Energy-momentum tensor

In 1923, Herman Weyl studied the problem of the representation of the energy distribution at large scales within the general theory of relativity. Considering the *cosmological principle*, Weyl assumed that the universe contains a uniform substratum, within which galaxies behave like particles in a perfect fluid (e.g. see [54]). Describing such a fluid requires two variables, an *energy-matter density* ρ and *pressure* p, under the assumption of isotropy.[1] If we want its equability to be conserved, we must have insignificant relative motions of the particles and fluid's motion that has to be characterized by a common velocity with a *4-vector* u^μ (relative to the observer).

Within the GR, matter and energy distribution in the Universe can be described by a tensor which is defined as follows[53, 58]

$$T_{\mu\nu} = (\rho + p)u_\mu u_\nu - p \cdot g_{\mu\nu} \tag{2.3}$$

The aforementioned tensor is called the *energy-momentum tensor*. Moreover every tensor can be written in a matrix form (as every tensor which describe physical quantities). Considering

[1] Even though on large scales our Universe is considered isotropic and homogeneous, in smaller ones it is not. For this case the metric that describes such a spacetime has equal time components, however space is expanding or contracting at different rates in different directions, depending on the values of p_j[55–57].

homogeneity and isotropy, the stress-energy tensor takes the following form

$$T_{\mu\nu} = \begin{pmatrix} \rho & 0 & 0 & 0 \\ 0 & -g_{11}p & 0 & 0 \\ 0 & 0 & -g_{22}p & 0 \\ 0 & 0 & 0 & -g_{33}p \end{pmatrix} \tag{2.4}$$

How do the density and pressure evolve with time? In Minkowski space, energy and momentum are conserved. These conservation laws can be combined into a four-component conservation equation for the stress-energy tensor[53]

$$\frac{\partial T_{\mu\nu}}{\partial x^{\nu}} = 0 \tag{2.5}$$

Eq.(2.5) is completely correct when it comes to a Minkowski space. However, when the spacetime is curved the above equation is promoted to the covariant conservation equation[53]

$$\nabla_{\nu} T_{\mu\nu} \equiv \frac{\partial T_{\mu\nu}}{\partial x^{\nu}} - \Gamma^{a}_{\mu\nu} T_{a\nu} - \Gamma^{a}_{\nu\nu} T_{\mu a} = 0 \tag{2.6}$$

where ∇_{μ} is the *covariant derivative* and $\Gamma^{a}_{\mu\nu}$ are the *Christoffel's symbols* which are defined as[53]

$$\Gamma^{a}_{\mu\nu} = \frac{1}{2} g^{a\beta} \left(\frac{\partial g_{\beta\nu}}{\partial x^{\mu}} + \frac{\partial g_{\mu\beta}}{\partial x^{\nu}} - \frac{\partial g_{\mu\nu}}{\partial x^{\beta}} \right) \tag{2.7}$$

Here we have to comment that in the bibliography it is usual for simplicity that the differentiation regarding an index to be denoted by "," and the *covariant derivative* by ";".

2.3 Einstein's Field Equations

Einstein's dream was to connect the energy and matter distribution of spacetime to its resulting geometry. This particular equation must include tensors of the same order, in order to remain invariant under transformations. Even though, an energy-momentum tensor was easy to be constructed its connection to a gravitational one was a bit tricky. Einstein based on the assumption that the GR, for a weak gravitational field, should lead to Newtonian theory constructed the so called *Ricci Tensor*.

In the Newtonian Theory the gravitational potential, $\Phi(r)$, obeys the Poisson's Law that can describe a gravitational field, which can be written as[53]

$$\nabla^2 \Phi(r) = 4\pi G \rho \tag{2.8}$$

where G is Newton's constant. In GR this role can be played by the metric tensor $g_{\mu\nu}$ hence Einstein was looking for a tensor with second order derivatives of $g_{\mu\nu}$, in order to ensure the invariance. This tensor was the *Riemann's curvature tensor*, which is defined as[53, 59]

$$R^{\rho}{}_{\mu\sigma\nu} = \frac{\partial \Gamma^{\rho}_{\mu\nu}}{\partial x^{\sigma}} - \frac{\partial \Gamma^{\rho}_{\mu\sigma}}{\partial x^{\nu}} + \Gamma^{\rho}_{\alpha\sigma} \Gamma^{a}_{\mu\nu} - \Gamma^{\rho}_{a\nu} \Gamma^{a}_{\mu\rho} \tag{2.9}$$

The basic problem was that the *Riemann curvature tensor* and the energy-momentum tensor are not of the same order. However, the *Ricci tensor*, which can be obtained through the Riemann

curvature tensor if we make a contraction between two indices, is of the same order as the energy-momentum tensor. The *Ricci tensor* can be defined as[53, 59]

$$R_{\mu\nu} = R^{\rho}{}_{\mu\rho\nu} = \frac{\partial \Gamma^{\rho}_{\mu\nu}}{\partial x^{\rho}} - \frac{\partial \Gamma^{\rho}_{\mu\rho}}{\partial x^{\nu}} + \Gamma^{\rho}_{\alpha\rho}\Gamma^{a}_{\mu\nu} - \Gamma^{\rho}_{a\nu}\Gamma^{a}_{\mu\rho} \tag{2.10}$$

Then, Einstein managed to construct a new tensor, as a function of the *Ricci tensor* $R_{\mu\nu}$ and the *Ricci scalar*. The latter is simply the contraction between its two indices with the metric tensor, i.e. $R = g^{\mu\nu}R_{\mu\nu}$. That new tensor is the famous *Einstein's tensor* and it is calculated via the following equation[53, 59]

$$G_{\mu\nu} = R_{\mu\nu} - \frac{1}{2}g_{\mu\nu}R \tag{2.11}$$

Einstein also proved that the covariant derivative of $G_{\mu\nu}$ is equal to zero, i.e. $\nabla^{\mu}G_{\mu\nu} = 0$[2]. Since, the above equation is a non-linear second order differential equation for the metric, the following two equations had to be proportional to each other and satisfy the relation[53, 59]

$$G_{\mu\nu} = R_{\mu\nu} - \frac{1}{2}g_{\mu\nu}R = 8\pi G T_{\mu\nu} \tag{2.12}$$

In Eq.(2.12) the constant was selected by Einstein in order for the above equation to give Poisson's equation at the limit of a weak gravitational field.

2.4 Friedmann Equations

2.4.1 Basic Assumptions

Einstein's field equations can be used for plenty of gravitational systems. In this section we will study the Universe's dynamical evolution through the solution for the *scale factor* $a(t)$. The Friedmann equations start with the simplifying assumption that the universe is spatially homogeneous and isotropic, i.e. the *cosmological principle*, which is expressed by the following metric

$$\mathrm{ds}^2 = \alpha(t)^2 \mathrm{ds_3}^2 - c^2 \mathrm{dt}^2 \tag{2.13}$$

where $\mathrm{ds_3}^2$ is a three-dimensional metric that must be one of

a. flat space of zero curvature

b. a sphere of constant positive curvature, i.e $k = +1$, or

c. a hyperbolic space with constant negative curvature i.e. $k = -1$.

The parameter k, which describes the geometry of three-dimensional space, is the basic parameter characterizing the global properties of our Universe. An exact solution for this scale factor as a function of physical and conformal time is desirable for the analysis of several problems. The most general spatial metric which has constant curvature is

$$\mathrm{ds_3}^2 = \left[\frac{dr^2}{1-kr^2} + r^2(d\theta^2 + sin^2\theta d\phi^2)\right] \tag{2.14}$$

[2]For an analytical derivation see Appendix A.

Substituting Eq.(2.14) in Eq.(2.13) we obtain the general non-flat FRW metric, which is given by the line element[3]

$$ds^2 = c^2dt^2 - \alpha^2(t)\left[\frac{dr^2}{1-kr^2} + r^2(d\theta^2 + sin^2\theta d\phi^2)\right] \tag{2.15}$$

where the metric tensor notation is $g_{\mu\nu} = (+,-,-,-)$. Within this chapter this is the notation that we adopted. One could rewrite Eq.(2.1) in a more convenient form as follows

$$ds^2 = g_{\mu\nu}dx^\mu dx^\nu \tag{2.16}$$

Comparing the two equation and demanding the equivalence of the aforementioned equations we produce the components of the metric tensor

$$g_{00} = c^2 = 1, \qquad g_{11} = \frac{-\alpha^2}{1-kr^2}, \qquad g_{22} = -\alpha^2r^2 \qquad g_{33} = -\alpha^2r^2sin^2\theta$$

or equivalently for the inverse metric tensor

$$g^{00} = c^2 = 1, \qquad g^{11} = \frac{1-kr^2}{-\alpha^2}, \qquad g^{22} = -\frac{1}{\alpha^2r^2} \qquad g^{33} = -\frac{1}{\alpha^2r^2sin^2\theta}$$

Therefore, we may write the metric in matrix form such as

$$g_{\mu\nu} = \begin{pmatrix} 1 & 0 & 0 & 0 \\ 0 & \frac{-\alpha^2}{1-kr^2} & 0 & 0 \\ 0 & 0 & -\alpha^2r^2 & 0 \\ 0 & 0 & 0 & -\alpha^2r^2sin^2\theta \end{pmatrix} \tag{2.17}$$

2.4.2 Christoffel's Symbols

Thereafter, we compute the Christoffel symbols for the FRW metric, i.e Eq.(2.15), using the definition

$$\Gamma^\rho_{\mu\nu} = \frac{1}{2}g^{\rho\sigma}(g_{\sigma\nu,\mu} + g_{\mu\beta,\nu} - g_{\mu\nu,\sigma}) \tag{2.18}$$

Of course the definitions of Eq.(2.7) and Eq.(2.18) are equivalent. Taking in consideration these definitions, one can calculate the non-zero Christoffel's symbols as follows

- $$\Gamma^0_{11} = \frac{1}{2}g^{0\sigma}\left(\frac{\partial g_{\sigma 1}}{\partial x^1} + \frac{\partial g_{1\sigma}}{\partial x^1} - \frac{\partial g_{11}}{\partial x^\sigma}\right) = \frac{1}{2}g^{00}\left(\frac{\partial g_{01}}{\partial r} + \frac{\partial g_{10}}{\partial r} - \frac{\partial g_{11}}{\partial t}\right) = \\ = \frac{1}{\cancel{2}}\cdot 1\cdot\frac{1}{1-kr^2}\cancel{2}\alpha\dot{\alpha} = \frac{\alpha\dot{\alpha}}{1-kr^2}$$

- $$\Gamma^0_{22} = \frac{1}{2}g^{0\sigma}\left(\frac{\partial g_{\sigma 2}}{\partial x^2} + \frac{\partial g_{2\sigma}}{\partial x^2} - \frac{\partial g_{22}}{\partial x^\sigma}\right) = \frac{1}{2}g^{00}\left(\frac{\partial g_{02}}{\partial x^2} + \frac{\partial g_{20}}{\partial x^2} - \frac{\partial g_{22}}{\partial t}\right) = \\ = \frac{1}{\cancel{2}}\cdot 1\cdot r^2\cancel{2}\alpha\dot{\alpha} = \alpha\dot{\alpha}r^2$$

[3]According to Sylvester's law of inertia[60], the signature of the scalar product g does not depend on the choice of basis. Moreover, for every metric g of signature $(p;q;r)$ there exists a basis such that $g_{ab} = +1$ for $a = b = 1,\ldots,p$, $g_{ab} = -1$ for $a = b = p+1,\ldots,p+q$ and $g_{ab} = 0$ otherwise. It follows that there exists an isometry if and only if the signatures of g_1 and g_2 are equal. That's the reason why the the spacetime identities does not change regardless the signature of the metric that is chosen.

- $$\Gamma^0_{33} = \frac{1}{2}g^{0\sigma}\Big(\frac{\partial g_{\sigma 3}}{\partial x^3} + \frac{\partial g_{3\sigma}}{\partial x^3} - \frac{\partial g_{33}}{\partial x^\sigma}\Big) = \frac{1}{2}g^{00}\Big(\frac{\partial g_{03}}{\partial x^3} + \frac{\partial g_{30}}{\partial x^3} - \frac{\partial g_{33}}{\partial t}\Big) =$$
$$= \frac{1}{\cancel{2}} \cdot 1 \cdot sin^2\theta r^2 \cancel{2}\alpha\dot{\alpha} = \alpha\dot{\alpha}r^2 sin^2\theta$$

- $$\Gamma^1_{11} = \frac{1}{2}g^{1\sigma}\Big(\frac{\partial g_{\sigma 1}}{\partial x^1} + \frac{\partial g_{1\sigma}}{\partial x^1} - \frac{\partial g_{11}}{\partial x^\sigma}\Big) = \frac{1}{2}g^{11}\Big(\frac{\partial g_{11}}{\partial r} + \frac{\partial g_{11}}{\partial r} - \frac{\partial g_{11}}{\partial r}\Big) =$$
$$= \frac{1}{\cancel{2}} \cdot \Big(-\frac{1-kr^2}{\cancel{\alpha^2}}\Big) \cdot \Big(-\cancel{\alpha^2}\frac{1}{(1-kr^2)^2}\Big)\cancel{2}kr = \frac{kr}{1-kr^2}$$

- $$\Gamma^1_{22} = \frac{1}{2}g^{1\sigma}\Big(\frac{\partial g_{\sigma 2}}{\partial x^2} + \frac{\partial g_{2\sigma}}{\partial x^2} - \frac{\partial g_{22}}{\partial x^\sigma}\Big) = \frac{1}{2}g^{11}\Big(\frac{\partial g_{12}}{\partial \theta} + \frac{\partial g_{21}}{\partial \theta} - \frac{\partial g_{22}}{\partial r}\Big) =$$
$$= \frac{1}{\cancel{2}} \cdot \Big(-\frac{1-kr^2}{\alpha^2}\Big) \cdot \cancel{2}\alpha^2 r = -r(1-kr^2)$$

- $$\Gamma^1_{33} = \frac{1}{2}g^{1\sigma}\Big(\frac{\partial g_{\sigma 3}}{\partial x^3} + \frac{\partial g_{3\sigma}}{\partial x^3} - \frac{\partial g_{33}}{\partial x^\sigma}\Big) = \frac{1}{2}g^{11}\Big(\frac{\partial g_{13}}{\partial \phi} + \frac{\partial g_{31}}{\partial \phi} - \frac{\partial g_{33}}{\partial r}\Big) =$$
$$= \frac{1}{\cancel{2}} \cdot \Big(-\frac{1-kr^2}{\alpha^2}\Big) \cdot \cancel{2}\alpha^2 sin^2\theta r = -r sin^2\theta(1-kr^2)$$

- $$\Gamma^1_{01} = \frac{1}{2}g^{1\sigma}\Big(\frac{\partial g_{\sigma 1}}{\partial x^0} + \frac{\partial g_{0\sigma}}{\partial x^1} - \frac{\partial g_{01}}{\partial x^\sigma}\Big) = \frac{1}{2}g^{11}\Big(\frac{\partial g_{11}}{\partial t} + \frac{\partial g_{01}}{\partial r} - \frac{\partial g_{01}}{\partial r}\Big) =$$
$$= \frac{1}{\cancel{2}} \cdot \Big(-\frac{\cancel{1-kr^2}}{\alpha^2}\Big)\Big(-\frac{1}{\cancel{1-kr^2}}\Big) \cdot \cancel{2}\alpha\dot{\alpha} = \frac{\dot{\alpha}}{\alpha}$$

- $$\Gamma^2_{02} = \frac{1}{2}g^{2\sigma}\Big(\frac{\partial g_{\sigma 2}}{\partial x^0} + \frac{\partial g_{0\sigma}}{\partial x^2} - \frac{\partial g_{02}}{\partial x^\sigma}\Big) = \frac{1}{2}g^{22}\Big(\frac{\partial g_{22}}{\partial t} + \frac{\partial g_{02}}{\partial \theta} - \frac{\partial g_{02}}{\partial \theta}\Big) =$$
$$= \frac{1}{\cancel{2}} \cdot \Big(-\frac{1}{\alpha^2 r^2}\Big)\Big(-r^2\cancel{2}\alpha\dot{\alpha}\Big) = \frac{\dot{\alpha}}{\alpha}$$

- $$\Gamma^3_{03} = \frac{1}{2}g^{3\sigma}\Big(\frac{\partial g_{\sigma 3}}{\partial x^0} + \frac{\partial g_{0\sigma}}{\partial x^3} - \frac{\partial g_{03}}{\partial x^\sigma}\Big) = \frac{1}{2}g^{33}\Big(\frac{\partial g_{33}}{\partial t} + \frac{\partial g_{03}}{\partial \phi} - \frac{\partial g_{03}}{\partial \phi}\Big) =$$
$$= \frac{\dot{\alpha}}{\alpha}$$

- $$\Gamma^2_{12} = \frac{1}{2}g^{2\sigma}\Big(\frac{\partial g_{\sigma 2}}{\partial x^1} + \frac{\partial g_{1\sigma}}{\partial x^2} - \frac{\partial g_{12}}{\partial x^\sigma}\Big) = \frac{1}{2}g^{22}\Big(\frac{\partial g_{22}}{\partial r} + \frac{\partial g_{12}}{\partial \theta} - \frac{\partial g_{12}}{\partial \theta}\Big) =$$
$$= \frac{1}{\cancel{2}} \cdot \Big(-\frac{1}{\cancel{\alpha^2}r^2}\Big)\Big(-\cancel{2}\cancel{\alpha^2}r\Big) = \frac{1}{r} = \Gamma^3_{13}$$

- $$\Gamma^2_{33} = \frac{1}{2}g^{2\sigma}\Big(\frac{\partial g_{\sigma 3}}{\partial x^3} + \frac{\partial g_{3\sigma}}{\partial x^3} - \frac{\partial g_{33}}{\partial x^\sigma}\Big) = \frac{1}{2}g^{22}\Big(\frac{\partial g_{23}}{\partial \phi} + \frac{\partial g_{32}}{\partial \phi} - \frac{\partial g_{33}}{\partial \theta}\Big) =$$
$$= \frac{1}{\cancel{2}}\cdot\Big(-\frac{1}{\cancel{\alpha^2 r^2}}\Big)\Big(\cancel{2}\cancel{\alpha^2 r^2} sin\theta cos\theta\Big) = -sin\theta cos\theta$$

- $$\Gamma^3_{23} = \frac{1}{2}g^{3\sigma}\Big(\frac{\partial g_{\sigma 3}}{\partial x^2} + \frac{\partial g_{2\sigma}}{\partial x^3} - \frac{\partial g_{23}}{\partial x^\sigma}\Big) = \frac{1}{2}g^{33}\Big(\frac{\partial g_{33}}{\partial \theta} + \frac{\partial g_{23}}{\partial \phi} - \frac{\partial g_{23}}{\partial \phi}\Big) =$$
$$= \frac{1}{\cancel{2}}\cdot\Big(-\frac{1}{\cancel{\alpha^2 r^2} sin^2\theta}\Big)\Big(-\cancel{2}\cancel{\alpha^2 r^2} sin\theta cos\theta\Big) = \frac{cos\theta}{sin\theta}$$

The non-zero Christoffel symbols are summarised in the following Table

Christoffel Symbols		
$\Gamma^0_{11} = \frac{\alpha\dot{\alpha}}{1-kr^2}$	$\Gamma^0_{22} = \alpha\dot{\alpha}r^2$	$\Gamma^0_{33} = \alpha\dot{\alpha}r^2 sin^2\theta$
$\Gamma^1_{11} = \frac{kr}{1-kr^2}$	$\Gamma^1_{22} = -r(1-kr^2)$	$\Gamma^1_{33} = -rsin^2\theta(1-kr^2)$
$\Gamma^1_{01} = \Gamma^2_{02} = \frac{\dot{\alpha}}{\alpha}$	$\Gamma^3_{03} = \frac{\dot{\alpha}}{\alpha}$	$\Gamma^2_{12} = \frac{1}{r}$
$\Gamma^3_{13} = \frac{1}{r}$	$\Gamma^2_{33} = -sin\theta cos\theta$	$\Gamma^3_{23} = \frac{cos\theta}{sin\theta}$

2.4.3 Ricci Scalar

In order to compute the Ricci Scalar we will use the above calculated Christoffel's symbols along with the definition

$$R_{\mu\nu} = R^\rho{}_{\mu\rho\nu} = \Gamma^\rho_{\mu\nu,\rho} - \Gamma^\rho_{\mu\rho,\nu} + \Gamma^\rho_{\sigma\rho}\Gamma^\sigma_{\mu\nu} - \Gamma^\rho_{\sigma\nu}\Gamma^\sigma_{\mu\rho} \tag{2.19}$$

Hence, we may have for the (00) component

$$R_{00} = \cancelto{0}{\frac{\partial\Gamma^\rho_{00}}{\partial x^\rho}} - \frac{\partial\Gamma^\rho_{0\rho}}{\partial x^0} + \cancelto{0}{\Gamma^\rho_{\sigma\rho}\Gamma^\sigma_{00}} - \Gamma^\rho_{\sigma 0}\Gamma^\sigma_{0\rho} =$$
$$= -\frac{\partial\Gamma^1_{01}}{\partial t} - \frac{\partial\Gamma^2_{02}}{\partial t} - \frac{\partial\Gamma^3_{03}}{\partial t} - \Gamma^1_{10}\Gamma^1_{01} - \Gamma^2_{20}\Gamma^2_{02} - \Gamma^3_{30}\Gamma^3_{03} =$$
$$= -3\Big(\frac{\partial\Gamma^1_{01}}{\partial t} + \Gamma^1_{10}\Gamma^1_{01}\Big) = -3\Big(\frac{\ddot{a}}{a} - \frac{\dot{\alpha}^2}{\alpha^2} + \frac{\dot{\alpha}^2}{\alpha^2}\Big) = -3\frac{\ddot{a}}{a}$$

In a similar way one can calculate the rest of the Ricci tensor components. Then the Ricci scalar is written

$$R = g^{\mu\nu}R_{\mu\nu} = g^{00}R_{00} + g^{11}R_{11} + g^{22}R_{22} + g^{33}R_{33} =$$
$$= -3\frac{\ddot{a}}{a} - \frac{1-kr^2}{\alpha^2}\frac{\alpha\ddot{\alpha} + 2\dot{\alpha}^2 + 2k}{1-kr^2} - \frac{1}{\alpha^2 r^2}r^2(\alpha\ddot{\alpha} + 2\dot{\alpha} + 2k) - \frac{1}{\alpha^2 r^2 sin^2\theta}r^2(a\ddot{a} + 2\dot{a}^2 + 2k)sin^2\theta \Rightarrow$$
$$\Rightarrow R = -6\Big(\frac{\ddot{\alpha}}{\alpha} + \frac{\dot{\alpha}^2}{\alpha^2} + \frac{k}{\alpha^2}\Big) \tag{2.20}$$

2.4.4 Calculating Friedmann Equations

As we already described, within the GR, matter and energy distribution in the Universe, must be described by a tensor. The simplest form of a tensor, which can describe the uniform motion of a perfect fluid within a curved gravitation background is given by Eq.(2.3), i.e.

$$T_{\mu\nu} = (\rho + p)u_\mu u_\nu - pg_{\mu\nu} \tag{2.21}$$

That is, as we already mentioned, the *energy-momentum tensor*. One could think naively, the *energy-momentum tensor* as a measure of the "matter content" of the Universe. As there are not any preferable reference frames we will use the one most simplified and suited to our needs. The only non-zero component of u^μ for a comoving observer is the time component, which we normalize to 1, so we can write $u^\mu = (1, 0, 0, 0)$. Hence the energy-momentum tensor for the perfect fluid can be written as

$$T_{\mu\nu} = (\rho + p)g_{\mu 0}g_{\nu 0} - pg_{\mu\nu} \tag{2.22}$$

Furthermore, any tensor can take the form of a matrix as we already discussed. As a result, the $T_{\mu\nu}$ in this case, takes the form

$$T_{\mu\nu} = diag\{\rho, -p, -p, -p\} \tag{2.23}$$

Now we are ready to compute the non-zero components of the Einstein field equations[58]

- <u>The (00)-component</u>

$$\begin{aligned} R_{00} - \frac{1}{2}g_{00}R &= 8\pi G T_{00} \Rightarrow \\ \Rightarrow -3\frac{\ddot{\alpha}}{\alpha} - \left(\frac{1}{2}\right)\cdot 1 \cdot \left[-6\left(\frac{\ddot{\alpha}}{\alpha} + \frac{\dot{\alpha}^2}{\alpha^2} + \frac{k}{\alpha^2}\right)\right] &= 8\pi G\rho \Rightarrow \\ \Rightarrow -3\frac{\ddot{\alpha}}{\alpha} + 3\left(\frac{\ddot{\alpha}}{\alpha} + \frac{\dot{\alpha}^2}{\alpha^2} + \frac{k}{\alpha^2}\right) &= 8\pi G\rho \Rightarrow \\ \left(\frac{\dot{\alpha}}{\alpha}\right)^2 &= \frac{8\pi G}{3}\rho - \frac{k}{\alpha^2} \end{aligned} \tag{2.24}$$

  which is also known as the *first (order) Friedmann Equation.*

- <u>The (11)-component</u>

$$\begin{aligned} R_{11} - \frac{1}{2}g_{11}R &= 8\pi G T_{11} \Rightarrow \\ \frac{\alpha\ddot{\alpha} + 2\dot{\alpha}^2 + 2k}{1 - kr^2} - 3\frac{\alpha^2}{1 - kr^2}\left(\frac{\ddot{\alpha}}{\alpha} + \frac{\dot{\alpha}^2}{\alpha^2} + \frac{k}{\alpha^2}\right) &= -8\pi G\left(-\frac{\alpha^2}{1 - kr^2}\right)p \Rightarrow \\ 2\frac{\ddot{\alpha}}{\alpha} + \frac{\dot{\alpha}^2}{\alpha^2} + \frac{k}{\alpha^2} &= -8\pi G p. \end{aligned} \tag{2.25}$$

  One can easily show that the (22)-component and (33)-component give rise to the same Eq.(2.25). Now, substituting Eq.(2.24) into Eq.(2.25), we end up with[58]

$$\frac{\ddot{\alpha}}{\alpha} = -\frac{4\pi G}{3}(\rho + 3p) \tag{2.26}$$

Eq.(2.26), in this form, is known as *Raychaudhuri Equation or Acceleration Equation*, given the fact that there is only the second derivative term of the scale factor. According to Newton and Eq.(2.8), the pressure does not interact with gravity. However Einstein, according to Eq.(2.25), proves that pressure interacts with gravity and considering $p > 0$, pressure causes deceleration of the expansion just like density.

The above equations determine the evolution of the scale factor $\alpha(t)$ in time as a function of the energy density and pressure of the perfect fluid that the Universe contains. A third relevant but dependent equation is the *conservation of energy equation or the continuity equation* as we know. The continuity equation can be written as[58]

$$\dot{\rho} + 3\frac{\dot{\alpha}}{\alpha}(\rho + p) = 0 \tag{2.27}$$

We notice that this is derivable from the other two, therefore it is not independent[4] . Furthermore, due to the uniformity of the energy and matter distribution in the Universe, energy density as well as pressure are considered functions only of the time coordinate t. As we can see in the above equation, there are two terms that contribute to variation of the energy density within the Universe; the first term in the parenthesis decreases the energy density because of the universe expansion, as is expected and the second one gives energy loss due to pressure's work from the matter in the universe.

Although we need one more equation so we can solve the system (our components are not independent). We will use, of course, the equation that connects energy density with perfect fluid's pressure

$$p = w\rho \tag{2.28}$$

The proportionality factor w, it may generally be a function of the time and not a constant as it is assumed here. To summarize, the Friedmann equations are

Friedmann Equations for Standard Cosmology

$$\left(\frac{\dot{\alpha}}{\alpha}\right)^2 = \frac{8\pi G}{3}\rho - \frac{k}{\alpha^2}$$
$$\frac{\ddot{\alpha}}{\alpha} = -\frac{4\pi G}{3}(\rho + 3p)$$
$$\dot{\rho} + 3\frac{\dot{\alpha}}{\alpha}(\rho + p) = 0$$
$$p = w\rho$$

All these equations lead to the determination of the scale factor $\alpha(t)$ and the dynamical evolution of the Universe in time. From the system of the first three equations only the 2 are independent.

[4]For an analytical derivation see Appendix A. An alternative way to prove that this equation is dependent is through the Bianchi identities. This is also shown in Appendix A

2.5 Mathematical Approach for Calculating Friedmann Equations

The method that we used in the previous sections in order to obtain the Friedmann Equations is somewhat instinctive and historic. One could follow a more mathematical approach to derive the Friedmann Equations. In general, there are two basic methods in order to derive the equations of motion from a given action

a. By varying the action with a general metric, derive Einstein Equations and then use FRW metric.

b. By using the FRW metric directly in the Einstein Hilbert Action and vary with respect to the scale factor to obtain Friedmann equations.

In this section we will derive Friedmann equations using both methods.

2.5.1 First Method: Variation of the Action with General Metric

Let us first consider the full Einstein-Hilbert action

$$S = \int d^4x \sqrt{-g} \left[\frac{1}{2\kappa} R + \mathscr{L}_{matter} \right] \tag{2.29}$$

Eq.(2.29) consists of two terms. The first is the geometric one, where $g = det(g_{\mu\nu})$ is the determinant of the metric tensor matrix, R is the *Ricci scalar*, $\kappa = 8\pi G c^{-4}$ is Einstein's constant and the other term is the Lagrangian that describes any matter fields appearing in the theory.

Following the action principle, we require that the variation of the action with respect to the inverse metric is zero, i.e

$$\begin{aligned} \frac{\delta S}{\delta g^{\mu\nu}} = 0 \Rightarrow \int d^4x \left[\frac{1}{2\kappa} \frac{\delta \left(R\sqrt{-g}\right)}{\delta g^{\mu\nu}} + \frac{\delta \left(\mathscr{L}_{matter}\sqrt{-g}\right)}{\delta g^{\mu\nu}} \right] \delta g^{\mu\nu} = 0 \Rightarrow \\ \Rightarrow \int d^4x \left[\frac{1}{2\kappa} \left(\frac{\delta R}{\delta g^{\mu\nu}} \sqrt{-g} + R \frac{\delta \sqrt{-g}}{\delta g^{\mu\nu}} \right) + \frac{\delta \left(\mathscr{L}_{matter}\sqrt{-g}\right)}{\delta g^{\mu\nu}} \right] \delta g^{\mu\nu} = 0 \xRightarrow{\times \frac{\sqrt{-g}}{\sqrt{-g}}} \\ \Rightarrow \int d^4x \sqrt{-g} \left[\frac{1}{2\kappa} \left(\frac{\delta R}{\delta g^{\mu\nu}} + \frac{R}{\sqrt{-g}} \frac{\delta \sqrt{-g}}{\delta g^{\mu\nu}} \right) + \frac{\delta \left(\mathscr{L}_{matter}\sqrt{-g}\right)}{\sqrt{-g}\, \delta g^{\mu\nu}} \right] \delta g^{\mu\nu} = 0 \end{aligned} \tag{2.30}$$

Since Eq.(2.30) should be zero for any variation $\delta g^{\mu\nu}$ it implies that

$$\frac{\delta R}{\delta g^{\mu\nu}} + \frac{R}{\sqrt{-g}} \frac{\delta \sqrt{-g}}{\delta g^{\mu\nu}} = -\frac{2\kappa}{\sqrt{-g}} \frac{\delta \left(\mathscr{L}_{matter}\sqrt{-g}\right)}{\delta g^{\mu\nu}} \tag{2.31}$$

Eq.(2.31) is the equation of motion for the metric field. We now bodly define the right hand side of this equation as the *stress-energy tensor*[61]

$$T_{\mu\nu} \equiv \frac{-2}{\sqrt{-g}} \frac{\delta \left(\mathscr{L}_{matter}\sqrt{-g}\right)}{\delta g^{\mu\nu}} \tag{2.32}$$

which describes the density and flux of energy and momentum in spacetime.

2.5.1.1 Variation of Riemann tensor, Ricci tensor and Ricci scalar

Next we will try to calculate the left hand side of Eq.(2.31). For that we need the variations of the Ricci scalar R and the determinant of the metric. It is straightforward to show that[5]

$$\delta R = R_{\mu\nu}\delta g^{\mu\nu} + \nabla_\sigma \left(g^{\mu\nu}\delta\Gamma^\sigma_{\mu\nu} - g^{\mu\sigma}\delta\Gamma^\rho_{\rho\mu}\right) \tag{2.33}$$

where in Eq.(2.33) we used the metric compatibility of the covariant derivative $\nabla_\sigma g^{\mu\nu} = 0$[5]. The last term, $\nabla_\sigma \left(g^{\mu\nu}\delta\Gamma^\sigma_{\nu\mu} - g^{\mu\sigma}\delta\Gamma^\rho_{\rho\mu}\right)$, multiplied by $\sqrt{-g}$ becomes a total derivative, since

$$\sqrt{-g}A^\mu{}_{;\mu} = \sqrt{-g}\,\nabla_\mu A^\mu = \partial_\mu\left(\sqrt{-g}A^\mu\right) = \left(\sqrt{-g}A^\mu\right)_{,\mu} \tag{2.34}$$

and thus by Stoke's theorem only yields a boundary term when integrated. Therefore when the variation of the metric $\delta g^{\mu\nu}$ vanishes at infinity, this term does not contribute to the variation of the action. Thus we obtain

$$\frac{\delta R}{\delta g^{\mu\nu}} = R_{\mu\nu} \tag{2.35}$$

2.5.1.2 Variation of the determinant

Jacobi's formula, the rule of differentiating a determinant, gives[5]

$$\delta g = \delta \det\left(g^{\mu\nu}\right) = g g^{\mu\nu}\delta g_{\mu\nu} \tag{2.36}$$

Using this we are ready to prove that

$$\delta\left(\sqrt{g}\right) = \frac{1}{2\sqrt{g}}\delta g = -\frac{1}{2}\frac{(\sqrt{g})^{\cancel{2}}}{\cancel{\sqrt{g}}}g_{a\beta}\delta g^{a\beta} = -\frac{1}{2}\sqrt{g}g_{a\beta}\delta g^{a\beta} \Rightarrow$$
$$\Rightarrow \delta\left(\sqrt{g}\right) = -\frac{1}{2}\sqrt{g}g_{a\beta}\delta g^{a\beta} \tag{2.37}$$

Now, in order to get the expression for the 4-dimensional pseudo-Riemannian space of General Relativity, we simply replace $g \to -g$ and let the indices run from 0 to 3 (the usual greek ones). We then have

$$\delta\left(\sqrt{-g}\right) = -\frac{1}{2}\sqrt{-g}g_{\mu\nu}\delta g^{\mu\nu} \tag{2.38}$$

where $\mu, \nu = 0, 1, 2, 3$ as usual and we used the fact that $g_{\mu\nu}\delta g^{\mu\nu} = -g^{\mu\nu}\delta g_{\mu\nu}$ which follows from the rules for differentiating the inverse of a matrix, $\delta g^{\mu\nu} = -g^{\mu\alpha}\left(\delta g_{\alpha\beta}\right)g^{\beta\nu}$.

Now, we have all the necessary variations at our disposal, hence one can obtain the *Einstein's Field Equations*

$$R_{\mu\nu} - \frac{1}{2}g_{\mu\nu}R = \frac{8\pi G}{c^4}T_{\mu\nu} \tag{2.39}$$

Lastly, let us re-express Eq.(2.39) in a more compact defining the Einstein tensor as $G_{\mu\nu} = R_{\mu\nu} - \frac{1}{2}g_{\mu\nu}R$, which is as we mentioned already in Eq.(2.12), the symmetric second rank tensor and use the geometrized units, where $c = 1$. Therefore the *Einstein's Field Equations* are given by

$$G_{\mu\nu} = 8\pi G T_{\mu\nu} \tag{2.40}$$

Comparing Eq.(2.12) and Eq.(2.40) one can see that these particular equations are exactly the same, as it was expected. It has to be mentioned that Eq.(2.24) and Eq.(2.25) can be obtained from the Einstein Equations following the same procedure as shown in the previous sections.

[5]For an analytical derivation see Appendix A.

2.5.2 Second Method: Variation of the action with FRW metric

An alternative way to derive Eq.(2.24) and Eq.(2.25) is through the second method that we described[62, 63]. Under the assumption that the spacetime manifold is described by a FRW metric and preserve the same notation as before, i.e. $g_{\mu\nu} = (+, -, -, -)$ and taking into account the *Ricci scalar* $R = -6\left(\frac{\ddot{\alpha}}{\alpha} + \frac{\dot{\alpha}^2}{\alpha^2} + \frac{k}{\alpha^2}\right)$ the action (also known as the *Einstein-Hilbert action*) has the simple form[64]

$$S_{EH} = -\int \frac{R}{16\pi}\sqrt{-g}\, d^4x \tag{2.41}$$

where $\sqrt{-g}\, d^4x$ is the differential 4-volume element. By using the Ricci scalar and the metric tensor for an FRW universe, the new action can be re-expressed as

$$\begin{aligned} S_{EH} &= -\int -\frac{6}{16\pi}\left(\frac{\ddot{\alpha}}{\alpha} + \frac{\dot{\alpha}^2}{\alpha^2} + \frac{k}{\alpha^2}\right)\sqrt{-g}\, d^4x = \int \frac{3}{8\pi}\left(\frac{\ddot{\alpha}}{\alpha} + \frac{\dot{\alpha}^2}{\alpha^2} + \frac{k}{\alpha^2}\right)\alpha^3\, d^3x\, dt \Rightarrow \\ &\Rightarrow S_{EH} = \frac{3}{8\pi}\int d^3x\, dt\left(\alpha^2\ddot{\alpha} + \alpha\dot{\alpha}^2 + \alpha k\right) = \frac{3V}{8\pi}\int\left(\ddot{\alpha}\alpha^2 + \alpha\dot{\alpha}^2 + \alpha k\right) dt \end{aligned} \tag{2.42}$$

But $\frac{d\left(\alpha^2\dot{\alpha}\right)}{dt} = 2\alpha\dot{\alpha}^2 + \alpha^2\ddot{\alpha}$, therefore Eq.(2.42) takes the following form

$$S_{EH} = \cancelto{0}{\frac{3V}{8\pi}\alpha^2\dot{\alpha}\Big|_{t_1=0}^{t_2=\infty}} + \frac{3V}{8\pi}\int\left(-2\alpha\dot{\alpha}^2 + \alpha\dot{\alpha}^2 + \alpha k\right) dt \Rightarrow S_{EH} = \frac{3V}{8\pi}\int\left(-\alpha\dot{\alpha}^2 + \alpha k\right) dt \tag{2.43}$$

We could also introduce the action for a point particle of mass m is $S_{part} = -m\int d\tau$, where $d\tau$ is is the differential of proper time τ. However, if these particles are at rest in the comoving frame (i.e. $d\tau = dt$), and ρ_0 is the density of the ideal fluid (where $\rho_0 = m/V$), then this action reduces to

$$S_{part} = -\rho_0 \cdot V\int dt \tag{2.44}$$

Combining Eq.(2.43) and Eq.(2.44) we conclude that the total action is

$$S_{total} = S_{EH} + S_{part} = \frac{3V}{8\pi}\int\left(-\alpha\dot{\alpha}^2 + \alpha k - \frac{8\pi}{3}\rho_0\right) dt \tag{2.45}$$

Now, considering that the action is typically represented as an integral over time, $S = \int dt\mathscr{L}$, where $\mathscr{L}$ is the Lagrangian density and remembering that we are working in a homogenous Universe, i.e V can be neglected, we deduce that

$$\mathscr{L}_{total} = \frac{3}{8\pi}\left(-\dot{\alpha}^2\alpha + \alpha k - \frac{8\pi}{3}\rho_0\right) = -\frac{3}{8\pi}\dot{\alpha}^2\alpha + \frac{3k\alpha}{8\pi} - \rho_0 \tag{2.46}$$

If the above action is varied with fixed $t_1; t_2; \alpha(t_1)$ and $\alpha(t_2)$, allowing the trajectory of $\alpha(t)$ to vary in between the initial and the final times, the Euler-Lagrange equation gives rise to the second order equation. Indeed

$$\begin{aligned} &\frac{d}{dt}\left(\frac{\partial\mathscr{L}_{total}}{\partial\dot{\alpha}}\right) = \frac{\partial\mathscr{L}_{total}}{\partial\alpha} \Rightarrow \frac{d}{dt}\left(\frac{-3\dot{\alpha}\alpha}{4\pi}\right) = -\frac{3\dot{\alpha}^2}{8\pi} + \frac{3k}{8\pi} \Rightarrow -\frac{3}{4\pi}\left(\ddot{\alpha}\alpha + \dot{\alpha}^2\right) = -\frac{3}{8\pi}\dot{\alpha}^2 + \frac{3k}{8\pi} \Rightarrow \\ &\Rightarrow -2\left(\ddot{\alpha}\alpha + \dot{\alpha}^2\right) = -\dot{\alpha}^2 + k \Rightarrow -2\ddot{\alpha}\alpha - 2\dot{\alpha}^2 = -\dot{\alpha}^2 + k \Rightarrow \frac{\ddot{\alpha}}{\alpha} = -\frac{1}{2}\frac{\dot{\alpha}^2}{\alpha^2} - \frac{k}{2\alpha^2} \end{aligned} \tag{2.47}$$

The Friedmann equation Eq.(2.25) imply the above for $p = 0$[6].

Rewriting the action in terms of of $t(\alpha)$ one can see that the action can be calculated

$$S_{total} = \frac{3V}{8\pi}\int\left(-\alpha\dot{\alpha}^2 + \alpha k - \frac{8\pi}{3}\rho_0\right)dt = V\int\left(-\frac{3}{8\pi}\alpha\dot{\alpha}^2 + \frac{3}{8\pi}\alpha k - \rho_0\right)\frac{dt}{d\alpha}d\alpha =$$
$$= V\int\left(-\frac{3}{8\pi}\alpha\dot{\alpha}^2 + \frac{3}{8\pi}\alpha k - \rho_0\right)\dot{t}d\alpha = V\int\left(-\frac{3\alpha}{8\pi\,\dot{t}^2} + \frac{3}{8\pi}\alpha k - \rho_0\right)\dot{t}d\alpha \Rightarrow$$
$$\Rightarrow S_{total} = V\int\left(-\frac{3\alpha}{8\pi\,\dot{t}} + \frac{3}{8\pi}\alpha k\dot{t} - \rho_0\dot{t}\right)d\alpha \tag{2.48}$$

Accordingly, the new Lagrangian density is

$$\mathscr{L}_{total} = -\frac{3\alpha}{8\pi\,\dot{t}} + \frac{3}{8\pi}\alpha k\dot{t} - \rho_0\dot{t} \tag{2.49}$$

Allowing general variations with t_1 and t_2 free but fixing α_1 and α_2, we get the first order equation as follows

$$\frac{d}{d\alpha}\left(\frac{\partial\mathscr{L}_{total}}{\partial\dot{t}}\right) = \frac{d\mathscr{L}_{total}}{dt} \Rightarrow \frac{d}{d\alpha}\left(-\frac{3\alpha}{8\pi}\cdot\left(-\frac{1}{\dot{t}^2}\right) + \frac{3\alpha k}{8\pi} - \rho_0\right) = 0 \Rightarrow \frac{3\alpha}{8\pi\dot{t}^2} + \frac{3\alpha k}{8\pi} - \rho_0 = c(t) \xRightarrow[c(t)=0]{\dot{t}=\frac{1}{\dot{\alpha}}}$$
$$\Rightarrow \frac{3\alpha}{8\pi}\dot{\alpha}^2 + \frac{3\alpha k}{8\pi} - \rho_0 = 0 \Rightarrow \alpha\dot{\alpha}^2 + \alpha k - \frac{8\pi\rho_0}{3} = 0 \xRightarrow{:\alpha^3} \frac{\dot{\alpha}^2}{\alpha^2} = \frac{8\pi\rho_0}{3\alpha^3} - \frac{k}{\alpha^2} \xRightarrow{G=1} \frac{\dot{\alpha}^2}{\alpha^2} = \frac{8\pi G\rho_0}{3\alpha^3} - \frac{k}{\alpha^2} \tag{2.50}$$

This is equivalent to the first Friedmann equation, i.e Eq.(2.24) for $\rho = \rho_m$.

This particular method holds true only for matter for the case of Standard Cosmology. There is a similar way to derive the Friedmann equations following the same procedure as in Ref.[65]. Let us start from Eq.(2.29) and substituting the Ricci scalar we get

$$S = \int d^4x\sqrt{-g}\left[\frac{1}{2\kappa}R + \mathscr{L}_{matter}\right] = \int d^4\sqrt{-g}\left[-\frac{3}{\kappa}\left(\frac{\ddot{\alpha}}{\alpha} + \frac{\dot{\alpha}^2}{\alpha^2} + \frac{k}{\alpha}\right) + \mathscr{L}_{matter}\right] =$$
$$= \int d^4x\left[\alpha^3\left(-\frac{3}{\kappa}\right)\left(\frac{\ddot{\alpha}}{\alpha} + \frac{\dot{\alpha}^2}{\alpha^2} + \frac{k}{\alpha}\right) + \mathscr{L}_{matter}\sqrt{-g}\right] = \int d^4x\left[-\frac{3}{\kappa}\left(\ddot{\alpha}\alpha^2 + \dot{\alpha}^2\alpha + \alpha k\right) + \mathscr{L}_{matter}\sqrt{-g}\right]$$

However using the chain rule $\ddot{\alpha} = \frac{d}{dt}\dot{\alpha} = \frac{d\alpha}{dt}\frac{d}{d\alpha}\dot{\alpha}$, therefore varying the action with respect to α one can see

$$\delta_\alpha S = 0 \Rightarrow \int d^4x\Big[-\frac{3\alpha^2}{\kappa}\delta\left(\frac{d\alpha}{dt}\frac{d}{d\alpha}\dot{\alpha}\right) + \left(-\frac{3}{\kappa}\right)2\alpha\ddot{\alpha}\delta\alpha + \left(-\frac{3}{\kappa}\right)\alpha\delta\dot{\alpha}^2 + \left(-\frac{3}{\kappa}\right)\dot{\alpha}^2\delta\alpha + \left(-\frac{3}{\kappa}\right)k\delta\alpha +$$
$$+\frac{\delta\left(\sqrt{-g}\mathscr{L}_m\right)}{\delta\alpha}\delta\alpha\Big] = -\frac{3}{\kappa}\int d^4x\left(-2\alpha\dot{\alpha}\delta\dot{\alpha} + 2\ddot{\alpha}\alpha\delta\alpha + 2\alpha\dot{\alpha}\delta\dot{\alpha} + \dot{\alpha}^2\delta\alpha + k\delta\alpha\right) + \int d^4x\frac{\delta\left(\sqrt{-g}\mathscr{L}_m\right)}{\delta\alpha}\delta\alpha =$$
$$= -\frac{3}{\kappa}\int d^4x\left(2\ddot{\alpha}\alpha\delta\alpha + \dot{\alpha}^2\delta\alpha + k\delta\alpha\right) + \int d^4x\frac{\delta\left(\sqrt{-g}\mathscr{L}_m\right)}{\delta g^{\mu\nu}}\frac{\delta g^{\mu\nu}}{\delta\alpha}\delta\alpha = 0 \Rightarrow$$
$$\Rightarrow -\frac{3}{\kappa}\int d^4x\left(2\ddot{\alpha}\alpha\delta\alpha + \dot{\alpha}^2\delta\alpha + k\delta\alpha\right) + \int d^4x\frac{(-2)\delta\left(\sqrt{-g}\mathscr{L}_m\right)}{\sqrt{-g}\delta g^{\mu\nu}}\frac{\sqrt{-g}}{(-2)}\frac{\delta g^{\mu\nu}}{\delta\alpha}\delta\alpha = 0 \xRightarrow{Eq.(2.32)}$$
$$\Rightarrow -\frac{3}{\kappa}\int d^4x\left(2\ddot{\alpha}\alpha\delta\alpha + \dot{\alpha}^2\delta\alpha + k\delta\alpha\right) + \int d^4x(T_{ij}\delta^{ij})\delta\alpha = 0 \tag{2.51}$$

[6] We have assumed a pressure-less fluid in Eq.(2.41)

Hence from Eq.(2.51) we derive

$$-\frac{3}{\kappa}\left(2\ddot{\alpha}\alpha+\dot{\alpha}^2+k\right)+T_{ij}\delta^{ij}=0\Rightarrow-\frac{3}{\kappa}\left(2\ddot{\alpha}\alpha+\dot{\alpha}^2+k\right)-3p\alpha^2=0\Rightarrow$$
$$2\ddot{\alpha}\alpha+\dot{\alpha}^2+k=-\kappa p\alpha^2\Rightarrow 2\frac{\ddot{\alpha}}{\alpha}+\frac{\dot{\alpha}^2}{\alpha^2}=-\kappa p=-8\pi Gp \tag{2.52}$$

i.e Eq.(2.25). Now in order to obtain the *first Friedmann Equation* we will use a common technique starting by the original form of a flat Robertson-Walker metric

$$ds^2=N^2(t)dt-\alpha^2(t)\left[\frac{dr^2}{1-kr^2}+r^2(d\theta^2+sin^2\theta d\phi^2)\right] \tag{2.53}$$

and we only take the gauge $N(t)=1$ after the variation with respect to $N(t)$ has been performed. For this particular variation we will need the following relations

$$R=g^{\mu\nu}R_{\mu\nu}=g^{00}R_{00}+g^{ij}R_{ij}=\frac{1}{N^2(t)}R_{00}+g^{ij}R_{ij}\Rightarrow$$
$$\Rightarrow\frac{\delta R}{\delta N}=\frac{\delta}{\delta N}\left(\frac{1}{N^2(t)}R_{00}+g^{ij}R_{ij}\right)=-\frac{2}{N^3}R_{00}$$
$$\frac{\delta\left(\sqrt{-g}\mathscr{L}_m\right)}{\delta N}=\frac{-2\delta\left(\sqrt{-g}\mathscr{L}_m\right)}{\sqrt{-g}\delta g^{\mu\nu}}\frac{\delta g^{\mu\nu}}{\delta N}\frac{\sqrt{-g}}{(-2)}=T_{\mu\nu}\frac{\delta g^{\mu\nu}}{\delta N}\left(-\frac{\alpha^3N}{2}\right)=T_{00}\frac{\delta g^{00}}{\delta N}\left(-\frac{\alpha^3N}{2}\right)=\frac{\alpha^3\rho}{N^2}$$

Now we are ready to vary the action Eq.(2.29) with respect to $N(t)$

$$\delta S=0\Rightarrow\int d^4x\sqrt{-g}\left[\frac{R}{2\kappa}+\mathscr{L}_m\right]=0\Rightarrow\int d^4x\left[\frac{\alpha^3N}{2\kappa}R+\sqrt{-g}\mathscr{L}_m\right]=0\Rightarrow$$
$$\Rightarrow\int d^4x\left[\delta\left(\frac{\alpha^3N}{2\kappa}\right)R+\frac{\alpha^3N}{2\kappa}\frac{\delta R}{\delta N}\delta N+\frac{\delta\left(\sqrt{-g}\mathscr{L}_m\right)}{\delta N}\delta N\right]=0\Rightarrow$$
$$\Rightarrow\int d^4x\left(\frac{\alpha^3R}{2\kappa}+\frac{\alpha^3N}{2\kappa}\left(-\frac{2}{N^3}R_{00}\right)+\frac{\alpha^3\rho}{N^2}\right)\delta N=0\Rightarrow\frac{\alpha^3R}{2\kappa}+\frac{\alpha^3N}{2\kappa}\left(-\frac{2}{N^3}R_{00}\right)+\frac{\alpha^3\rho}{N^2}=0\Rightarrow$$
$$\Rightarrow R-\frac{2}{N^2}R_{00}+\frac{2\kappa\rho}{N^2}\overset{N=1}{\Longrightarrow}R-2R_{00}=-2\kappa\rho\Rightarrow-6\left(\frac{\ddot{\alpha}}{\alpha}+\frac{\dot{\alpha}^2}{\alpha^2}+\frac{k}{\alpha^2}\right)-2\left(-3\frac{\ddot{\alpha}}{\alpha}\right)=-2\kappa\rho\Rightarrow$$
$$\Rightarrow-6\frac{\dot{\alpha}^2}{\alpha^2}-6\frac{k}{\alpha^2}=-2\kappa\rho\Rightarrow3\frac{\dot{\alpha}^2}{\alpha^2}=\kappa\rho-3\frac{k}{\alpha^2}\Rightarrow\frac{\dot{\alpha}^2}{\alpha^2}=\frac{8\pi G}{3}\rho-\frac{k}{\alpha^2} \tag{2.54}$$

i.e Eq.(2.24)

In conclusion, in this section we used a very useful method, the one of the variational approach. We simplified things and we easily found the equations of motion. This method is particularly useful when we have even more complicated systems and actions than the one we studied such the actions in f(R) modified gravity cases or scalar tensor quintessence theories[66–69]

2.6 *Einstein's Static Universe*

In 1917 it was not even clear that galaxies outside our own Milky Way existed, let alone universal expansion. Therefore in that period the most obvious theory was that of a "static infinite" Universe. Nevertheless the Friedmann equations with matter or radiation do not have

static solution. A static universe implies that $\alpha(t) = constant \Rightarrow \dot{\alpha} = \ddot{\alpha} = 0$. However, a Universe dominated by matter or radiation satisfies Eq.(2.26)

$$\frac{\ddot{\alpha}}{\alpha} = -\frac{4\pi G}{3}(\rho + 3p)$$

Since the right hand side of Eq.(2.26) is not zero this excludes the static solution. This can be also understand intuitively, since normal matter has attractive gravity, so each fluid element will attract each other element, causing the Universe to decelerate. This can be seen clearly in the following figure, where we used the same procedure as the one that follows setting $\Lambda = 0$ [70]

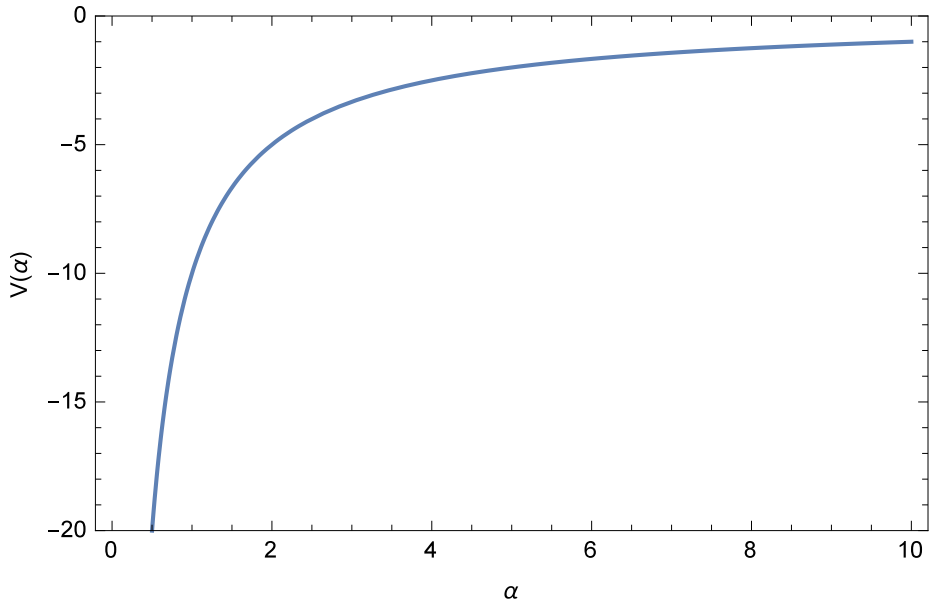

Figure 2.2: The "effective" potential $V(\alpha) = -\frac{A}{a}$, where $A = \frac{4\pi G}{3}\rho_0\alpha_0^3$, describing the expansion of the universe in the presence of matter or radiation. This particular equation for the potential was derived from Eq.(2.71) setting $\Lambda = 0$

Now the potential is everywhere negative as we can see from Fig.2.2, therefore the expansion can continue indefinitely. This is called the *Milne Universe*.

This was a real puzzle for Einstein who strongly believed that the Universe was static. Therefore he proposed, in 1917, the concept of the cosmological constant[71]. Einstein's Universe, also referred to as a "stationary" or "infinite" or "static infinite" Universe, is a cosmological model in which the universe is both spatially infinite and temporally infinite, and space is neither expanding nor contracting. In reality Einstein introduced in his field equations a constant Lorentz-invariant term, the cosmological constant Λ, which corresponds to a tiny correction to the geometry of the Universe. Hence Eq.(2.40), setting $c = 1$, became[58]

$$G_{\mu\nu} - \Lambda\, g_{\mu\nu} = R_{\mu\nu} - \frac{1}{2}g_{\mu\nu}R - \Lambda\, g_{\mu\nu} = 8\pi G\, T_{\mu\nu} \tag{2.55}$$

In contrast to the first two terms on the right-hand side, the $\Lambda\, g_{\mu\nu}$ term does not vanish in the limit of flat space-time. With this addition, Friedmann's equations take the form[5]

$$H^2 = \left(\frac{\dot{\alpha}}{\alpha}\right)^2 = \frac{8\pi G}{3}\rho + \frac{\Lambda}{3} - \frac{k}{\alpha^2} \tag{2.56}$$

$$\dot{H} + H^2 = \frac{\ddot{\alpha}}{\alpha} = -\frac{4\pi G}{3}(\rho + 3p) + \frac{\Lambda}{3} \tag{2.57}$$

Now let us discuss the deSitter expansion that we can derive from Eq.(2.56) and Eq.(2.57). In late times the cosmological constant term takes over. Therefore setting $\rho = 0$ in Eq.(2.56) we obtain the following equation

$$\frac{\dot{\alpha}}{\alpha} = \sqrt{\frac{\Lambda}{3}} - \frac{k}{\alpha^2} \xRightarrow{k=0} \frac{\dot{\alpha}}{\alpha} = \sqrt{\frac{\Lambda}{3}} \Rightarrow \frac{d\alpha}{dt}\frac{1}{\alpha} = \sqrt{\frac{\Lambda}{3}} \Rightarrow \alpha(t) \simeq e^{\sqrt{\frac{\Lambda}{3}}t} \tag{2.58}$$

For this scenario the Universe is expanding exponentially with time. This particular model is known as the *de Sitter* model.

Let us now return to the unstable Universe of Einstein. Einstein considered a closed Universe with cosmological constant, i.e. $k = 1$, and that the other component of the universe is matter, we derive that

$$\begin{aligned} \rho_{total} &= \rho_m \\ p_{total} &= p_m = w_m \rho_m \xRightarrow{w_m=0} p_{total} = 0 \end{aligned} \tag{2.59}$$

Now taking into consideration that $\rho = \rho_m = \frac{\rho_0}{\alpha^3}$, Eq.(2.56) and Eq.(2.57) take the final form

$$\begin{aligned} H^2 = \left(\frac{\dot{\alpha}}{\alpha}\right)^2 &= \frac{8\pi G}{3}\rho_m + \frac{\Lambda}{3} - \frac{1}{\alpha^2} = \frac{8\pi G}{3}\frac{\rho_0}{\alpha^3} + \frac{\Lambda}{3} - \frac{1}{\alpha^2} \\ \dot{H} + H^2 = \frac{\ddot{\alpha}}{\alpha} &= -\frac{4\pi G}{3}\frac{\rho_0}{\alpha^3} + \frac{\Lambda}{3} \end{aligned} \tag{2.60}$$

For a static universe we require $\dot{\alpha} = \ddot{\alpha} = 0$. Setting $\alpha = \alpha_c$ Eq.(2.60) can be written as

$$0 = -\frac{4\pi G}{3}\rho_m + \frac{\Lambda}{3} \Rightarrow \Lambda = 4\pi G \rho_m = 4\pi G \frac{\rho_0}{\alpha_c^3} \tag{2.61}$$

As we can see the cosmological constant is tuned to match exactly the matter density in this way.

As we have already proven the repulsion due to Λ balances the attraction of the matter. But what if the matter density is off by a tiny amount? (Equivalently we could ask, what if Λ is slightly bigger than half the matter density, or the universe is a bit bigger or smaller than its static solution?). It turns out that the solution is completely destroyed, leading to either runaway collapse driven by the matter, or runaway accelerated expansion driven by Λ.

To see this, let us consider a small perturbation of matter density around the static solution

$$\rho_m = \rho'_m(1 + \delta(t)), \quad \text{with} \quad \mid \delta \mid \ll 1 \tag{2.62}$$

In Eq.(2.62), $\rho' = \frac{\Lambda}{4\pi G}$ is the density of a static universe. We know from the fluid conservation equation that the matter density evolves as $\alpha(t)^{-3}$, and if we normalize the scale factor to $\alpha = 1$ in the static solution, we can write the conservation equation simply as

$$\rho_m = \rho'_m \cdot \alpha(t)^{-3} \tag{2.63}$$

Comparing Eq.(2.62) and Eq.(2.63) we can read of the density perturbation in terms of the scale factor as $\delta(t) = \alpha(t)^{-3} - 1$. Since δ is much smaller than unity then $\alpha(t)$ should also differ by a small amount

$$\alpha(t) = 1 + \epsilon(t) \tag{2.64}$$

Rewriting Eq.(2.57) in terms of ρ_m one can see that

$$\frac{\ddot{\alpha}}{\alpha} = -\frac{4\pi G}{3}\rho'_m \cdot \alpha(t)^{-3} + \frac{\Lambda}{3} = \frac{4\pi G \rho'_m}{3}\left(1 - \alpha(t)^3\right) \tag{2.65}$$

Plugging our perturbative expansion for $\alpha(t)$ into Eq.(2.65) all terms of $O(\epsilon^2)$ and higher, we find

$$\ddot{\alpha} = \ddot{\epsilon} = \frac{\Lambda}{3}\left(\alpha - \alpha^{-2}\right) \approx \frac{\Lambda}{3}\left(1 + \epsilon - (1 - 2\epsilon)\right) \approx \Lambda\epsilon \Rightarrow \ddot{\epsilon} \approx \Lambda\epsilon \tag{2.66}$$

Eq.(2.66) has exponentials as solutions, i.e

$$\epsilon = c_1 \cdot \epsilon^{\sqrt{\Lambda}t} + c_2 \cdot \epsilon^{-\sqrt{\Lambda}t} \tag{2.67}$$

From the above equation one can see that the growing mode will grow exponentially and, depending on the sign of c_1 (which in turn depends on the sign of the initial perturbation δ), either lead to runaway expansion or collapse to a Big Crunch. Regardless the solution this particular model leads clearly to an unstable universe.

Finally one could make an analogy concerning the *Einstein's universe* and classical mechanics and in particular this type of universe can be recast to look like a point particle on the surface of a sphere. Let us start with Eq.(2.57) which can be rewritten as

$$\frac{\ddot{\alpha}}{\alpha} = -\frac{4\pi G}{3}(\rho + 3p) + \frac{\Lambda}{3} \Rightarrow \ddot{\alpha} = -\frac{4\pi G}{3}\alpha(\rho + 3p) + \frac{\Lambda\,\alpha}{3} \tag{2.68}$$

Setting now $R \equiv \alpha \Rightarrow \ddot{R} \equiv \ddot{\alpha}$ as the radius, the previous equation takes the form

$$\begin{aligned}\ddot{R} = -\frac{4\pi G}{3}R(\rho + 3p) + \frac{\Lambda\,R}{3} \Rightarrow -\frac{4\pi G}{3}\frac{R^3}{R^2}(\rho + 3p) + \frac{\Lambda\,R}{3} \Rightarrow \\ \Rightarrow \ddot{R} = -\frac{G\,M}{R^2} + \frac{\Lambda}{3}R\end{aligned} \tag{2.69}$$

where $M = \frac{4\pi}{3}R^3(\rho+3p)$. From Eq.(2.69) we find that a particle on the sphere feels both attractive and repulsive forces. The repulsive force is $F_{rep} = \frac{\Lambda}{3}R$ if $\Lambda > 0$ is induced by the cosmological constant and increases with distance. Of course if $\Lambda < 0$ the force becomes attractive.

For our purpose it will be sufficient to note that the qualitative behaviour of the universe in the presence of a cosmological term which is either constant or time varying, can be understood very simply by rewriting Eq.(2.56) as follows

$$\begin{aligned}\left(\frac{\dot{\alpha}}{\alpha}\right)^2 = \frac{8\pi G}{3}\rho + \frac{\Lambda}{3} - \frac{k}{\alpha^2} \Rightarrow 3\left(\frac{\dot{\alpha}}{a}\right)^2 = 8\pi G\rho + \Lambda - \frac{3k}{\alpha^2} \Rightarrow 3\dot{\alpha}^2 = 8\pi G\alpha^2 + \Lambda\alpha^2 - 3k \Rightarrow \\ \Rightarrow \dot{\alpha}^2 = \frac{8\pi G\rho}{3}\alpha^2 + \frac{\Lambda}{3}\alpha^2 - k \overset{\times\frac{1}{2}}{\Longrightarrow} \frac{1}{2}\dot{\alpha}^2 = \frac{4\pi G\,\rho}{3} + \frac{\Lambda\,\alpha^2}{6} - \frac{k}{2} \Rightarrow \frac{1}{2}\dot{\alpha}^2 + V(\alpha) = E\end{aligned} \tag{2.70}$$

where $V(\alpha) = -\left(\frac{4\pi G}{3}\rho\alpha^2 + \frac{\Lambda\,\alpha^2}{6}\right)$ and $E = -\frac{k}{2}$. Assuming now that $\rho = \rho_{matter} = \rho_0\left(\frac{\alpha_0}{\alpha}\right)^{3(1+0)} = \rho_0\left(\frac{a_0}{a}\right)^3$ one can easily derive

$$V(\alpha) = -\frac{4\pi G}{3}\rho_0\frac{\alpha_0^3}{\alpha^{\cancel{3}}}\alpha^{\cancel{2}} - \frac{\Lambda\alpha^2}{6} = -\frac{4\pi G}{3}\cdot\frac{\rho_0\alpha_0^3}{\alpha} - \frac{\Lambda\alpha^2}{6} = -\left(\frac{A}{\alpha} + \frac{\Lambda\alpha^2}{6}\right) \tag{2.71}$$

where $A = \frac{4\pi G}{3}\rho_0\alpha_0^3$.

Eq.(2.70) can be seen as a classical motion with conserved energy E in a one dimensional potential $V(\alpha)$ whose generic form is shown in the figure below[70]

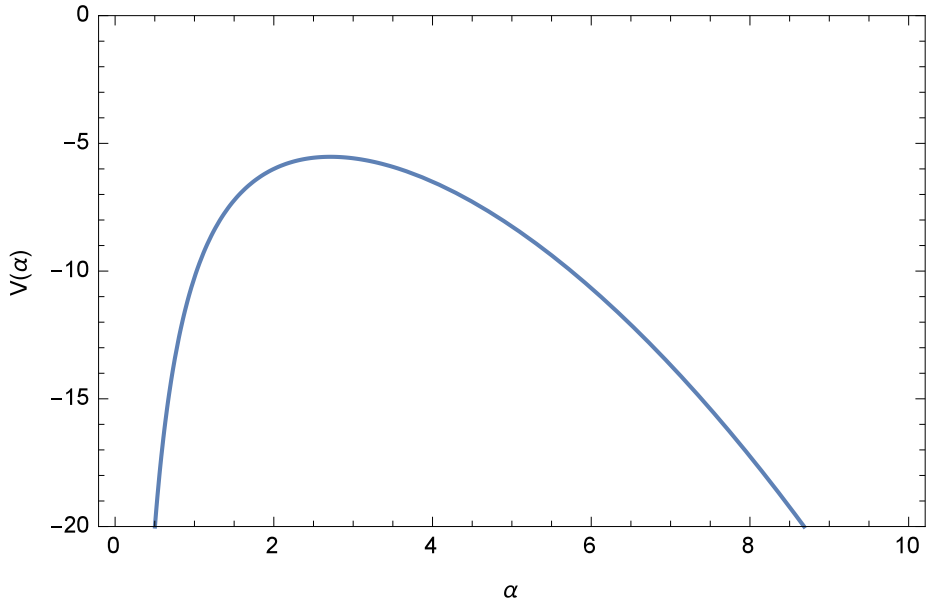

Figure 2.3: The "effective" potential $V(\alpha)$ describing the expansion of the universe in the presence of matter and a cosmological constant

Once again, from Fig.2.3, one can see clearly the instability of this particular model.

2.7 Cosmological Constant and the ΛCDM Model

Due to the instability of this particular model the cosmological constant was abandoned. The instability of the *Einstein's Universe* was also proven from Eddington in 1930, e.g see[72]. In accordance to these theoretical implications many observations indicated that the concept of a static Universe was incorrect. The biggest indication was the discovery of *Edwin Hubble* in 1929 when he discovered that all galaxies inside the Milky Way Galaxy are moving away from each other, implying an overall *expanding universe*[7]. From 1929 until the early 1990s, most cosmology researchers assumed the cosmological constant to be zero. This led Einstein to remark that *"the introduction of the cosmological term was the biggest blunder of my life"*.

Since the 1990s, several developments in observational cosmology[74, 75], especially the discovery of the accelerating universe from distant supernovae in 1998[76–78] (in addition to independent evidence from the cosmic microwave background and large galaxy redshift surveys [79]), have shown that a mere 4% is ordinary observable matter, such as atoms. Dark matter, on the other hand, accounts for an estimated 22%. In astronomy and cosmology, dark matter is hypothetical matter that does not interact with the electromagnetic force, but whose presence can be inferred from gravitational effects on visible matter. Dark matter is required to explain the stability of galaxies and the rate of formation of large-scale structures. The remaining 74% of the universe is filled with an *unknown component* called *dark energy*. Dark energy is however a

[7]Hubble discovered via observations that the velocity of the distant galaxies was proportional to each object's relative distance. This is known as Hubble's law and is given by[73]

$$\vec{u} = H_0 \, \vec{d}$$

wher u is is the vector of velocity of the receding object, d is is the vector of relative distance and H_0 is present value of the Hubble constant.

purely hypothetical concept, put in by hand so we can explain the observed accelerated expansion of the universe as it has never been detected in the laboratory. Determining the nature of dark energy is one of the most important problems in modern cosmology and particle physics.

Dark energy is a repulsive force that opposes the self-attraction of matter and causes the expansion of the universe to accelerate. While dark energy is poorly understood at a fundamental level, the main required properties of it are that it functions as a type of anti-gravity, it dilutes much more slowly than matter as the universe expands, and it clusters much more weakly than matter, or perhaps not at all. In order to shed light to this problem many models have been introduced through the years in order to explain the existence of this mysterious dark energy. The simplest candidate model is non other than the cosmological constant that has negative pressure, with its equation of state to be written $w = -1$. That leads to the current standard model of cosmology known as the ΛCDM model, which provides an excellent fit to many cosmological observations as of 2017. The background equations for the ΛCDM model are Eq.(2.55)-(2.57)

2.8 Challenges of the ΛCDM model

Although, the ΛCDM model provides an excellent fit to the cosmological data and has the additional advantage of simplicity due to a single free parameter it is somewhat problematic as it faces two major issues/problems[58]

- *The Cosmological Constant Problem*
- *The Cosmic Coincidence Problem*

2.8.1 *The Cosmological Constant Problem*

From the point of view of particle physics, the cosmological constant naturally arises as an energy density of the vacuum. Moreover, the energy scale of Λ should be much larger than that of the present Hubble constant H_0, if it originates from the vacuum energy density, as we have already discussed in the Introduction. This is the *Cosmological Constant Problem* and there have been a number of attempts to solve it.

If the cosmological constant originates from a vacuum energy density, then this suffers from a severe fine-tuning problem. Observationally we know that Λ is of order the present value of the Hubble parameter H_0, that is

$$\Lambda \approx {H_0}^2 = \left(100h\frac{km}{sec\,Mpc}\right)^2 = \left(100h\frac{3.24078\times10^{-20}\cancel{Mpc}}{sec\,\cancel{Mpc}}\right)^2 = \left(324.078h\times10^{-20}s^{-1}\right)^2 = \left(324.078\times10^{-20}\cdot6.58\times10^{-25}GeV\right)^2 = \left(2.13h\times10^{-42}GeV\right)^2 \tag{2.72}$$

where $h \approx 0.7$ is the dimensionless parameter for the Hubble constant. This corresponds to a critical density ρ_Λ

$$\frac{\Lambda}{3} = \frac{8\pi G}{3}\rho_\Lambda \Rightarrow \Lambda = 8\pi G\rho_\Lambda \Rightarrow \rho_\Lambda = \frac{\Lambda}{8\pi G} = \frac{\Lambda {m_{pl}}^2}{8\pi} = \frac{4.5369\cdot0.49\times10^{-84}\cdot1.4884\times10^{38}GeV^4}{8\pi} \Rightarrow \Rightarrow \rho_\Lambda = \frac{3.309}{8\pi}\times10^{-46}GeV^4 \approx 10^{-47}GeV^4 \tag{2.73}$$

Meanwhile the vacuum energy density evaluated by the sum of zero-point energies of quantum fields with mass m is given by[80]

$$\rho_{vac} = \frac{1}{2}\int_0^\infty \frac{d^3\vec{k}}{(2\pi)^3}\sqrt{k^2+m^2} = \frac{1}{4\pi^2}\int_0^\infty dk\,k^2\,\sqrt{k^2+m^2} \tag{2.74}$$

This exhibits an ultraviolet divergence $\rho_{vac} \propto k^4$. However we expect that quantum field theory is valid up to some cut-off scale k_{max} in which case the integral in Eq.(2.65) is finite[80]

$$\rho_{vac} \approx \frac{k_{max}^4}{16\pi^2} \tag{2.75}$$

For the extreme case of General Relativity we expect it to be valid to just below the Planck scale, where $m_{pl} = 1.22 \times 10^{19} GeV$. Hence if we pick up $k_{max} = m_{pl}$, we find that the vacuum energy density in this case is estimated as

$$\rho_{vac} \approx 10^{74} GeV^4 \tag{2.76}$$

Now comparing Eq.(2.73) and Eq.(2.76) one can see that ρ_{vac} is 10^{121} orders of magnitude larger than the observed value.

2.8.2 *The Cosmic Coincidence Problem*

If one accepts the implications of current observations then it seems that we live at a singularly remarkable point in the universe's history since the two energy components, ρ_m and ρ_Λ, which evolve completely differently and independently, are of the same order of magnitude. If dark energy is indeed a cosmological constant then the epoch when its energy density is the same order of magnitude as that of matter is a mere blip in the universe's lifetime. Thus a *fine tuning problem* has to be taken into account[8].

Since the missing energy density and the matter density decrease their ratio must be set to a specific, infinitesimal value in the very early universe in order for the two densities to nearly coincide today at different rates as the universe expands which may require anthropic principle arguments in order to be solved[81].

These particular problems led to a variety of alternative models that can provide a solution, in order to explain the nature of the Cosmological Constant. Perhaps the standard ΛCDM model is only a limiting case of a more complete, and less puzzling, cosmological model.

[8]The term *fine tuning* refers to circumstances when the parameters of the model must be adjusted very precisely in order to agree with observations. Theories requiring fine tuning are regarded as problematic in the absence of a known mechanism to explain why the parameters of the model happen to have precisely the needed values This is referred to the bibliography as the *Fine Tuning Problem*

Chapter 3

Dark Energy in General Relativity - Quintessence Models

The idea of modifying gravity on cosmological scales has really taken off over the past decade[82]. This has been triggered, in part, by theoretical developments involving higher dimensional theories, as well as new developments in constructing re-normalizable theories of gravity[83–86]. The effect of gravity on matter is tightly constrained to be mediated by interactions of the matter fields with a single rank-2 tensor field such as the metric $g_{\mu,\nu}$. The term "gravitational theory" can then be functionally defined by the set of field equations obeyed by the rank-2 tensor, and any other non-matter fields it interacts with. If these equations are anything other than Einstein's equations, then we consider it to be a "modified theory of gravity". This particular definition is independent of the action or the Lagrangian of the particular model.

In an effort to adress the *Cosmological Constant Problem* and the *Cosmic Coincidence Problem* many alternatives have been proposed. One of the possible solutions is that the role of dark energy can be played by a scalar field. Scalar fields are extremely important when it comes to modern physics. By being invariant under coordinate transformations, they are the simplest tensor fields, with a zero order. Hence it is reasonable to presume that dark energy may also be described by a scalar field, instead of using the cosmological constant.

In this particular category of models belongs the *quintessence models*[1][87–90]. A quintessence model is a scalar field minimally coupled to gravity. Let us present in this chapter this particular category of models.

3.1 Energy Momentum Tensor and Equation of State

The expansion history of the Universe can be summarized as follows: The Universe originated to a density singularity known as the *Big Bang*. Soon after that it entered a phase of accelerating expansion known as *inflation*. During inflation causally connected regions of the Universe exited out of the horizon, the Universe approached spatial flatness, monopoles were diluted and the first particles that gave rise to structure were created. At the end of inflation the Universe was initially dominated by radiation and afterward by matter, whose attractive gravitational properties induced a decelerating expansion. Despite that, recent cosmological observation [74, 75] that will be analysed in Section 5.1 indicate that the universe have entered a phase of accelerating expansion which have been attributed in dark energy.

[1]The ancient Greeks proposed Quintessence (quinta essentia) as the fifth element after air, earth, fire and water to describe a sublime perfect substance.

The obvious question to address is therefore "What are the properties of the additional component required to support this acceleration?". To address this issue we must consider the Friedmann equation that determines the evolution of the scale factor $a(t)$, i.e Eq.(2.26). Considering a Universe containing matter and dark energy, Eq.(2.26) can be written as[2]

$$\frac{\ddot{a}}{a} = -\frac{4\pi G}{3}\sum_i (\rho_i + 3p_i) = -\frac{4\pi G}{3}\left(\rho_m + 3\cancelto{0}{p_m} + \rho_X + 3p_X\right) = -\frac{4\pi G}{3}\left(\rho_m + \rho_X + 3p_X\right) \tag{3.1}$$

where ρ_X and p_X are the energy density and the pressure of the dark energy respectively. The only directly detected fluids in the universe are matter and the sub-dominant radiation. Both of these fluids are unable to cancel the minus sign on the right hand side of the Eq.(3.1) leading to decelerating expansion. Accelerating expansion in the context of GR can only be obtained by assuming the existence of an additional component, such as the dark energy $(\rho_X, p_X = w \cdot \rho_X)$, which could potentially change the minus sign, i.e a field which violates the strong energy condition $\rho + 3p \geq 0$(see [91]).

Rewriting Eq.(3.1) in terms of the dark energy equation of state parameter w as

$$\frac{\ddot{a}}{a} = -\frac{4\pi G}{3}\left[\rho_m + \rho_X\left(1 + 3w\right)\right] \tag{3.2}$$

It becomes clear from Eq.(3.2) that a $w < -\frac{1}{3}$ is required for accelerating expansion implying repulsive gravitational properties for dark energy. Let us, now, examine the quintessence field as a candidate for dark energy.

Quintessence fields are described by an ordinary scalar field minimally coupled to gravity and their Lagrangian density can be written as[92]

$$\mathscr{L} = \frac{1}{2}\dot{\phi}^2 - V(\phi) \tag{3.3}$$

The above Lagrangian Eq.(3.3) corresponds to the action

$$S = \int d^4x\sqrt{-g}\left(\frac{1}{2}g^{\mu\nu}\partial_\mu\phi\partial_\nu\phi - V(\phi)\right) \tag{3.4}$$

The variation of this action with respect to the inverse metric is zero, yielding

$$\delta S = \int d^4x\delta\sqrt{-g}\left(\frac{1}{2}g^{\mu\nu}\partial_\mu\phi\partial_\nu\phi - V(\phi)\right) + \int d^4x\sqrt{-g}\left(\frac{1}{2}\delta g^{\mu\nu}\partial_\mu\phi\partial_\nu\phi\right) \tag{3.5}$$

However, we have already proven that $\delta\sqrt{-g} = -\frac{1}{2}\sqrt{-g}g_{\mu\nu}\delta g^{\mu\nu}$, so Eq.(3.5) can be written as

$$0 = \delta S = \int d^4x\Big(-\frac{1}{2}\Big)\sqrt{-g}g_{\mu\nu}\delta g^{\mu\nu}\Big[\frac{1}{2}g^{\alpha\beta}\partial_\alpha\phi\partial_\beta\phi - V(\phi)\Big] + \int d^4x\sqrt{-g}\Big(\frac{1}{2}\delta g^{\mu\nu}\partial_\mu\phi\partial_\nu\phi\Big) \Rightarrow$$
$$\Rightarrow \int d^4x\sqrt{-g}\Big[-\frac{1}{2}g_{\mu\nu}\Big(\frac{1}{2}g^{\alpha\beta}\partial_\alpha\phi\partial_\beta\phi - V(\phi)\Big) + \frac{1}{2}\partial_\mu\phi\partial_\nu\phi\Big]\delta g^{\mu\nu} = 0$$

The term in brackets equals half of the energy-momentum tensor, which is therefore given by

$$T_{\mu\nu} = -g_{\mu\nu}\Big(\frac{1}{2}\partial_\alpha\phi\partial^\alpha\phi - V(\phi)\Big) + \partial_\mu\phi\partial_\nu\phi \tag{3.6}$$

[2]For simplicity we denoted the *scale factor* as a instead of $\alpha(t)$ for the rest of our work.

We have already mentioned that the cosmological principle implies homogeneity, so all spatial derivatives vanish in this cosmological model. For that reason the stress energy tensor takes the form

$$T_{\mu\nu} = \dot{\phi}^2 \delta^0_\mu \delta^0_\nu - g_{\mu\nu}\left(\frac{1}{2}\dot{\phi}^2 - V(\phi)\right) \tag{3.7}$$

Comparing it to the energy-momentum tensor of a perfect fluid, which is as we recall

$$T_{\mu\nu} = (\rho + p)u_\mu u_\nu + g_{\mu\nu} p$$

one can "read" the energy density as well as the pressure, which are given in this case, by

$$\begin{aligned} \rho &= T_{00} = \frac{1}{2}\dot{\phi}^2 + V(\phi) \\ p &= -g^{ii}T_{ii} = \frac{1}{2}\dot{\phi}^2 - V(\phi) \end{aligned} \tag{3.8}$$

Thus the corresponding equation of state parameter is[92]

$$w = \frac{p}{\rho} = \frac{\frac{1}{2}\dot{\phi}^2 - V(\phi)}{\frac{1}{2}\dot{\phi}^2 + V(\phi)} \tag{3.9}$$

A careful inspection of Eq.(3.9), leads to the possible range of w, i.e. $-1 \leq w \leq 1$. The state parameter presents a unique minimum $w = -1$ for $\dot{\phi} = 0$ and a unique maximum $w = 1$ for $V(\phi) = 0$. From Eq.(3.9) it is clear that it is impossible for w to cross the Phantom Divide Line $w = -1$, hereafter PDL, in a continuous manner. The reason for that is that for $w = -1$ a zero kinetic term $\dot{\phi}^2$ is required and the continuous transition from $w < -1$ to $w > -1$ (or vice versa) would require a change of sign of the kinetic term. The sign of this term however is fixed in quintessence models. This difficulty in crossing the PDL $w = -1$ could play an important role in identifying the correct model for dark energy.

3.2 Cosmological Equations of Quintessence

Now, considering a potential of the form $V(\phi) = -s\,\phi$ the equations of motion are[92]

$$\frac{\ddot{a}}{a} = -\frac{1}{3{M_p}^2}\left(\dot{\phi}^2 + s\phi\right) - \frac{\Omega_{0m}{H_0}^2}{2a^3} \text{ and} \tag{3.10}$$

$$\ddot{\phi} + 3\frac{\dot{a}}{a}\dot{\phi} - s = 0 \tag{3.11}$$

These equations can be easily derived from Eq.(2.26) and Eq.(2.27) using Eq.(3.8) as follows

$$\begin{aligned} \frac{\ddot{a}}{a} &= -\frac{4\pi G}{3}\left(\frac{1}{2}\dot{\phi}^2 + V(\phi) + \frac{3}{2}\dot{\phi}^2 - 3V(\phi)\right) - \frac{4\pi G}{3}\rho_m(t) \Rightarrow \\ \Rightarrow \frac{\ddot{a}}{a} &= -\frac{4\pi G}{3}\left(2\dot{\phi}^2 - 2V(\phi)\right) - \frac{4\pi G}{3}\frac{\rho_{0,m}}{a^3(t)} \Rightarrow \\ \Rightarrow \frac{\ddot{a}}{a} &= -\frac{8\pi G}{3}\left(\dot{\phi}^2 - V(\phi)\right) - \frac{4\pi G}{3a^3}\rho_{crit}\frac{\rho_{0,m}}{\rho_{crit}}. \end{aligned}$$

Substituting $\rho_{crit} = \dfrac{3H_0^2}{8\pi G}$ and $\Omega_{0,m} \equiv \dfrac{\rho_{0,m}}{\rho_{crit}}$ we end up with

$$\begin{aligned}
\frac{\ddot{a}}{a} &= -\frac{8\pi G}{3}\left(\dot{\phi}^2 - V(\phi)\right) - \frac{\Omega_{0,m}{H_0}^2}{2a^3} \Rightarrow \\
\Rightarrow \frac{\ddot{a}}{a} &= -\frac{8\pi G}{3}\left(\dot{\phi}^2 + s\phi\right) - \frac{\Omega_{0,m}{H_0}^2}{2a^3} \Rightarrow \\
\Rightarrow \frac{\ddot{a}}{a} &= -\frac{1}{3M_p^2}\left(\dot{\phi}^2 + s\phi\right) - \frac{\Omega_{0,m}{H_0}^2}{2a^3}
\end{aligned} \tag{3.12}$$

where $M_p = (8\pi G)^{-1/2}$ is the Planck mass. Similarly for the ϕ field we derive

$$\begin{aligned}
\dot{\rho} + 3\frac{\dot{a}}{a}(\rho + p) = 0 \Rightarrow \frac{d}{dt}\left(\frac{1}{2}\dot{\phi}^2 + V(\phi)\right) + 3\frac{\dot{a}}{a}\left(\frac{1}{2}\dot{\phi}^2 + V(\phi) + \frac{1}{2}\dot{\phi}^2 - V(\phi)\right) = 0 \Rightarrow \\
\Rightarrow \ddot{\phi}\,\dot{\phi} + \frac{dV}{d\phi}\frac{d\phi}{dt} + 3\frac{\dot{a}}{a}\dot{\phi}^2 = 0 \overset{:\dot{\phi}}{\Rightarrow} \ddot{\phi} + 3\frac{\dot{a}}{a}\dot{\phi} - s = 0
\end{aligned} \tag{3.13}$$

Afterwards, we will make another rescaling (in order to be consistent with the Ref.[92]) by setting

$$\begin{aligned}
H_0 t \to t \Rightarrow H_0 = 1 \\
\frac{\phi}{\sqrt{3}M_p} \to \phi \\
\frac{s}{\sqrt{3}M_p{H_0}^2} \to s
\end{aligned} \tag{3.14}$$

Taking the derivative of Eq.(3.14) we derive $\frac{\dot{\phi}}{\sqrt{3}M_p} \to \dot{\phi} \Rightarrow \frac{1}{3{M_p}^2}\dot{\phi}^2 \to \dot{\phi}^2$. Hence Eq.(3.12) can be written as[92]

$$\begin{aligned}
\frac{\ddot{a}}{a} = -\frac{1}{3{M_p}^2}\dot{\phi}^2 - \frac{s}{3{M_p}^2}\phi - \frac{\Omega_{0m}}{2a^3} = -\frac{1}{3{M_p}^2}\dot{\phi}^2 - \frac{s}{\sqrt{3}M_p{\bar{H}_0}^2}\frac{1}{\sqrt{3}M_p}\phi - \frac{\Omega_{0m}}{2a^3} \overset{(3.14)}{\Longrightarrow} \\
\overset{(3.14)}{\Longrightarrow} \frac{\ddot{a}}{a} = -\dot{\phi}^2 - s\phi - \frac{\Omega_{0m}}{2a^3} \Rightarrow \frac{\ddot{a}}{a} = -\left(\dot{\phi}^2 + s\phi\right) - \frac{\Omega_{0m}}{2a^3}
\end{aligned} \tag{3.15}$$

Of course the scalar field equation Eq.(3.13) remains unchanged. It has to be mentioned that the equations of motion can be derived following the aforementioned methods presented in Chapter 2 considering an appropriate action[2, 89, 90]

Chapter 4

Modified Gravity - Scalar Tensor Quintessence Models

According to the information presented in the previous chapters, many theories have been proposed to solve the problems of the ΛCDM model. In this category as we mentioned is the *quintessence models*, which theoretical background was presented in Chapter 3. Even though the *quintessence* field has dynamical evolution and thus can solve coincidence problem[81], the origin of the scalar field remains a problem. To overcome this problem scalar tensor quintessence models have been proposed, which have the additional advantage of providing a potential solution to the origin problem as the physical origin of the scalar field is the dynamical "Newtons constant". The model that we will study in this chapter is a general scalar tensor quintessence field[93–95].

4.1 Dynamical Cosmological Equations in Scalar Tensor Quintessence

Let us start with the most general action involving gravity nonminimally coupled with one scalar field in four dimensions, which has the form[69, 94]

$$S = \int d^4x\sqrt{-g}\left[\frac{F(\phi)}{2}R - \frac{1}{2}g^{\mu\nu}\partial_\mu\phi\partial_\nu\phi - V(\phi)\right] + S_m \tag{4.1}$$

where S_m is the action related to the Lagrangian $\mathscr{L}[\psi_m; g_{\mu\nu}]$ of the matter source.

As we mentioned earlier, there are two basic methods in order to derive the equations of motion from a given action. Once again, in this section, we will prove the dynamical equation, i.e. the equations of motion using both methods.

4.1.1 First Method: Variation of the Action with General Metric

Let us start by varying the action. In order to calculate the dynamical equations we will use the identities that we have already proven in Appendix A

$$\delta R = R_{\mu\nu}\delta g^{\mu\nu} + \nabla_\sigma\left(g^{\mu\nu}\delta\Gamma^\sigma_{\mu\nu} - g^{\mu\sigma}\delta\Gamma^\rho_{\rho\mu}\right) \tag{4.2}$$

$$\delta\sqrt{-g} = -\frac{1}{2}\sqrt{-g}g_{\mu\nu}\delta g^{\mu\nu} \tag{4.3}$$

Next, it is straightforward to prove that[1]

$$g^{\mu\nu}\delta\Gamma^\sigma_{\mu\nu} = -\nabla_a\delta g^{a\sigma} + \frac{1}{2}g_{a\beta}\nabla^\sigma\delta g^{a\beta} \tag{4.4}$$

[1]For the analytical proof of these equations see Appendix B

and

$$g^{\mu\sigma}\delta\Gamma^{\lambda}_{\lambda\mu} = -\frac{1}{2}g_{a\beta}\nabla^{\sigma}\delta g^{a\beta} \tag{4.5}$$

which implies that

$$\delta R = R_{\mu\nu}\delta g^{\mu\nu} - \nabla_{\sigma}\nabla_{a}\delta g^{a\sigma} + g_{a\beta}\nabla_{\sigma}\nabla^{\sigma}\delta g^{a\beta} = R_{\mu\nu}\delta g^{\mu\nu} - \nabla_{\mu}\nabla_{\nu}\delta g^{\mu\nu} + g_{\mu\nu}\nabla_{\sigma}\nabla^{\sigma}\delta g^{\mu\nu} \tag{4.6}$$

Returning to the variation of the action with respect to the inverse metric and using Eq.(4.2)-(4.6), one can see that

$$\begin{aligned}
\delta S = 0 \Rightarrow \int d^4x\, \delta\sqrt{-g}\left[\frac{F(\phi)}{2}R - \frac{1}{2}g^{\mu\nu}\partial_{\mu}\phi\partial_{\nu}\phi - V(\phi)\right] + \delta S_{matter} + \\
+ \int d^4x\sqrt{-g}\left[F(\phi)\delta R - \frac{1}{2}\,\delta g^{\mu\nu}\partial_{\mu}\phi\partial_{\nu}\phi\right] = 0 \Rightarrow \\
\Rightarrow \int d^4x\,\sqrt{-g}\Big[-\frac{1}{2}g_{\mu\nu}\left(\frac{F(\phi)}{2}R - \frac{1}{2}g^{a\beta}\partial_{a}\phi\partial_{\beta}\phi - V(\phi)\right) + \frac{\delta S_m}{\sqrt{-g}\delta g^{\mu\nu}} + \frac{F(\phi)}{2}R_{\mu\nu} - \nabla_{\mu}\nabla_{\nu}\frac{F(\phi)}{2} + \\
+ g_{\mu\nu}\nabla_{\sigma}\nabla^{\sigma}\frac{F(\phi)}{2} - \frac{1}{2}\partial_{\mu}\phi\partial_{\nu}\phi\Big]\delta g^{\mu\nu} = 0 \Rightarrow -\frac{F(\phi)}{2}\frac{g_{\mu\nu}}{2}R + \frac{1}{4}g_{\mu\nu}g^{a\beta}\partial_{a}\phi\partial_{\beta}\phi + \frac{V(\phi)}{2}g_{\mu\nu} - \\
-\frac{T^{matter}_{\mu\nu}}{2} + \frac{F(\phi)}{2}R_{\mu\nu} - \nabla_{\mu}\nabla_{\nu}\frac{F(\phi)}{2} + g_{\mu\nu}\nabla_{\sigma}\nabla^{\sigma}\frac{F(\phi)}{2} - \frac{1}{2}\partial_{\mu}\phi\partial_{\nu}\phi = 0 \xRightarrow{\times\frac{2}{F(\phi)}} R_{\mu\nu} - \frac{1}{2}g_{\mu\nu}R + \\
+\frac{1}{2F(\phi)}g_{\mu\nu}g^{a\beta}\partial_{a}\phi\partial_{\beta}\phi + \frac{V(\phi)}{F(\phi)}g_{\mu\nu} - \frac{T^{matter}_{\mu\nu}}{F(\phi)} - \frac{1}{F(\phi)}\nabla_{\mu}\nabla_{\nu}F(\phi) + \frac{g_{\mu\nu}}{F(\phi)}\nabla_{\sigma}\nabla^{\sigma}F(\phi) - \frac{1}{F(\phi)}\partial_{\mu}\phi\partial_{\nu}\phi = 0 \\
\Rightarrow F(\phi)G_{\mu\nu} = T^{matter}_{\mu\nu} + \nabla_{\mu}\nabla_{\nu}F(\phi) + \partial_{\mu}\phi\partial_{\nu}\phi - \frac{1}{2}g_{\mu\nu}g^{a\beta}\partial_{a}\phi\partial_{\beta}\phi - V(\phi)g_{\mu\nu} - g_{\mu\nu}\nabla_{\sigma}\nabla^{\sigma}F(\phi)
\end{aligned} \tag{4.7}$$

where $G_{\mu\nu} = R_{\mu\nu} - \frac{1}{2}Rg_{\mu\nu}$ is the Einstein tensor. Eq.(4.7) represents the generalised Einstein's equations for the case of modified gravity.

An alternative form for Eq.(4.7) is

$$G_{\mu\nu} = \frac{1}{F(\phi)}(T^{matter}_{\mu\nu} + T^{(\phi)}_{\mu\nu}) = \frac{1}{F(\phi)}T^{total}_{\mu\nu} \tag{4.8}$$

where $T^{(\phi)}_{\mu\nu} = \nabla_{\mu}\nabla_{\nu}F(\phi) + \partial_{\mu}\phi\partial_{\nu}\phi - \frac{1}{2}g_{\mu\nu}g^{a\beta}\partial_{a}\phi\partial_{\beta}\phi - V(\phi)g_{\mu\nu} - g_{\mu\nu}\nabla_{\sigma}\nabla^{\sigma}F(\phi)$. The term $\dfrac{1}{F(\phi)}$ is playing the role of the effective gravitational constant $8\pi G_{eff}$ in this theory. If we look more carefully, the "new Newton's constant" presents dynamics which can solve the physical origin of the scalar field problem. Here, the tensor $T^{(m)}_{\mu\nu}$ is the standard perfect fluid matter source (we consider the matter fluid presurreless) and $T^{(\phi)}_{\mu\nu}$ is the energy-momentum tensor relative to the scalar field. Hence we can see clearly once more that in our model the universe consists of matter and a scalar field which plays the role of dark energy.

As we have proven in Eq.(4.8) the term $\dfrac{1}{F(\phi)}$ is playing the role of the effective gravitational constant $8\pi G_{eff}$ in this theory. However this particular equation hold true only for this kind of scalar tensor quintessence models. In scalar-tensor theories, in general, the effective Newton's constant with respect to the redshift z is given by[47, 96]

$$G_{eff} = \frac{1}{F(\phi)}\left(\frac{2F + 4\left(\frac{dF}{d\phi}\right)^2}{2F + 3\left(\frac{dF}{d\phi}\right)^2}\right)$$

After some manipulation we obtain the final result

$$G_{eff} = \frac{1}{F(\phi)} \frac{F(\phi) + 2\left(\frac{dF}{d\phi}\right)^2}{F(\phi) + \frac{3}{2}\left(\frac{dF}{d\phi}\right)^2} \propto \frac{1}{F(\phi)} \tag{4.9}$$

The approximation in the above equation is for consistency with solar system tests, which indicate that $\frac{dF}{d\phi} \sim \frac{dF}{dz} \sim 0$(see [97, 98]) and holds true only for low redshifts.

Now, in order to produce the first dynamical equation, we consider the (00) component of Eq.(4.7). Fixing the homogenous and isotropic FRW metric and using the metric tensor notation $g_{\mu\nu} = (-,+,+,+)$[2] with calculations similar to those of Chapter 2 we derive that $R_{00} = -3\frac{\ddot{a}}{a}$ and $R = 6\left(\frac{\ddot{a}}{a} + \frac{\dot{a}^2}{a^2}\right)$. Thus Eq.(4.7) for the (00) component can be written as

$$\left(R_{00} - \frac{1}{2}g_{00}R\right)F(\phi) = T_{00}^{matter} + \nabla_0\nabla_0 F(\phi) + \partial_0\phi\partial_0\phi - \frac{1}{2}g_{00}g^{00}\partial_0\phi\partial_0\phi - V(\phi)g_{00} - g_{00}\Box F(\phi) \tag{4.10}$$

where $\Box = \nabla_\sigma\nabla^\sigma$ is the d'Alembertian operator. Let us now calculate the Left-Hand Side(LHS) and Right-Hand Side(RHS) of Eq.(4.10) separately

$$LHS = F(\phi)\left[-3\frac{\ddot{a}}{a} + 3\left(\frac{\ddot{a}}{a} + \frac{\dot{a}^2}{a^2}\right)\right] = 3F(\phi)\frac{\dot{a}^2}{a^2}$$
$$RHS = \rho_m - 3\frac{\dot{a}}{a}\dot{F} + \dot{\phi}^2 - \frac{1}{2}\dot{\phi}^2 + V(\phi)$$

Hence demanding LHS=RHS we derive[69, 94]

$$3F(\phi)H^2 = \rho_m + \frac{\dot{\phi}^2}{2} + V(\phi) - 3H\dot{F} \tag{4.11}$$

where $H = \frac{\dot{a}}{a}$.

Accordingly, for the (11) component we obtain (we study again the LHS and RHS of Eq.(4.10) setting $\mu = \nu = 1$)

$$LHS = F(\phi)\left[R_{11} - \frac{1}{2}g_{11}R\right] = F(\phi)\left[a\ddot{a} + 2\dot{a}^2 - \frac{1}{2}(a^2)R\right] =$$
$$= F(\phi)\left[a\ddot{a} - 3\ddot{a}a + 2\dot{a}^2 - 3\dot{a}^2\right] = F(\phi)\left[-2a\ddot{a} - \dot{a}^2\right]$$
$$RHS = \cancelto{0}{T_{11}^m} + \nabla_1\nabla_1 F(\phi) + \cancelto{0}{\partial_1\phi\partial_1\phi} - \frac{1}{2}g_{11}g^{00}\partial_0\phi\partial_0\phi - V(\phi)g_{11} - g_{11}\nabla_\sigma\nabla^\sigma F(\phi) =$$
$$= -\partial_\kappa F(\phi)\Gamma_{11}^\kappa + \frac{1}{2}a^2\dot{\phi}^2 - a^2V(\phi) - g_{11}\left(\partial_\sigma\partial^\sigma + \Gamma_{\sigma\lambda}^\sigma\partial^\lambda\right)F(\phi) =$$
$$= -\dot{F}\Gamma_{11}^0 + \frac{a^2}{2}\dot{\phi}^2 - a^2V(\phi) - g_{11}g^{00}\partial_0\partial_0 F(\phi) - 3g_{11}\frac{\dot{a}}{a}\partial^0 F(\phi) =$$
$$= -\dot{F}a\dot{a} + \frac{a^2}{2}\dot{\phi}^2 - a^2V(\phi) + a^2\ddot{F} + 3a^{\cancel{2}}\frac{\dot{a}}{\cancel{a}}\dot{F} =$$
$$= 2\dot{F}a\dot{a} + \frac{a^2}{2}\dot{\phi}^2 - a^2V(\phi) + a^2\ddot{F}$$

[2]This notation is adopted for the rest of this thesis

Hence demanding LHS=RHS we see that

$$F(\phi)\left[-2\ddot{a}a-\dot{a}^2\right]=2\dot{F}a\dot{a}+\frac{a^2}{2}\dot{\phi}^2-a^2V(\phi)+a^2\ddot{F}\overset{:a^2}{\Longrightarrow}F(\phi)\left[-2\frac{\ddot{a}}{a}-\frac{\dot{a}^2}{a^2}\right]=2\dot{F}\frac{\dot{a}}{a}+\frac{\dot{\phi}^2}{2}-V(\phi)+\ddot{F} \tag{4.12}$$

However, Eq.(4.11) imposes that

$$-V=\rho_m+\frac{\dot{\phi}^2}{2}-3F\frac{\dot{a}^2}{a^2}-3\frac{\dot{a}}{a}\dot{F} \tag{4.13}$$

Consequently, substituting Eq.(4.13) to Eq.(4.12) one can derive[69, 94]

$$\begin{aligned}-2F\frac{\ddot{a}}{a}-F\frac{\dot{a}^2}{a^2}&=2\dot{F}\frac{\dot{a}}{a}+\frac{1}{2}\dot{\phi}^2+\rho_m+\frac{\dot{\phi}^2}{2}-3F\frac{\dot{a}^2}{a^2}-3\frac{\dot{a}}{a}\dot{F}+\ddot{F}\\ -2F(\phi)\left(\frac{\ddot{a}}{a}-\frac{\dot{a}^2}{a^2}\right)&=\rho_m+\dot{\phi}^2+\ddot{F}-H\dot{F}\end{aligned} \tag{4.14}$$

Finally, we will vary the action with respect to the ϕ field, in order to derive the Klein-Gordon equation for the case of the modified gravity. Once again the action principle tells us that the variation of this action with respect to the ϕ field is zero

$$\begin{aligned}\delta S=0\Rightarrow\int d^4x\sqrt{-g}\left[\frac{R}{2}\delta F(\phi)-\delta V(\phi)-\frac{1}{2}\delta\left(g^{\mu\nu}\nabla_\mu\phi\nabla_\nu\phi\right)\right]&=0\\ \Rightarrow\int d^4x\sqrt{-g}\left[\frac{R}{2}\delta F(\phi)-\delta V(\phi)+\frac{\cancel{2}}{\cancel{2}}g^{\mu\nu}\nabla_\mu\nabla_\nu\phi\delta\phi\right]&=0\\ \Rightarrow\int d^4x\sqrt{-g}\left[\frac{R}{2}\frac{dF(\phi)}{d\phi}-\frac{dV(\phi)}{d\phi}+\nabla_\mu\nabla^\mu\phi\right]d\phi=0\Rightarrow\frac{R}{2}F_\phi-V_\phi+\nabla_\mu\nabla^\mu\phi&=0\Rightarrow\\ \Rightarrow-\nabla_\mu\nabla^\mu\phi+V_\phi=\frac{F_\phi}{2}R\Rightarrow\ddot{\phi}+3\frac{\dot{a}}{a}\dot{\phi}+V_\phi&=F_\phi\frac{R}{2}\end{aligned} \tag{4.15}$$

and substituting the Ricci scalar $R=6\left(\frac{\ddot{a}}{a}+\frac{\dot{a}^2}{a^2}\right)$ in Eq.(4.15) we obtain[69, 94]

$$\begin{aligned}\ddot{\phi}+3\frac{\dot{a}}{a}\dot{\phi}+V_\phi&=\frac{6}{2}\left(\frac{\ddot{a}}{a}+\frac{\dot{a}^2}{a^2}\right)F_\phi\Rightarrow\\ \ddot{\phi}+3\frac{\dot{a}}{a}\dot{\phi}-3\left(\frac{\ddot{a}}{a}+\frac{\dot{a}^2}{a^2}\right)F_\phi+V_\phi&=0\end{aligned} \tag{4.16}$$

4.1.2 Second Method: Variation of the action with FRW metric

In this section we will use an alternative way[62, 63] to derive Eq.(4.11), Eq.(4.14) and Eq.(4.16), i.e. the equations of motion. That is the Lagrangian method. Let us assume, as before, that the spacetime manifold is described by a flat FRW metric, that is homogenous and isotropic. Also we preserve the same notation as before, i.e. $g_{\mu\nu}=(-,+,+,+)$ and $R=6\left(\frac{\ddot{a}}{a}+\frac{\dot{a}^2}{a^2}\right)$. As a result the general action is written

$$\begin{aligned}S&=\int d^4x\sqrt{-g}\left[\frac{F(\phi)}{2}6\left(\frac{\ddot{a}}{a}+\frac{\dot{a}^2}{a^2}\right)-\frac{1}{2}(-1)\dot{\phi}^2-V(\phi)+\mathscr{L}_m\right]=\\ &=\int d^4x\sqrt{-g}\left[3F(\phi)\frac{\ddot{a}}{a}+3F(\phi)\frac{\dot{a}^2}{a^2}+\frac{\dot{\phi}^2}{2}-V(\phi)+\mathscr{L}_m\right]=\\ &=\int d^3xdt\sqrt{-g}\left[3F(\phi)\frac{\ddot{a}}{a}+3F(\phi)\frac{\dot{a}^2}{a^2}+\frac{\dot{\phi}^2}{2}-V(\phi)+\mathscr{L}_m\right]\end{aligned}$$

Using, now, the "transformation" of derivatives for $\ddot{a}$ one can obtain that $\ddot{a} = \frac{d}{dt}\dot{a} = \frac{d}{d\phi}\frac{d\phi}{dt}\dot{a} = \frac{d}{d\phi}\left(\dot{a}\dot{\phi}\right)$. Thus the action of modified gravity can be written as

$$S = \int d^3x dt\sqrt{-g}\frac{3F(\phi)}{a}\frac{d}{d\phi}\left(\dot{a}\dot{\phi}\right) + \int d^3x dt\sqrt{-g}\left[3F(\phi)\frac{\dot{a}^2}{a^2} + \frac{\dot{\phi}^2}{2} - V(\phi) + \mathscr{L}_m\right]$$

$$= \cancelto{0}{\frac{3\sqrt{-g}F(\phi)}{a}\dot{a}\dot{\phi}\Big|_{-\infty}^{\infty}} - \int d^3x\, dt\, \dot{a}\,\dot{\phi}\frac{d}{d\phi}\left(\frac{3F(\phi)\sqrt{-g}}{a}\right) + \int d^3x\, dt\,\sqrt{-g}\left[3F(\phi)\frac{\dot{a}^2}{a^2} + \frac{\dot{\phi}^2}{2} - V(\phi) + \mathscr{L}_m\right] =$$

$$= -\int d^3x\, dt\, \dot{a}\,\cancel{\dot{\phi}}\frac{d}{dt}\frac{\cancel{dt}}{\cancel{d\phi}}\left(\frac{3F(\phi)\sqrt{-g}}{a}\right) + \int d^3x\, dt\sqrt{-g}\left[3F(\phi)\frac{\dot{a}^2}{a^2} + \frac{\dot{\phi}^2}{2} - V(\phi) + \mathscr{L}_m\right] =$$

$$= -\int d^3x\, dt\, 3\dot{a}\left[\frac{\sqrt{-g}}{a}\dot{F} + F\frac{d}{dt}\left(\frac{\sqrt{-g}}{a}\right)\right] + \int d^3x\, dt\,\sqrt{-g}\left[3F(\phi)\frac{\dot{a}^2}{a^2} + \frac{\dot{\phi}^2}{2} - V(\phi) + \mathscr{L}_m\right] =$$

$$= -\int d^3x\, dt\, 3\dot{a}\left[\frac{\sqrt{-g}}{a}\dot{F} + F\frac{d}{dt}a^2\right] + \int d^3x\, dt\,\sqrt{-g}\left[3F(\phi)\frac{\dot{a}^2}{a^2} + \frac{\dot{\phi}^2}{2} - V(\phi) + \mathscr{L}_m\right] =$$

$$= -\int d^3x\, dt\, 3\dot{a}\left[\frac{\sqrt{-g}}{a}\dot{F} + 2Fa\dot{a}\right] + \int d^3x\, dt\,\sqrt{-g}\left[3F(\phi)\frac{\dot{a}^2}{a^2} + \frac{\dot{\phi}^2}{2} - V(\phi) + \mathscr{L}_m\right] =$$

$$= \int d^3x\, dt\, a^3\left[-6\frac{\dot{a}^2}{a^3}aF - 3\dot{F}\frac{\dot{a}}{a} + 3F(\phi)\frac{\dot{a}^2}{a^2} + \frac{\dot{\phi}^2}{2} - V(\phi) + \mathscr{L}_m\right]$$

$$= \int d^3x\, dt\sqrt{-g}\left[-3\frac{\dot{a}^2}{a^2}F(\phi) - 3\frac{\dot{a}}{a}\dot{F} + \frac{\dot{\phi}^2}{2} - V(\phi) + \mathscr{L}_m\right] \tag{4.17}$$

Considering that the action is typically represented an integral over time, $S = \int dt\mathscr{L}$, where $\mathscr{L}$ is the Lagrangian density we deduce that

$$\mathscr{L}_{total} = \sqrt{-g}\left[-3\frac{\dot{a}^2}{a^2}F(\phi) - 3\frac{\dot{a}}{a}\dot{F} + \frac{\dot{\phi}^2}{2} - V(\phi)\right] + \mathscr{L}_m$$

where the standard matter contribution acts essentially as a density term, i.e. $\mathscr{L}_m = -\sqrt{-g}\rho_m$. Here we have to mention that during our calculation we considered a homogenous spacetime, therefore neglecting the volume. Also that $\sqrt{-g} = a^3$. Consequently the final Lagrangian takes the form

$$\mathscr{L}_{total} = a^3\left[-3\frac{\dot{a}^2}{a^2}F(\phi) - 3\frac{\dot{a}}{a}\dot{F} + \frac{\dot{\phi}^2}{2} - V(\phi) - \rho_m\right] \tag{4.18}$$

Eq.(4.18) can be seen as a "point-like" Lagrangian on the configuration space (a,ϕ). For this reason, we can solve the problem as an exercise of classical mechanics calculating the "*Euler-Lagrange*" equations. Let us remind that the energy function relative to $\mathscr{L}$ is given by

$$\mathscr{E}_t = \frac{\partial\mathscr{L}}{\partial\dot{a}}\,\dot{a} + \frac{\partial\mathscr{L}}{\partial\dot{\phi}}\,\dot{\phi} - \mathscr{L} \tag{4.19}$$

Now, we will express our Lagrangian density as follows

$$\mathscr{L}_{total} = \sqrt{-g}\left[-3\frac{\dot{a}^2}{a^2}F(\phi) - 3\frac{\dot{a}}{a}\dot{F} + \frac{\dot{\phi}^2}{2} - V(\phi) - \rho_m\right] = a^3\left[-3\frac{\dot{a}^2}{a^2}F(\phi) - 3\frac{\dot{a}}{a}\dot{F} + \frac{\dot{\phi}^2}{2} - V(\phi) - \rho_m\right] =$$
$$= -3F(\phi)\dot{a}^2 a - 3\dot{a}a^2\dot{F} + a^3\left(\frac{\dot{\phi}^2}{2} - V(\phi) - \rho_m\right)$$

From the above equation we observe that $\mathscr{L}$ has no explicit time dependence, therefore the energy function relative to $\mathscr{L}$ is conserved. From the equations of motion one can deduce that this constant plays the role of the curvature. However we have assumed a flat Universe, therefore this constant should be equal to zero. It is straightforward, then, to obtain Eq.(4.11), as follows

$$\mathscr{E}_t = 0 \Rightarrow \frac{\partial\mathscr{L}}{\partial\dot{a}}\dot{a} + \frac{\partial\mathscr{L}}{\partial\dot{\phi}}\dot{\phi} - \mathscr{L} = 0 \Rightarrow$$
$$\Rightarrow \left(-3\dot{F}a^2 - 6F\dot{a}a\right)\dot{a} + \left(-3a^2\dot{a}F_\phi + a^3\dot{\phi}\right)\dot{\phi} + 3F(\phi)\dot{a}^2 a + 3\dot{a}a^2\dot{F} - a^3\left(\frac{\dot{\phi}^2}{2} - V(\phi) - \rho_m\right) = 0 \Rightarrow$$
$$\Rightarrow -3\dot{F}a^2\dot{a} - 6F\dot{a}^2 a - \cancel{3a^2\dot{a}\dot{\phi}F_\phi} + a^3\dot{\phi}^2 + 3F\dot{a}^2 a + \cancel{3\dot{a}a^2\dot{F}} - a^3\left(\frac{\dot{\phi}^2}{2} - V(\phi) - \rho_m\right) = 0 \Rightarrow$$
$$\Rightarrow -3\dot{F}a^2\dot{a} - 3F\dot{a}^2 a + a^3\left(\frac{\dot{\phi}^2}{2} + V(\phi) + \rho_m\right) = 0 \overset{:a^3}{\Longrightarrow} -3\dot{F}\frac{\dot{a}}{a} - 3F\frac{\dot{a}^2}{a^2} + \frac{\dot{\phi}^2}{2} + V(\phi) + \rho_m = 0 \Rightarrow$$
$$\Rightarrow 3F(\phi)H^2 = \rho_m + \frac{\dot{\phi}^2}{2} + V(\phi) - 3H\dot{F} \tag{4.20}$$

Next we will calculate the "*Euler-Lagrange*" equation for a, relative to $\mathscr{L}$, using Eq.(4.18), as follows

$$\frac{d}{dt}\left(\frac{\partial\mathscr{L}}{\partial\dot{a}}\right) = \frac{\partial\mathscr{L}}{\partial a} \tag{4.21}$$

Let us calculate each term separately

$$\frac{\partial\mathscr{L}}{\partial\dot{a}} = \sqrt{-g}\left[-6\frac{\dot{a}^2}{a^2}F - 3\frac{\dot{F}}{a}\right] = a^3\left[-6\frac{\dot{a}^2}{a^2}F - 3\frac{\dot{F}}{a}\right] = -6a\dot{a}F(\phi) - 3\dot{F}a^2$$
$$\frac{d}{dt}\left(\frac{\partial\mathscr{L}}{\partial\dot{a}}\right) = -6\dot{a}^2F(\phi) - 6a\ddot{a}F(\phi) - 6a\dot{a}\dot{F} - 3\frac{d\phi}{dt}\frac{d}{d\phi}F_\phi\dot{\phi}a^2 - 6\dot{F}a\dot{a} =$$
$$= -6\dot{a}^2F(\phi) - 6a\ddot{a}F(\phi) - 12\dot{F}a\dot{a} - 3\ddot{F}a^2$$
$$\frac{\partial\mathscr{L}}{\partial a} = \frac{\partial\sqrt{-g}}{\partial a}\left[-3\frac{\dot{a}^2}{a^2}F(\phi) - 3\frac{\dot{a}}{a}\dot{F} + \frac{\dot{\phi}^2}{2} - V(\phi) - \rho_m\right] + \sqrt{-g}\frac{\partial}{\partial a}\left[-3\frac{\dot{a}^2}{a^2}F(\phi) - 3\frac{\dot{a}}{a}\dot{F} + \frac{\dot{\phi}^2}{2} - V(\phi) - \rho_m\right]$$
$$= 3a^2\left[-3\frac{\dot{a}^2}{a^2}F(\phi) - 3\frac{\dot{a}}{a}\dot{F} + \frac{\dot{\phi}^2}{2} - V(\phi) - \frac{\rho_{0,m}}{a^3}\right] + a^3\left[6\frac{\dot{a}^2}{a^3}F(\phi) + 3\frac{\dot{a}}{a^2}\dot{F} + 3\frac{\rho_{0,m}}{a^4}\right] =$$
$$= 3a^2\left[-3\frac{\dot{a}^2}{a^2}F(\phi) - 3\frac{\dot{a}}{a}\dot{F} + \frac{\dot{\phi}^2}{2} - V(\phi) - \frac{\rho_{0,m}}{a^3}\right] + 6\dot{a}^2F(\phi) + 3\dot{a}a\dot{F} + 3\frac{\rho_{0,m}}{a}$$
$$= 3a^2\left[-3\frac{\dot{a}^2}{a^2}F(\phi) - 3\frac{\dot{a}}{a}\dot{F} + \frac{\dot{\phi}^2}{2} - V(\phi) - \cancel{\frac{\rho_{0,m}}{a^3}} + 2\frac{\dot{a}^2}{a^2}F + \frac{\dot{a}}{a}\dot{F} + \cancel{\frac{\rho_{0,m}}{a^3}}\right] =$$

$$= 3a^2\left[-\frac{\dot{a}^2}{a^2}F(\phi) - 2\frac{\dot{a}}{a}\dot{F} + \frac{\dot{\phi}^2}{2} - V(\phi)\right] = -3\dot{a}^2F - 6a\dot{a}\dot{F} + \frac{3a^2}{2}\dot{\phi} - 3a^2V(\phi)$$

where we used the fact that

$$\ddot{F} = \frac{d}{dt}\dot{F} = \frac{d}{dt}\left(F_\phi \cdot \dot{\phi}\right) = \frac{d\phi}{dt}\frac{d}{d\phi}F_\phi\dot{\phi}$$

Then, Eq.(4.21) can be written as

$$\frac{d}{dt}\left(\frac{\partial\mathscr{L}}{\partial\dot{a}}\right) = \frac{\partial\mathscr{L}}{\partial a} \Rightarrow -6\dot{a}^2F(\phi) - 6a\ddot{a}F(\phi) - 12\dot{F}a\dot{a} - 3\ddot{F}a^2 = -3\dot{a}^2F - 6a\dot{a}\dot{F} + \frac{3a^2}{2}\dot{\phi} - 3a^2V(\phi) \Rightarrow$$

$$\Rightarrow -3\dot{a}^2F(\phi) - 6a\ddot{a}F(\phi) - 6\dot{F}a\dot{a} - 3\ddot{F}a^2 = \frac{3a^2}{2}\dot{\phi} - 3a^2V(\phi) \xRightarrow{:3a^2}$$

$$\xRightarrow{:3a^2} -\frac{\dot{a}^2}{a^2}F(\phi) - 2\frac{\ddot{a}}{a}F(\phi) - \ddot{F} - 2\dot{F}\frac{\dot{a}}{a} = \frac{\dot{\phi}^2}{2} - V(\phi) \Rightarrow \frac{\dot{\phi}^2}{2} - V(\phi) + \ddot{F} + 2F\frac{\dot{a}}{a} = F(\phi)\left[-2\frac{\ddot{a}}{a} - \frac{\dot{a}^2}{a^2}\right] \tag{4.22}$$

Taking in consideration, Eq.(4.13) it is trivial to obtain Eq.(4.14) as follows

$$-2F(\phi)\frac{\ddot{a}}{a} - F\frac{\dot{a}^2}{a^2} = 2\dot{F}\frac{\dot{a}}{a} + \frac{1}{2}\dot{\phi}^2 + \rho_m + \frac{\dot{\phi}^2}{2} - 3F\frac{\dot{a}^2}{a^2} - 3\frac{\dot{a}}{a}\dot{F} + \ddot{F}$$

$$\Rightarrow -2F(\phi)\left(\frac{\ddot{a}}{a} - \frac{\dot{a}^2}{a^2}\right) = \rho_m + \dot{\phi}^2 + \ddot{F} - H\dot{F} \tag{4.23}$$

Similarly, the "*Euler-Lagrange*" equation for the scalar field ϕ is

$$\frac{d}{dt}\left(\frac{\partial\mathscr{L}}{\partial\dot{\phi}}\right) = \frac{\partial\mathscr{L}}{\partial\phi} \tag{4.24}$$

Studying each term separately as before we obtain

$$\frac{\partial\mathscr{L}}{\partial\dot{\phi}} = \left(-3\frac{\dot{a}}{a}F_\phi + \dot{\phi}\right)a^3 = -3\dot{a}a^2F_\phi + a^3\dot{\phi}$$

$$\frac{d}{dt}\left(\frac{\partial\mathscr{L}}{\partial\dot{\phi}}\right) = -3\ddot{a}a^2F_\phi - 6\dot{a}^2aF_\phi - 3\dot{a}a^2\dot{\phi}F_{\phi\phi} + 3a^2\dot{\phi}\dot{a} + a^3\ddot{\phi}$$

$$\frac{\partial\mathscr{L}}{\partial\phi} = \sqrt{-g}\left[-3\frac{\dot{a}^2}{a^2}F_\phi - 3\frac{\dot{a}}{a}F_{\phi\phi}\dot{\phi} - V_\phi\right] = -3a\dot{a}^2F_\phi - 3\dot{a}a^2F_{\phi\phi}\dot{\phi} - a^3V_\phi$$

Therefore, we derive the "*Euler-Lagrange*" equation for the scalar field

$$\frac{d}{dt}\left(\frac{\partial\mathscr{L}}{\partial\dot{\phi}}\right) = \frac{\partial\mathscr{L}}{\partial\phi} \Rightarrow -3\ddot{a}a^2F_\phi - 6\dot{a}^2aF_\phi - \cancel{3\dot{a}a^2\dot{\phi}F_{\phi\phi}} + 3a^2\dot{\phi}\dot{a} + a^3\ddot{\phi} = -3a\dot{a}^2F_\phi - \cancel{3\dot{a}a^2F_{\phi\phi}\dot{\phi}} - a^3V_\phi \Rightarrow$$

$$\Rightarrow -3\ddot{a}a^2F_\phi - 3\dot{a}^2aF_\phi + 3a^2\dot{\phi}\dot{a} + a^3\ddot{\phi} = -a^3V_\phi \xRightarrow{:a^3} -3\frac{\ddot{a}}{a}F_\phi - 3\frac{\dot{a}^2}{a^2}F_\phi + 3\frac{\dot{a}}{a}\dot{\phi} + \ddot{\phi} + V_\phi = 0 \Rightarrow$$

$$\Rightarrow \ddot{\phi} + 3\frac{\dot{a}}{a}\dot{\phi} - 3\left(\frac{\ddot{a}}{a} + \frac{\dot{a}^2}{a^2}\right)F_\phi + V_\phi = 0 \tag{4.25}$$

i.e Eq.(4.16).

From our calculation, we conclude that regardless of what method we follow we end up to the same equations. The equations of motion for the case of modified gravity are summarised in the table below

Equations of Motion For Modified Gravity

$$3F(\phi)H^2 = \rho_m + \frac{\dot{\phi}^2}{2} + V(\phi) - 3H\dot{F}$$
$$-2F(\phi)\left(\frac{\ddot{a}}{a} - \frac{\dot{a}^2}{a^2}\right) = \rho_m + \dot{\phi}^2 + \ddot{F} - H\dot{F}$$
$$\ddot{\phi} + 3\frac{\dot{a}}{a}\dot{\phi} - 3\left(\frac{\ddot{a}}{a} + \frac{\dot{a}^2}{a^2}\right)F_\phi + V_\phi = 0$$

Only the two out of three equations are independent and the third one can be used as a constraint in the solution derived from the other two.

Next let us rescale the dynamical equation with respect with the present day Hubble parameter H_0 (setting $H = \bar{H}H_0$, $t = \frac{\bar{t}}{H_0}$, $V = \bar{V}{H_0}^2$ and $\rho_m = \bar{\rho}_m {H_0}^2$). Thus Eq.(4.11) can be written as

$$3F(\phi)\bar{H}^2 = \bar{\rho}_m + \frac{\dot{\phi}^2}{2} + \bar{V} - 3\bar{H}\dot{F} \Rightarrow 3F(\phi)\bar{H}^2 = \frac{\rho_m}{{H_0}^2} + \frac{\dot{\phi}^2}{2} + \bar{V} - 3\bar{H}\dot{F} \tag{4.26}$$

and considering a universe which contains matter and dark energy we obtain

$$\Omega_m = \frac{\rho_m}{3F\bar{H}^2{H_0}^2} \Rightarrow \Omega_{0m} = \frac{\rho_{0m}}{3F_0\bar{H}_0^2{H_0}^2} \xrightarrow{\bar{H}_0^2=1} \Omega_{0m} = \frac{\rho_{0m}}{3F_0{H_0}^2} \tag{4.27}$$

In a similar way, we derive for the ϕ field

$$\Omega_\phi = \frac{1}{3F\bar{H}^2}\left(\frac{\dot{\phi}^2}{2} + \bar{V} - 3\bar{H}\dot{F}\right) = \frac{1}{3F\bar{H}^2}\left(\frac{\dot{\phi}^2}{2} + \bar{V}\right) - \frac{\cancel{3}\cancel{\bar{H}}}{\cancel{3}\bar{H}^{\cancel{2}}}\frac{\dot{F}}{F} = \frac{1}{3F\bar{H}^2}\left(\frac{\dot{\phi}^2}{2} + \bar{V}\right) - \frac{1}{\bar{H}}\frac{\dot{F}}{F} \Rightarrow$$
$$\Rightarrow \Omega_{0\phi} = \frac{1}{3F_0\bar{H}_0^2}\left(\frac{{\dot{\phi}_0}^2}{2} + \bar{V}_0\right) - \frac{1}{\bar{H}_0}\frac{\dot{F}_0}{F_0} \xrightarrow{\bar{H}_0=1} \Omega_{0\phi} = \frac{1}{3F_0}\left(\frac{{\dot{\phi}_0}^2}{2} + \bar{V}_0\right) - \frac{\dot{F}_0}{F_0} \tag{4.28}$$

Next, let us rewrite Eq.(4.11) and Eq.(4.14) in the rescaled form as follows

$$3F(\phi)\bar{H}^2 = \bar{\rho}_m + \frac{\dot{\phi}^2}{2} + \bar{V}(\phi) - 3\bar{H}\dot{F} \tag{4.29}$$
$$-2F(\phi)\left(\frac{\ddot{a}}{a} - \frac{\dot{a}^2}{a^2}\right) = \bar{\rho}_m + \dot{\phi}^2 + \ddot{F} - \bar{H}\dot{F} \tag{4.30}$$

Consequently, one could obtain the rescaled dynamical equation for the scale factor

$$-2F(\phi)\left(\frac{\ddot{a}}{a} - \frac{\dot{a}^2}{a^2}\right) = \bar{\rho}_m + \dot{\phi}^2 + \ddot{F} - \bar{H}\dot{F} \Rightarrow \frac{\ddot{a}}{a} = \frac{\dot{a}^2}{a^2} - \frac{\bar{\rho}_m}{2F} - \frac{\dot{\phi}^2}{2F} - \frac{\ddot{F}}{2F} + \bar{H}\frac{\dot{F}}{2F}$$

But from Eq.(4.29) we obtain

$$\frac{\dot{a}^2}{a^2} = \bar{H}^2 = \frac{\bar{\rho}_m}{3F} + \frac{\dot{\phi}^2}{6F} + \frac{\bar{V}}{3F} - \bar{H}\frac{\dot{F}}{F}$$

therefore

$$\frac{\ddot{a}}{a} = \frac{\bar{\rho}_m}{3F} + \frac{\dot{\phi}^2}{6F} + \frac{\bar{V}}{3F} - \bar{H}\frac{\dot{F}}{F} - \frac{\bar{\rho}_m}{2F} - \frac{\dot{\phi}^2}{2F} - \frac{\ddot{F}}{2F} + \bar{H}\frac{\dot{F}}{2F} \Rightarrow$$
$$\Rightarrow \frac{\ddot{a}}{a} = -\frac{\bar{\rho}_m}{6F} - \frac{\dot{\phi}^2}{3F} + \frac{\bar{V}}{3F} - \frac{\ddot{F}}{2F} - \bar{H}\frac{\dot{F}}{2F} \Rightarrow \frac{\ddot{a}}{a} = -\frac{\rho_m}{6F{H_0}^2} - \frac{\dot{\phi}^2}{3F} + \frac{\bar{V}}{3F} - \frac{\ddot{F}}{2F} - \bar{H}\frac{\dot{F}}{2F} \xRightarrow{Eq.(4.27)}$$
$$\Rightarrow \frac{\ddot{a}}{a} = -\frac{\rho_{0m}}{3F_0{H_0}^2}\frac{F_0}{2Fa^3} - \frac{\dot{\phi}^2}{3F} + \frac{\bar{V}}{3F} - \frac{\ddot{F}}{2F} - \bar{H}\frac{\dot{F}}{2F} \Rightarrow \frac{\ddot{a}}{a} = -\frac{\Omega_{0m}F_0}{2Fa^3} - \frac{\dot{\phi}^2}{3F} + \frac{\bar{V}}{3F} - \frac{\ddot{F}}{2F} - \bar{H}\frac{\dot{F}}{2F} \tag{4.31}$$

Of course, setting $F = F_0 = M_p = (8\pi G)^{-1/2} = 1$ we recover Eq.(3.11) and Eq.(3.15) as it was expected. With this we conclude our theoretical framework of the modified gravity case and we are free to proceed to the final chapter of the thesis where we we consider observational tests constraining scalar field evolution parameters.

Chapter 5

Observationals Tests

As we have already discussed, recent cosmological data indicate that the universe has recently entered a phase of accelerating expansion attributed to an unknown component called *dark energy*, which can induce repulsive gravity and thus cause accelerated expansion. This unknown component represents the 74% of our universe.

Several models have been proposed to explain the nature of *dark energy*, which can be classified essentially into two groups

- The first class assumes that GR is valid at cosmological scales and attributes the accelerating expansion to a dark energy component which has repulsive gravitational properties due to its negative pressure. The role of dark energy is usually played by a scalar field minimally coupled to gravity called *quintessence*. Alternatively, the role of dark energy can be played by various perfect fluids (eg Chaplygin gas[51, 52]) topological defects[99], holographic dark energy[45, 100, 101] etc.)

- The second class of models attributes the accelerating expansion to modifications and extensions of GR, which converts gravity to a repulsive interaction at late times and on cosmological scales, such as scalar-tensor theories, f(R) extended gravity theories[102], braneworld models[103] etc.

In the first section of this chapter we will make a short introduction in the observational cosmology and describe the basic quantities used in astronomy. Next we will focus on the first class of models, i.e *quintessence* models and investigate the goodness of fit to the Union2.1 and Gold Dataset for this kind of category. In the final sections of the chapter we will investigate the cosmological dynamics for general scalar tensor quintessence field and find the goodness of fit to the Union2.1 dataset, i.e focus on the second category of models.

5.1 Observational Probes for Cosmological Observations

The accelerated expansion have been attributed either to DE or generalised theories of gravity. Both of these models have some characteristic predictions. These predictions concern the calculation of $H(z)$ and $G_{eff}(z)$. These predictions can be categorised into two groups[104]

- Geometric Probes: These kind of methods detect the geometry of the Universe in large scales and measure the equation of state parameter using cosmological distances, such as luminosity distance[76, 77] as a function of the redshift and the baryon acoustic oscillations[105].

- Dynamical Probes: These kind of methods detect the dynamical evolution of density perturbations as an independent test of dark energy and general relativity, such as the gravitational lensing measurements[106]. An example of such a dynamical probe is the growth function of the linear matter density contrast defined as $\delta \equiv \frac{\delta\rho_m}{\rho_m}$, where ρ_m represents the background matter density and $\delta\rho_m$ its first order perturbation. In many classes of modified gravity the growth factor $\delta(a)$ satisfies the following equation[107]

$$\delta''(a) + \left(\frac{3}{a} + \frac{H'(a)}{H(a)}\right)\delta'(a) - \frac{3}{2}\frac{\Omega_m G_{eff}(k,a)/G_N}{a^5 H(a)^2/{H_0}^2} \tag{5.1}$$

where primes denote differentiation with respect to the scale factor and $H(a) = \frac{\dot{a}}{a}$ is the Hubble parameter and $G_{eff}(a,k)$ is the effective Newton's constant which is constant and equal to G_N in GR. In modified gravity theories G_{eff} depends on both the scale factor a (or equivalently the redshift z) and the scale k. From dynamical probes we obtain information for $G_{eff}(k,a)$ and $H(a)$ simultaneously. Eq.(5.1) is an equation with two unknown quantities, $H(a)$ and $G_{eff}(k,a)$. However from geometrical probes one could calculate $H(a)$ and substituting this in Eq.(5.1) we could calculate $G_{eff}(k,a)$. In reality a robust measurable quantity in redshift surveys is not the growth factor $\delta(a)$ but the combination

$$f\sigma_s(a) \equiv f(a)\cdot\sigma(a) = \frac{\sigma(s)}{\delta(1)}a\cdot\delta'(a)$$

where $f(a) = \frac{dln\delta}{dlna}$ is the growth rate and $\sigma(a) = \sigma_s\frac{\delta(a)}{\delta(1)}$ is the redshift-dependent rms fluctuations of the linear density field within spheres of radius $R = 8h^{-1}Mpc$ while the parameter σ_s is its value today. A more detail analysis for the dynamical probes exceeds the purpose of this thesis since we focus on the geometrical probes(for more details concerning the dynamical probes see Ref.[107])

In cosmology the most direct way to detect dark energy geometrically, comes from measurements of supernovae Ia explosions. These supernovae explosions are caused by binary systems in which a compact object, usually a white dwarf, accumulates material from a companion star creating the so-called *accretion disk*

Figure 5.1: The accretion disk that is created around a compact object (The picture can be found in Ref.[108] and was used after permission of the author).

At a certain moment, the white dwarf will reach a critical mass, the Chandrasekhar limit[109]. The white dwarf is progressively compressed, and eventually sets off a runaway nuclear reaction inside that eventually leads to a cataclysmic supernova outburst.

Astronomical objects with a known luminosity, so called standard candles, enables us to measure the luminosity distance d_L and the redshift z simultaneously. So under the assumption that supernovae Ia explosions,and thus the related luminosities, are drawn from the same statistical sample, they can be considered as standard candles[1]. Measuring these quantities gives an expansion rate of the universe and leads to a density parameter $\Omega_\Lambda \approx 0.7$.

First of all, let us consider a luminous cosmological object emitting at total power L in radiation within a particular wavelength band. Also, one can imagine an observer at a distance d_L from the luminous object as it can be seen in the figure below

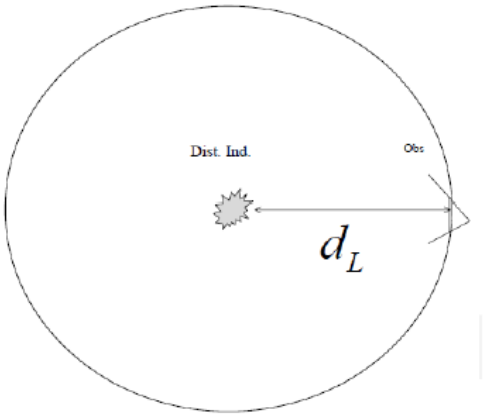

Figure 5.2: The *luminosity distance* of a luminous object (The picture can be found in Ref.[112] and was used after permission of the author.)

The function d_L is called a "distance" because its dimensionality is that of a distance, and because it is what the proper distance to the standard candle would be if the Universe were static and euclidean. In a static euclidean Universe, the propagation of light follows the inverse square law using the *flux* f as follows[113]

$$f = \frac{L}{4\pi {d_L}^2} \tag{5.2}$$

However our Universe is not static and euclidean and it is described by the FRW metric, i.e Eq.(2.15). When we observe a distant galaxy, we know its angular position very well, but not its distance. That is, we can point in its direction, but we don't know its *comoving coordinate distance* d. We can, however, measure the redshift z of the light we receive from the galaxy. Setting $c = 1$, the *comoving distance* d is given by the formula $d = \int_{t_e}^{t_0} \frac{dt}{a(t)}$ and holds true in any universe whose geometry is described by a flat FRW metric

$$d = \int_{t_e}^{t_0} \frac{dt}{a(t)} = \int_{t_e}^{t_0} \frac{1}{a}\frac{dt}{da} da = \int_{a(t_e)}^{a(t_0)} \frac{1}{a}\frac{1}{\dot{a}} da \xRightarrow{a(t_0)=1} \int_{a(t_e)}^{1} \frac{da}{H\,a^2} = \int_{a(t_e)}^{1} \frac{1}{H\,a^2}\frac{da}{dz} dz \tag{5.3}$$

where t_e is the emission time. However the redshift z can be defined as

$$1 + z = \frac{a(t_0)}{a(t_e)} \Rightarrow 1 + z = \frac{1}{a} \Rightarrow dz = -\frac{da}{a^2} \Rightarrow \frac{da}{dz} = -a^2 \tag{5.4}$$

[1]There are other possible candles that have been proposed and are actively being investigated. One such approach has been to use FRIIb radio galaxies[110]. Another suggested standard candle is that of Gamma Ray Bursts (GRB), which may enable the expansion rate of our Universe to be measured out to very high redshifts[111].

Substituting Eq.(5.4) in Eq.(5.3), it is trivial to show that[114]

$$d = -\int_{z(t_e)}^{0} \frac{1}{H(z)\cancel{a^2}}\cancel{a^2}dz \Rightarrow d = \int_{0}^{z(t_e)} \frac{dz}{H(z)} \tag{5.5}$$

Nevertheless in a Universe characterized by an expansion $a(t)$, the object (standard candle), is not stationary, so the energy of photons emitted at time t_e is redshifted by the factor $(1+z) = a^{-1}(t_e)$. Moreover, the arrival rate of the photons suffers time dilation by another factor $(1+z)$, often called the *energy effect*. In that Universe the *flux* is given by[113]

$$f = \frac{L}{4\pi d^2(1+z)^2} \tag{5.6}$$

Comparing Eq.(5.2) and Eq.(5.6), the *luminosity distance* is defined as $d_L = d(1+z)$, therefore one can easily derive that, for a flat Universe

$$d_L = (1+z)\int_{0}^{z(t_e)} \frac{dz'}{H(z')} \tag{5.7}$$

Eq.(5.3) is valid only for a flat Universe. Let us provide for completeness the methodology for a non flat Universe. Light that was emitted by a distant galaxy at a time t_e is observed by us at a time t_0. During its travel from the distant galaxy to us, the light travelled along a null geodesic, with $ds = 0$. A null geodesic has θ and ϕ constant since we conside a homogeneous and isotropic Universe. Therefore considering Eq.(2.15) we derive[113]

$$\int_{t_e}^{t_0} \frac{dt}{a(t)} = -\int_{r_e}^{0} \frac{dr}{\sqrt{1-kr^2}} \tag{5.8}$$

where r_e is the distance of the distant galaxy to us. Let us now focus on the right hand side of Eq.(5.8) setting the three values of the *scalar curvature* which describe an open, a flat and a closed Universe

- $\underline{k=1}$: This particular case corresponds to an open Universe and Eq.(5.8) is written as

$$-\int_{r_e}^{0} \frac{dr}{\sqrt{1-r^2}} = -\int_{r_e}^{0} d\left(arcsin(r)\right) = -\cancelto{0}{arcsin(0)} + arcsin(r_e) = sin^{-1}(r_e) = sin^{-1}(d) \tag{5.9}$$

  Therefore, Eq.(5.8) is rewritten as

$$sin^{-1}(d) = \int_{t_e}^{t_0} \frac{dt}{a(t)} \Rightarrow d = sin\left(\int_{t_e}^{t_0} \frac{dt}{a(t)}\right) = sin\left(\int_{0}^{z(t_e)} \frac{dz}{H(z)}\right) \tag{5.10}$$

  Hence the *luminosity distance* for an open Universe is

$$d_L = (1+z)sin\left(\int_{0}^{z(t_e)} \frac{dz}{H(z)}\right) \tag{5.11}$$

- $\underline{k=0}$: This case describes a flat Universe and following the same procedure we obtain Eq.(5.7)

- $k = -1$: The final value of the *scalar curvature* describes a closed Universe. For that case Eq.(5.8) takes the following form

$$-\int_{r_e}^{0} \frac{dr}{\sqrt{1+r^2}} = -\int_{r_e}^{0} d\left(arcsinh(r)\right) = -\cancelto{0}{arcsinh(0)} + arcsinh(r_e) = sinh^{-1}(r_e) = sinh^{-1}(d) \tag{5.12}$$

As a result, Eq.(5.8) is rewritten as

$$sinh^{-1}(d) = \int_{t_e}^{t_0} \frac{dt}{a(t)} \Rightarrow d = sinh\left(\int_{t_e}^{t_0} \frac{dt}{a(t)}\right) = sinh\left(\int_{0}^{z(t_e)} \frac{dz}{H(z)}\right) \tag{5.13}$$

Hence the *luminosity distance* for an open Universe is

$$d_L = (1+z)sinh\left(\int_{0}^{z(t_e)} \frac{dz}{H(z)}\right) \tag{5.14}$$

Now assuming the Universe to be composed of a set of independent components having density parameters $\Omega_i \equiv \rho_i/\rho_{crit}$, the Friedmann equation for a flat FRW universe, may be expressed as

$$\left(\frac{\dot{a}}{a}\right)^2 = {H_0}^2 \sum_i \Omega_i \left(\frac{a_0}{a}\right)^{3\,(1+w_i)} \tag{5.15}$$

where $H_0 \equiv H(t_0)$ is the present time value of the Hubble parameter, $a_0 \equiv a(t_0)$ is the current value of the scale parameter and the equation of state for each component is given by

$$p_i = w_i \rho_i. \tag{5.16}$$

Now rewriting Eq.(5.15) in terms of the redshift one can see that

$$\left(\frac{\dot{a}}{a}\right) = H^2 = H_0^2 \sum_i \Omega_i (1+z)^{3(1+w_i)} \tag{5.17}$$

which combined with Eq.(5.7) gives[80]

$$d_L = \frac{1+z}{H_0} \int_0^z \frac{dz'}{\sqrt{\sum_i \Omega_i (1+z')^{3(1+w_i)}}} \tag{5.18}$$

Measurements of the *luminosity distance* and the redshift can be compared with the theoretical function of d_L, i.e Eq.(5.18). Astronomers usually replace the flux f and the total power L by two empirically defined quantities, the *absolute magnitude* M of a luminous object and the *apparent magnitude* m. Let us define these quantities in order to be consistent.

The *apparent magnitude* of a light source in terms of intensity l, or flux f[2], as[115]

$$m = -2.5 log_{10} \frac{l}{l_x} \tag{5.19}$$

[2]For SnIa (the type of stars that we focus on) the flux f and the intensity l are practically the same because the angle θ is small.

where l_x is set as a value $l_x = 2.53 \times 10^{-8} watt\, m^{-2}$. Next let us consider two stars, namely 1 and 2 and taking the difference of their apparent magnitude we obtain

$$m_1 - m_2 = -2.5log_{10}\frac{l_1}{l_x} + 2.5log_{10}\frac{l_2}{l_x} = -2.5log_{10}\frac{l_1}{l_x} - 2.5log_{10}\frac{l_x}{l_2} \Rightarrow$$
$$\Rightarrow m_1 - m_2 = -2.5log_{10}\frac{l_1}{l_2} \tag{5.20}$$

Now we define the *absolute magnitude* M, which is a constant for type Ia supernovae, as the apparent magnitude of the same star at 10 parsec, therefore

$$m - M = -2.5log_{10}\frac{l(z)}{L}, \text{ where } L = l_2 \Rightarrow m - M = 2.5log_{10}\frac{L}{l(z)}$$

But one can be define intensity in terms of luminosity $\mathscr{L}$, as $l = \frac{\mathscr{L}}{4\pi d_L^2}$, hence

$$m - M = -2.5log_{10}\frac{\cancel{\frac{\mathscr{L}}{4\pi 10^2}}}{\cancel{\frac{\mathscr{L}}{4\pi d_L^2}}} \Rightarrow m - M = 2.5log_{10}\frac{d_L^2}{10^2} \Rightarrow m - M = 5log_{10}\frac{d_L(z)_{obs}}{10pc} \Rightarrow$$
$$\Rightarrow m - M = 5log_{10}\frac{d_L(z)_{obs}}{10^{-5}Mpc} = 5\left(log_{10}d_L(z)_{obs} - log_{10}10^{-5} - log_{10}Mpc\right) \Rightarrow$$
$$\Rightarrow m(z) - M - 25 = 5log_{10}\frac{d_L(z)_{obs}}{Mpc} \tag{5.21}$$

Eq.(5.21) can be re-expressed taking in account the corresponding Hubble free luminosity distance $D_L^{th}(z)$,which is defined as $D_L = \frac{H_0 d_L}{c}$, through

$$m_{th} = \bar{M}(M, H_0) + 5log_{10}\left(D_L(z; a_1, a_2, \ldots, a_n)\right) \tag{5.22}$$

In a flat cosmological model

$$D_L^{th}(z; a_1, a_2, \ldots, a_n) = (1+z)\int_0^z dz' \frac{H_0}{H(z'; a_1, a_2, \ldots, a_n)} \tag{5.23}$$

where "th" stands for theoretical, the quantities $(H_0 d_L), a_1, a_2, \ldots, a_n$ are the parameters of our theoretical model and $\bar{M}$ is the magnitude zero point offset. The proof of Eq.(5.22) is trivial. In order to derive it we will need the connection between the luminosity distance d_L and the corresponding Hubble free luminosity distance $D_L(z)$

$$D_L = \frac{H_0 d_L}{c} \Rightarrow d_L = \frac{c \cdot D_L}{H_0} \tag{5.24}$$

Substituting Eq.(5.24) in Eq.(5.21) one can see

$$m(z) - M - 25 = 5log_{10}\left(\frac{d_L(z)_{obs}}{Mpc}\right) \Rightarrow m(z) - M - 25 = 5log_{10}\left(\frac{\frac{c \cdot D_L}{H_0}}{Mpc}\right) \Rightarrow$$
$$\Rightarrow m(z) = M + 25 + 5log_{10}\left(\frac{c \cdot D_L}{H_0}\right) - 5log_{10}(1Mpc) \Rightarrow$$
$$\Rightarrow m(z) = M + 25 + 5log_{10}D_L + 5log_{10}(cH_0^{-1}) + 5log_{10}\left(\frac{1}{1Mpc}\right) \Rightarrow$$
$$\Rightarrow m(z) = M + 25 + 5log_{10}(D_L) + 5log_{10}\left(\frac{cH_0^{-1}}{1Mpc}\right) \Rightarrow$$
$$\Rightarrow m(z; a_1, \ldots, a_n) = \bar{M}(M, H_0) + 5log_{10}\left(D_L(z; a_1, \ldots, a_n)\right) \text{ where } \bar{M} = M + 5log_{10}\left(\frac{cH_0^{-1}}{1Mpc}\right) + 25 \tag{5.25}$$

Eq(5.25) can be written in a more convenient form using the dimensionless parameter for the Hubble constant as follows

$$m(z;a_1,a_2,\ldots,a_n)=\bar{M}(M,h)+5log_{10}\left(D_L(z;a_1,a_2,\ldots,a_n)\right)\ \text{where}\ \bar{M}(M,h)=M-5log_{10}h+42.38 \tag{5.26}$$

For the derivation of Eq.(5.26) we define the dimensionless parameter for the Hubble constant as

$$h=\frac{H}{100\,(km/sec)\,/Mpc} \tag{5.27}$$

Therefore Eq.(5.25) can be written as

$$\begin{aligned}
m(z;a_1,a_2,\ldots,a_n)&=M+5log_{10}\left(\frac{cH_0^{-1}}{1Mpc}\right)+25+5log_{10}\left(D_L(z;a_1,a_2,\ldots,a_n)\right)\Rightarrow\\
\Rightarrow m(z;a_1,a_2,\ldots,a_n)&=M+5log_{10}\left(\frac{c}{H_0Mpc}\right)+25+5log_{10}\left(D_L(z;a_1,a_2,\ldots,a_n)\right)\xRightarrow{Eq.(5.27)}\\
\Rightarrow m(z;a_1,a_2,\ldots,a_n)&=M+5log_{10}\left(\frac{c}{100hMpc\,\frac{km}{s\cdot Mpc}}\right)+25+5log_{10}\left(D_L(z;a_1,a_2,\ldots,a_n)\right)\Rightarrow\\
\Rightarrow m(z;a_1,a_2,\ldots,a_n)&=M+5log_{10}\left(\frac{3\times10^{5\cancel{\frac{km}{s}}}}{10^{2\cancel{\frac{km}{s}}}}\right)-5log_{10}h+25+5log_{10}\left(D_L(z;a_1,a_2,\ldots,a_n)\right)\Rightarrow\\
\Rightarrow m(z;a_1,a_2,\ldots,a_n)&=M-5log_{10}h+25+5log_{10}\left(3\times10^3\right)+5log_{10}\left(D_L(z;a_1,a_2,\ldots,a_n)\right)\Rightarrow\\
\Rightarrow m(z;a_1,a_2,\ldots,a_n)&\simeq M-5log_{10}h+25+17.38+5log_{10}\left(D_L(z;s)\right)\Rightarrow\\
\Rightarrow m(z;a_1,\ldots,a_n)&=\bar{M}(M,h)+5log_{10}\left(D_L(z;a_1,\ldots,a_n)\right)\ \text{where}\ \bar{M}(M,h)=M-5log_{10}h+42.38
\end{aligned} \tag{5.28}$$

Typically the points of the datasets, are given in terms of the distance modulus

$$\mu_{obs}(z_i)=m_{obs}(z_i)-M \tag{5.29}$$

The theoretical distance modulus can be associated with the apparent magnitude via the following equation

$$\mu_{th}(z_i)=m_{th}(z_i)-M=5log_{10}\left(D_L(z)\right)+\mu_0 \tag{5.30}$$

where $\mu_0=42.38-5log_{10}h$.

Eq.(5.30) can be proven as follows

$$\begin{aligned}
\mu_{th}(z_i)=m_{th}(z_i)-M&\xRightarrow{Eq.(5.28)}M-5log_{10}h+42.38+5log_{10}\left(D_L(z;a_1,a_2,\ldots,a_n)\right)-M\Rightarrow\\
&\Rightarrow\mu_{th}(z_i)=5log_{10}\left(D_L(z)\right)+\mu_0
\end{aligned} \tag{5.31}$$

This procedure, has been done for 170 supernovae explosions, by the supernovae cosmology project (SCP) and the high-z supernovae team (HSST). In 2004 (see [116]) 16 high redshift supernovae explosions have been observed with the Hubble Space Telescope (HST). Including these data with the other 170 previously found supernovae explosions[117] it was shown that the universe exhibited a transition from deceleration to acceleration with a confidence level $> 99\%$[3]. A best-fit value for Ω_{0m} was found to be $\Omega_{0m}=0.31$ and $\Omega_{0\Lambda}=0.69$ as it can be seen in the following Fig.5.3[70]

[3]See also Refs.[115, 118, 119] for recent papers about the SN Ia data analysis.

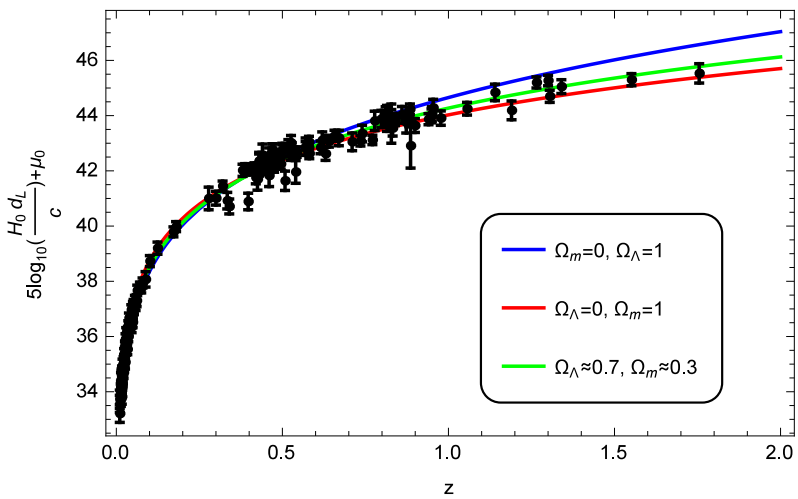

Figure 5.3: The apparent magnitude $m(z)$ versus the redshift z for a flat cosmological model, using the Gold Dataset[116].

In Fig.5.3 the theoretical curves can be derived from Eq.(5.31). This figure is the same as the one in Ref.[80]

Another interesting piece of evidence for the existence of dark energy is the Cosmic Microwave Background (CMB)[5, 120] and the large scale structure formation observations[121, 122]in the context of ΛCDM. Let us present the CMB method of measurement. In order to do we have to define another distance, which is commonly used in astronomy, the *angular diameter distance* d_A. To calculate this distance we need the angle θ subtended by an object of known physical size r_s. The distance to that object (under the assumption of small angle) is

$$d_A(z) = \frac{r_s}{\theta} \tag{5.32}$$

This distance is called the *angular diameter distance*. The *angular diameter distance* in an expanding Universe we first note that the comoving size of the object is $\frac{r_s}{a}$, therefore the angle θ in terms of the comoving distance d is

$$\theta = \frac{\frac{r_s}{a}}{d} \tag{5.33}$$

Taking in account Eq.(5.33) the *angular diameter distance* for an expanding Universe is

$$d_A(z) = \frac{r_s}{\theta} \Rightarrow d_A(z) = \frac{r_s}{\frac{\frac{r_s}{a}}{d}} \Rightarrow d_A(z) = a \cdot d = \frac{d}{1+z} \tag{5.34}$$

Now that we have derived the *angular diameter distance* for an expanding Universe let us prove that the *angular diameter distance* is connected with $H(z)$ from the relation that follows

$$d_A(z) = \frac{1}{1+z}\int_0^z \frac{dz'}{H(z')} \tag{5.35}$$

The proof of Eq.(5.35) is trivial. Setting $dr = d\phi = dt = 0$, $c = 1$ and considering an FRW metric we obtain

$$ds^2 = a^2\, r^2\, d\theta^2 \Rightarrow ds = r_s = a(t_e) \cdot d \cdot d\theta \Rightarrow ds = \frac{1}{1+z}\int_0^z \frac{dz'}{H(z')}\theta \Rightarrow d_A = \frac{r_s}{\theta} = \frac{1}{1+z}\int_0^z \frac{dz'}{H(z')}$$

i.e. Eq.(5.35).

We are thus faced with the following question "What kind of stellar objects that we have to use?" or "What is the proper physical size of an object in order to taking into account?". The most common object that we use is the horizon as it is measured in the time of the last scattering of the photons using the CMB. The measured[74] angular diameter distance to the horizon $r_s(z_{rec})$ at recombination is given by Eq.(5.35)

$$d_A(z_{rec}) = \frac{1}{1+z_{rec}} \int_0^{z_{rec}} \frac{dz'}{H(z')} \tag{5.36}$$

The expansion history of the Universe is determined by a set of the dimensionless density parameters

$$\Omega_{0m} + \Omega_{0R} + \Omega_{0\Lambda} + \Omega_{0k} = 1 \tag{5.37}$$

where Ω_{0m} is the present mean mass density of non-relativistic matter which mainly consists of baryons and non-baryonic cold dark matter (CDM), Ω_{0R} is the present mass density in the relativistic CMB radiation accompanying the low mass neutrinos that almost homogeneously fills the space, $\Omega_{0\Lambda}$ is the present dark energy density and Ω_{0k} is an effect of the curvature of spacetime. Using this relation the cross-checks for the existence of dark energy are[123]

- The Universe has to be older than the oldest stars. If there is no cosmological constant or other form of dark energy, it is not possible to create a universe that is old enough. If the Universe contains only matter, then the scale factor is given by the relation $a(t) \propto t^{2/3}$. Considering the Hubble constant we derive

$$H_0 = \left(\frac{\dot{a}}{a}\right)_0 = \frac{2}{3t_0} \Rightarrow t_0 = \frac{2}{3H_0} = \frac{640}{H_0} \times 10^9 years = \frac{640}{67} \times 10^9 years \Rightarrow t_0 \simeq 9.5 \times 10^9 years \tag{5.38}$$

However this answer is not satisfactory because it is smaller that the older stars. Let us do the same for the case of matter and ΛCDM and for $k = 0$

$$\frac{\dot{a}^2}{a^2} = \frac{8\pi G}{3}\left(\frac{\rho_0}{a^3} + \Lambda\right) = \frac{8\pi G}{3}\rho_c\left(\frac{\rho_0/\rho_c}{a^3} + \frac{\Lambda}{\rho_c}\right) = {H_0}^2\left[\frac{a_0^3}{a^3}(1-\Omega_\Lambda) + \Omega_\Lambda\right] \xRightarrow{a(t_0)=1}$$
$$\Rightarrow H_0 = \frac{\dot{a}}{a}\frac{1}{\sqrt{\frac{1-\Omega_\Lambda}{a^3} + \Omega_\Lambda}} = \frac{da}{dt}\frac{\sqrt{a}}{\sqrt{1-\Omega_\Lambda + \Omega_\Lambda\, a^3}} \tag{5.39}$$

However $H_0\, t_0 = \int_0^{t_0} H_0 dt$ and substituting Eq.(5.39) one can see

$$H_0 t_0 = \int_0^{t_0} \frac{\sqrt{a}}{\sqrt{1-\Omega_\Lambda + \Omega_\Lambda\, a^3}}\frac{da}{dt}dt = \int_0^{a(t_0)} \sqrt{\frac{a}{1-\Omega_\Lambda + \Omega_\Lambda a^3}}da = \int_0^1 \sqrt{\frac{a}{1-\Omega_\Lambda + \Omega_\Lambda a^3}}da \tag{5.40}$$

and solving Eq.(5.40) we obtain

$$H_0 t_0 = \frac{2}{3\sqrt{\Omega_\Lambda}} sinh^{-1}\left(\sqrt{\frac{\Omega_\Lambda}{1-\Omega_\Lambda}}\right) = \frac{2}{3\sqrt{0.7}} sinh^{-1}\left(\sqrt{\frac{0.7}{1-0.7}}\right) \Rightarrow t_0 = 13.7 \times 10^9 years \tag{5.41}$$

- The angular power spectrum of fluctuations in the temperature of the 3K thermal cosmic background (CMB) radiation across the sky indicates that Ω_{0k} is almost 0 and $\Omega_{0R} \approx 10^{-4}$.
- The power spectrum of the spatial distributions of large scale structures give $\Omega_{0m} \approx 0.3$.

All these observations give the values $\Omega_{0m} \approx 0.3$ and $\Omega_{0\Lambda} \approx 0.7$.

5.2 Constraints on Quintessence Models

Having already presented the theoretical background of quintessence models in Chapter 3 we are ready to study this kind of models numerically.

5.2.1 Numerical Solution of Scalar Field Evolution

Now we are ready to solve the system of Eq.(3.13) and Eq.(3.15) numerically considering a potential of the form $V(\phi) = -s\,\phi$ and using the initial conditions for matter dominated Universe at early times we solve numerically the following system [92]

$$\ddot{\phi} = -3\frac{\dot{a}}{a}\dot{\phi} + s$$
$$\frac{\ddot{a}}{a} = -\left(\dot{\phi}^2 + s\phi\right) - \frac{\Omega_{0m}}{2a^3}$$
$$a(t_i) = \left(\frac{9\Omega_{0m}}{4}\right)^{1/3} t_i^{2/3}$$
$$\phi(t_i) = \phi_i$$
$$\dot{\phi}(t_i) = 0$$

The value of ϕ_i is chosen for each value of the slope s such as that $\Omega_{0\phi} = \dot{\phi}^2(t_0) + V(\phi(t_0)) = 1 - \Omega_{0m}$ at the present time t_0, which is defined by $a(t_0) = H(t_0) = 1$. It has to be mentioned that the quantities $\phi(\dot{t}_0)$ and $V(\phi(t_0))$ are dimensionless, since we used the rescaling of Eq.(3.14). In what follows we have assumed a prior of $\Omega_{0m} = 0.3$. According to the numerical solution the field ϕ gets negative values (see Fig.5.4) since in order to obtain $\Omega_{0\phi} \approx 0.7$ and $H(z = 0) \approx 1$ at the present time we set the initial value of the ϕ field in negative values[70]

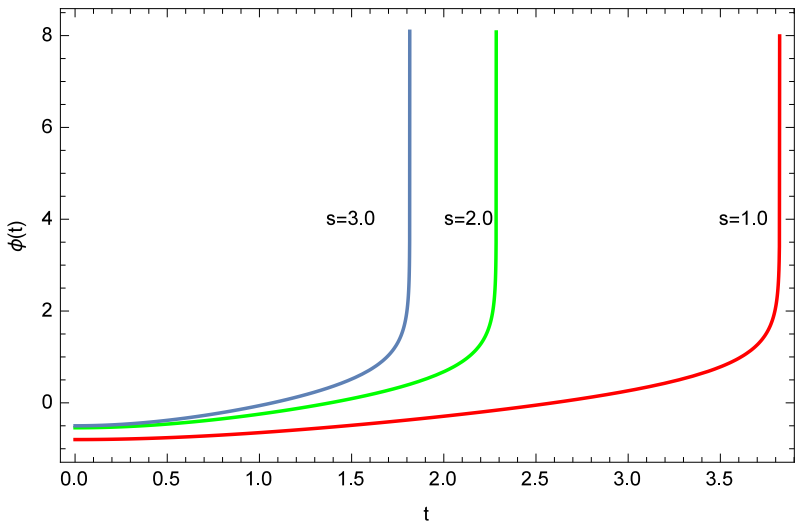

Figure 5.4: Evolution of the scalar field ϕ for quintessence models with linear potential for various slopes.

Assuming $s > 0$ and $\phi < 0$ our potential ($V = -s\,\phi$) is positive at early times. At approximately the present time when the matter density drops and the field potential begins to dominate the lower friction allows the field to move down the potential. This can be seen in the graphic below for the potential energy[70]

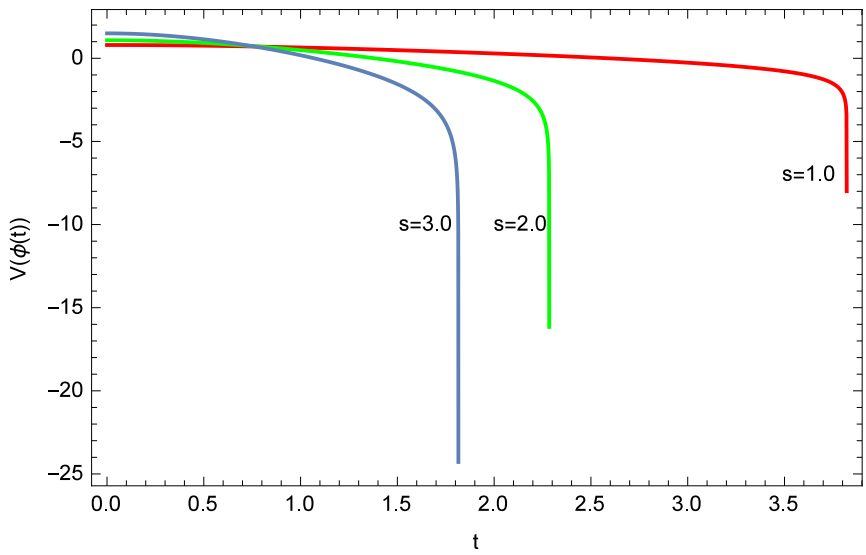

Figure 5.5: The potential energy evolution for quintessence models with linear potential for various slopes.

From the above graphic the following mechanism accrued. As the field moves down the potential energy becomes negative, ϕ becomes positive (See Fig.5.4), hence Eq.(3.15) becomes negative(attractive gravity). Thus the scale factor begins to decelerate until the Universe ends with a Big Crunch. This can be seen clearly in Fig.5.6[70]

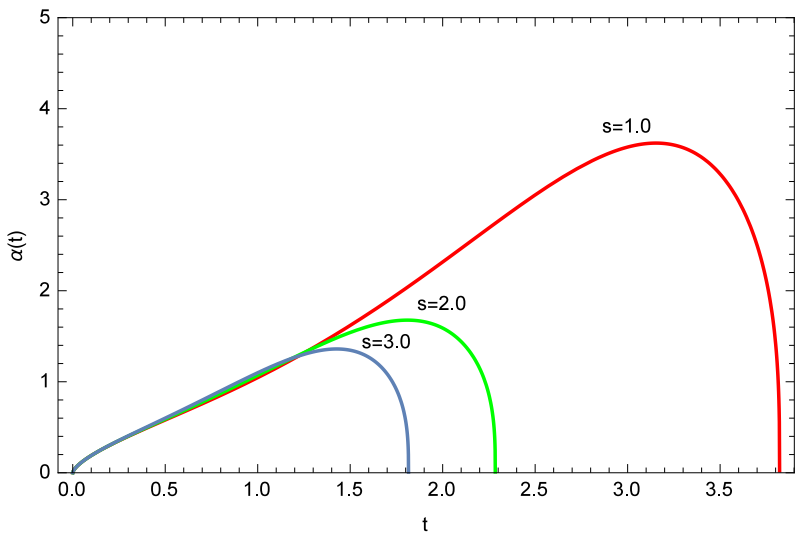

Figure 5.6: Evolution of the scale factor a for quintessence models with linear potential for various slopes.

This graphic is the same as the one in Ref.[124]

One feature of this evolution that is relevant for observational cosmology is that the equation of state for the scalar field changes in an unconventional manner. Using the numerical solution of the system we can evaluate the redshift dependence of the equation of state parameter

$$w(z) = \frac{p}{\rho} = \frac{\frac{1}{2}\dot{\phi}^2 - V(\phi)}{\frac{1}{2}\dot{\phi}^2 + V(\phi)} = \frac{\frac{1}{2}\dot{\phi}^2 + s\phi}{\frac{1}{2}\dot{\phi}^2 - s\phi} \tag{5.42}$$

The evolution of the state parameter as a function of the redshift z, is shown in the figure below in the redshift range $0 \leq z \leq 2$ for quintessence models for various slopes of s. It is clear from Fig.5.7, that the PDL is not crossed for any value of s, and instead $w(z)$ evolves towards positive values for a quintessence scalar field[70]

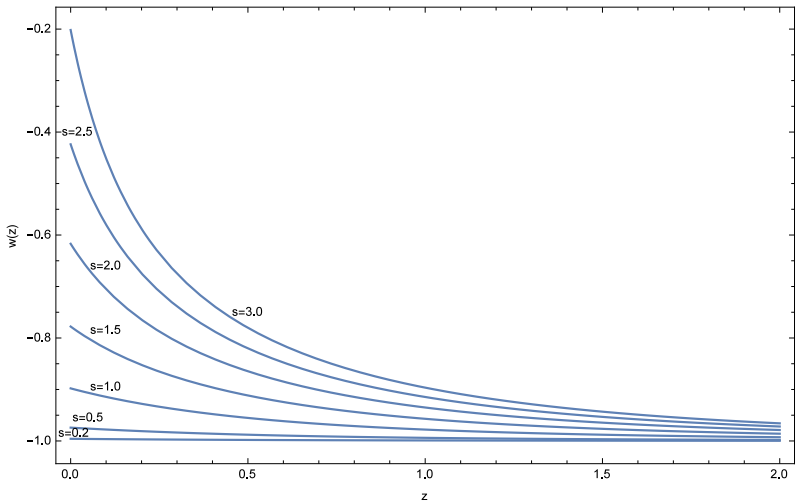

Figure 5.7: Evolution of the redshift for quintessence models with linear potential for different slopes.

To summarize, the main features of the evolution of quintessence models are as follows

- The universe is dominated by matter at early times, hence $a(t) \propto t^{2/3}$. At the same time the scalar field is moving slowly due to friction.
- After some time the matter density falls below of the scalar field potential energy and the evolution becomes scalar field dominated and we have the expansion that we observe today.
- Then the friction becomes smaller and the field starts to move. Therefore the kinetic term makes $w > -1$.
- As the field slips down the potential, the potential energy changes sign($V(\phi)$ becomes negative), since ϕ changes sign (ϕ becomes positive), hence $\ddot{a} < 0$. This epoch marks the turning point, where cosmic expansion becomes contraction.
- As the universe starts contracting, the kinetic energy of the scalar field comes to dominate however this makes the $\ddot{a}$ even more negative and the universe arrives rapidly at a new singularity, hereafter denotes as *Big Crunch* or *Cosmic Doomsday*.

5.2.2 Fit to SnIa Data

Having solved numerically the rescaled system we are ready to see if the quintessence model can play the role of dark energy. For this purpose, we will use two recent datasets of distant Type Ia supernovae (SnIa), such as the Gold Dataset[4] and Union2.1 Dataset[125], and obtain the

[4]The Gold Dataset dataset compiled by Riess et. al.[116] is a set of supernova data from various sources analysed in a consistent and robust manner with reduced calibration errors arising from systematics. It contains 143 points from previously published data plus 14 points with $z > 1$ discovered recently with the HST

"ideal" χ^2 *function*[5] and use it to fit the ΛCDM model. If the fit of the quintessence model is better, then this would be a clear indication that it could play the role of dark energy.

5.2.2.1 χ^2 Analysis for Gold Dataset

The Gold dataset[116] provides the apparent magnitude $m(z)$ of the supernovae at peak brightness after implementing some corrections. The goodness of fit, for the quintessence models that we studied earlier, corresponding to any slope s is determined by the probability distribution of s[126]

$$P(\bar{M}, s) = \mathcal{N} e^{-\chi^2(\bar{M},s)/2} \tag{5.43}$$

where

$$\chi^2(\bar{M}, s) = \sum_{i=1}^{157} \frac{\left[m^{obs}(z_i) - m^{th}(z_i; \bar{M}, s)\right]^2}{\sigma^2_{m^{obs}(z_i)}} \tag{5.44}$$

This is the quantity that we want to minimize. But as we have already mentioned the data points of the Gold dataset are given in terms of the distance modulus and in particular Eq.(5.31). Using Eq.(5.29) and Eq.(5.31) one can see that it is exactly the same instead of minimizing Eq.(5.44), to minimize the quantity

$$\chi^2\left(a_1, a_2, \ldots a_n\right) = \sum_{i=1}^{157} \frac{\left(\mu_{obs}(z_i) - \mu_{th}(z_i)\right)^2}{\sigma^2_{i,total}} \tag{5.45}$$

Eq.(5.45) is exactly the same as the general one from Ref.[126]. The process of minimization that we follow, is the one in the appendix from Ref.[127] and can be seen below

$$\chi^2\left(a_1, a_2, \ldots a_n\right) = \sum_{i=1}^{157} \frac{\left(\mu_{obs}(z_i) - \mu_{th}(z_i)\right)^2}{\sigma^2_{i,total}} \xRightarrow{Eq.(5.31)}$$

$$\Rightarrow \chi^2\left(a_1, a_2, \ldots a_n\right) = \sum_{i=1}^{157} \frac{\left(\mu_{obs}(z_i) - 5log_{10}\left(D_L(z; s)\right) - \mu_0\right)^2}{\sigma^2_{i,total}}$$

The parameter μ_0 is a nuisance parameter but it is constant, i.e. independent of the data points and the dataset. Now using the very well known identity $(a-b-c)^2 = a^2+b^2+c^2-2ab-2ac+2bc$ we derive[127]

$$\chi^2\left(a_1, a_2, \ldots a_n\right) = \sum_{i=1}^{157} \frac{1}{\sigma^2_{i,total}} (\mu^2_{obs}(z_i) + (5log_{10}D_L)^2 + \mu_0^2 - 2 \times 5log_{10}D_L \cdot \mu_{obs}(z_i) -$$

$$-2\mu_{obs}(z_i) \cdot \mu_0 + 2 \times 5log_{10}D_L \cdot \mu_0) = \sum_{i=1}^{157} \frac{\mu_0^2}{\sigma^2_{i,total}} - 2\mu_0 \sum_{i=1}^{157} \frac{(\mu_{obs}(z_i) - 5log_{10}D_L)}{\sigma^2_{i,total}} +$$

$$+ \sum_{i=1}^{157} \frac{\mu^2_{obs}(z_i) + (5log_{10}D_L)^2 - 2 \times 5log_{10}D_L \cdot \mu_{obs}(z_i)}{\sigma^2_{i,total}} =$$

$$= \sum_{i=1}^{157} \frac{\mu_0^2}{\sigma^2_{i,total}} - 2\mu_0 \sum_{i=1}^{157} \frac{(\mu_{obs}(z_i) - 5log_{10}D_L)}{\sigma^2_{i,total}} + \sum_{i=1}^{157} \frac{\mu^2_{obs}(z_i) - \mu^2_{th}(z_i; a_1, \ldots a_n, \mu_0 = 0) - 2\mu_{obs}(z_i) \cdot \mu_{th}(z_i)}{\sigma^2_{i,total}}$$

$$\Rightarrow \chi^2\left(a_1, a_2, \ldots a_n\right) = A(a_1, \ldots a_n) - 2\mu_0 B(a_1, \ldots a_n) + \mu_0^2 C(a_1, \ldots a_n) \tag{5.46}$$

[5]For an introduction to statistical physics and the χ^2 *function* see Chapter 15 from Ref.[126]

where[127]

$$A(a_1,\dots a_n)=\sum_{i=1}^{157}\frac{\left(\mu_{obs}(z_i)-\mu_{th}(z_i;\mu_0=0,a_1,\dots a_n)\right)^2}{\sigma^2_{i,total}}$$
$$B(a_1,\dots a_n)=\sum_{i=1}^{157}\frac{\mu_{obs}(z_i)-\mu_{th}(z_i;\mu_0=0,a_1,\dots a_n)}{\sigma^2_{i,total}}$$
$$C(a_1,\dots a_n)=\sum_{i=1}^{157}\frac{1}{\sigma^2_{i,total}} \tag{5.47}$$

Now we are ready to compute the minimum of Eq.(5.46) with respect to μ_0 as follows

$$\frac{d\chi^2(a_1,\dots,a_n)}{d\mu_0}=0\Rightarrow -2B+2\mu_0 C=0\Rightarrow \chi^2(a_1,\dots,a_n)\text{ has a minimum for }\mu_0=\frac{B}{C} \tag{5.48}$$

and the minimum of Eq.(5.48) is at

$$\chi^2(a_1,\dots,a_n)=A-\frac{2B^2}{C}+\frac{B^2}{C^{\cancel{2}}}\cdot\cancel{C}\Rightarrow\chi^2(a_1,\dots,a_n)=A(a_1,\dots a_n)-\frac{B(a_1,\dots a_n)^2}{C(a_1,\dots a_n)} \tag{5.49}$$

Thus we can minimize Eq.(5.49) instead of Eq.(5.46) which is independent of μ_0.

Alternatively we could have performed a uniform marginalization over the nuisance parameter μ_0 thus obtaining

$$\chi^2(a_1,\dots,a_n)=A(a_1,\dots a_n)-\frac{B(a_1,\dots a_n)^2}{C(a_1,\dots a_n)}+ln\left(\frac{C(a_1,\dots a_n)}{2\pi}\right) \tag{5.50}$$

to be minimized with respect to $a_1,\dots,a_n$. This is the particular quantity that we will minimize in our numerical analysis. The Eq.(5.50) for the ΛCDM model and quintessence model for various slopes of s can be seen in the matrix constructed for the Gold dataset[6] below[70]

Models for Study for Gold Dataset		
Type	s	$\chi^2_{s_i}$
ΛCDM	0	183.275
$QM_{s=0.1}$	0.1	183.332
$QM_{s=0.2}$	0.2	183.346
$QM_{s=0.5}$	0.5	183.497
$QM_{s=1.0}$	1.0	184.355
$QM_{s=1.5}$	1.5	186.593
$QM_{s=2.0}$	2.0	191.163
$QM_{s=2.5}$	2.5	198.511
$QM_{s=3.0}$	3.0	208.969

The 1σ error of s (1 parameter) is determined by the relation[115, 126]

$$\Delta\chi^2_{1\sigma}=\chi^2(s_{1\sigma})-\chi^2_{min}=1 \tag{5.51}$$

i.e. s in the range $[s_0;s_{1\sigma}]$ with 68% probability. Similarly the 2σ error (95.4% range) is determined by $\Delta\chi^2_{2\sigma}=4$ and the 3σ error (99% range) by $\Delta\chi^2_{3\sigma}=6.63$. These differences concern 1 parameter. For more parameters we construct the following table

[6]The Gold dataset points can be found in a txt form in [70]

Number of Parameters	1σ error	2σ error	3σ error
1	1	4	6.63
2	2.3	6.17	9.21
3	3.53	8.02	11.34

The following Fig.5.8 shows the plot of the differences $\Delta\chi^2(s) = \chi^2(s) - \chi^2(s \simeq 0)$ with respect to the cosmological constant for quintessence models[70]

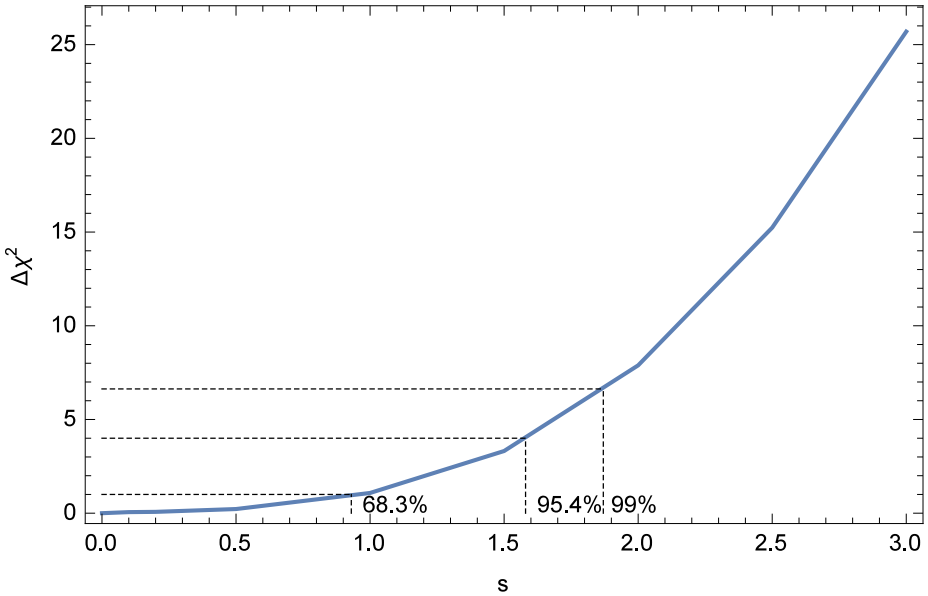

Figure 5.8: The differences $\Delta\chi^2(s) = \chi^2(s) - \chi^2(s \simeq 0)$ for quintessence models with various values of $s = \{0, 0.1, 0.2, 0.5, 1.0, 1.5, 2.0, 2.5, 3.0\}$.

As it can be seen for the matrix above and Fig.5.8 the best model fit is the ΛCDM model.

5.2.2.2 χ^2 Analysis for Union2.1 Dataset

Next we will follow the same procedure for another Dataset, the Union2.1[125], which is a complication of 580 data. Working as in Subsubsection 5.2.2.1, we can find the goodness of fit to the corresponding observed Hubble free luminosity distance coming from the SnIa of the Union2.1 Dataset[7]. Hence we construct the corresponding matrix[70]

Models for Study for Union2.1 Dataset		
Type	s	$\chi^2_{s_i}$
ΛCDM	0	570.264
$QM_{s=0.1}$	0.1	571.603
$QM_{s=0.2}$	0.2	571.742
$QM_{s=0.5}$	0.5	572.476
$QM_{s=1.0}$	1.0	576.598
$QM_{s=1.5}$	1.5	586.317
$QM_{s=2.0}$	2.0	605.752
$QM_{s=2.5}$	2.5	636.348
$QM_{s=3.0}$	3.0	679.423

and the same figure as Fig.5.8 as it can be seen below[70]

[7]The Union2.1 dataset points can be found here

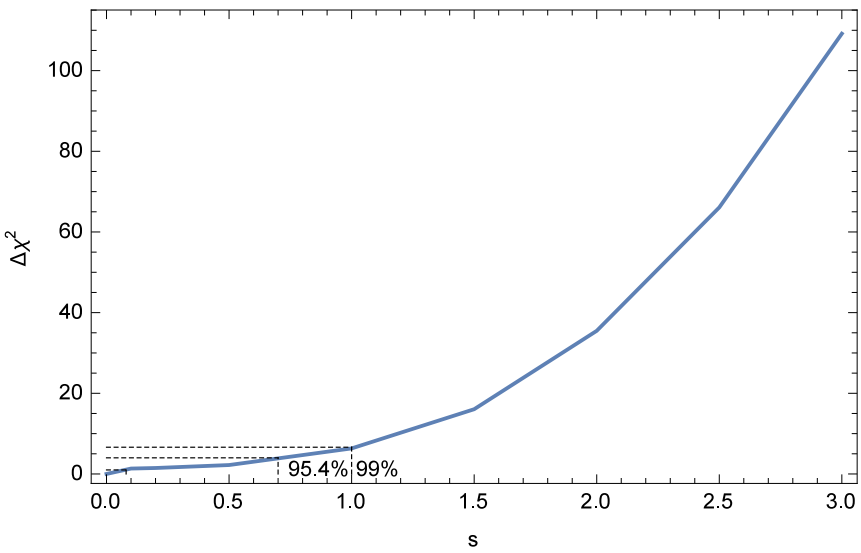

Figure 5.9: The differences $\Delta\chi^2(s) = \chi^2(s) - \chi^2(s \simeq 0)$ for quintessence models with various values of $s = \{0, 0.1, 0.2, 0.5, 1.0, 1.5, 2.0, 2.5, 3.0\}$.

From the above graphic, we conclude that the best fit provided for quintessence models is obtained for $s \simeq 0$. For $s = 0$ one can see that $\Delta\chi^2$ is smaller than any $\Delta\chi^2$ which corresponds to any value of s. That is due to the fact that the Union2.1 Dataset has 580 data, which makes our model more sensitive and gives larger initial value for χ^2. It is important to remember that in the aforementioned matrices the value of s that corresponds to the ΛCDM is not exactly zero. The quintessence model for small value of s (very close to zero) leads to a very small kinetic term of the field, mimicking the ΛCDM model.

From the above analysis we conclude that regardless of the dataset that we use the ΛCDM is the best fit and quintessence field theory models have serious difficulty to exceed the quality of fit for the particular potential of a cosmological constant despite of the additional parameters.

5.3 Fits to equation of state parametrizations

5.3.1 Linear Ansanz(L.A.)

We are thus faced with the following question "What are the particular features required by $w(z)$ for better fits to the SnIa data?". To address this question we can use arbitrary parametrizations of $w(z)$ and identify the forms of $w(z)$ that best fit the data. The best fit forms of $w(z)$ have the following common properties

- The value of $w(z = 0)$ at best fit was found to be in the range $-2 < w(z = 0) < -1$
- The function $w(z)$ at best fit was found to cross the PDL from below at least once with $\frac{dw}{dz} >$ in the range $0 < z < 1$.

As a possible solution, in order to find a better fit to data, one could consider two other dynamical parametrizations of dark energy which are commonly used in the literature considering the equation of state $w(z)$. The main advantage of such parametrizations is that we could introduce parameters and minimize the χ^2 below the χ^2 of ΛCDM model.

First let us consider a linear ansanz[115]

$$w(z) = w_0 + w_1 z \tag{5.52}$$

Let us be a little more explicit expressing the equation of state parameter in terms of $H(z)$, $\frac{dH}{dz}$ and Ω_{0m} using the definitions of Friedmann equation and of the deceleration parameter as follows

$$H^2 = \left(\frac{\dot{a}}{a}\right)^2 = \frac{8\pi G}{3}\left(\rho_m + \rho_{DE}\right) \Rightarrow \frac{3H^2}{8\pi G} = \rho_m + \rho_{DE} \text{ and} \tag{5.53}$$

$$q = -\frac{\ddot{a}}{aH^2} = \frac{4\pi G}{3H^2}\left[\rho_m + (\rho_{DE} + 3p_{DE})\right] \Rightarrow \frac{4\pi G}{3H^2}\cdot\frac{3H^2}{8\pi G} + 3p_{DE}\cdot\frac{4\pi G}{3H^2} \Rightarrow$$
$$\Rightarrow q = \frac{1}{2} + p_{DE}\frac{4\pi G}{H^2} \Rightarrow p_{DE} = \frac{H^2}{4\pi G}\left(q - \frac{1}{2}\right) \tag{5.54}$$

Using Eq.(5.53) and Eq.(5.54) one can see

$$w(z) = \frac{p_{DE}}{\rho_{DE}} = \frac{\frac{H^2}{4\pi G}\left(q - \frac{1}{2}\right)}{\frac{3H^2}{8\pi G} - \rho_m} = \frac{\frac{H^2}{4\pi G}\left(q - \frac{1}{2}\right)}{\frac{3H^2}{8\pi G}\left(1 - \frac{8\pi G}{3H^2}\rho_m\right)} = \frac{2\left(q - \frac{1}{2}\right)}{3\left(1 - \Omega_m\right)} = \frac{2q - 1}{3\left(1 - \Omega_m\right)} \tag{5.55}$$

where $\Omega_m = \rho_m \frac{8\pi G}{3H^2} = \Omega_{0m}(1+z)^3 \frac{{H_0}^2}{H^2}$. Using now the definitions of q and H it is easy to show that

$$q = -1 + (1+z)\frac{dlnH}{dz} \tag{5.56}$$

Substituting Eq.(5.56) in Eq.(5.55) we obtain

$$w(z) = \frac{2q-1}{3(1-\Omega_m)} = \frac{2\left(-1 + (1+z)\frac{dlnH}{dz}\right) - 1}{3(1-\Omega_m)} = \frac{-2 - 1 + 2(1+z)\frac{dlnH}{dz}}{3(1-\Omega_m)} = \frac{-3 + 2(1+z)\frac{dlnH}{dz}}{3(1-\Omega_m)} \Rightarrow$$
$$\Rightarrow w(z) = \frac{\frac{2}{3}(1+z)\frac{dlnH}{dz} - 1}{1 - \Omega_m} \Rightarrow w(z) = \frac{\frac{2}{3}(1+z)\frac{dlnH}{dz} - 1}{1 - \Omega_{0m}(1+z)^3\frac{{H_0}^2}{H^2}} \tag{5.57}$$

Using now Eq.(5.57) we can obtain the Hubble parameter $H(z)$, with the assistance of Mathematica, corresponding to the $w(z)$ of Eq(5.52) as

$$H^2(z) = {H_0}^2\left[\Omega_{0m}(1+z)^3 + (1-\Omega_{0m})(1+z)^{3(1+w_0-w_1)}e^{3w_1 z}\right] \tag{5.58}$$

Eq.(5.58) can now be used to obtain the $D_L^{th}(z; w_0, w_1)$ from Eq.(5.23) and minimize the χ^2 obtained from the Gold dataset. Using the Gold dataset, the best fit parameter values for this ansanz are $(w_0, w_1) = (-1.40 \pm 0.40, 1.66 \pm 1.42)$ giving $\chi^2 = 180.568$ at the minimum. However the difference lies in the 1σ error level as it can be seen in the following figure[70]

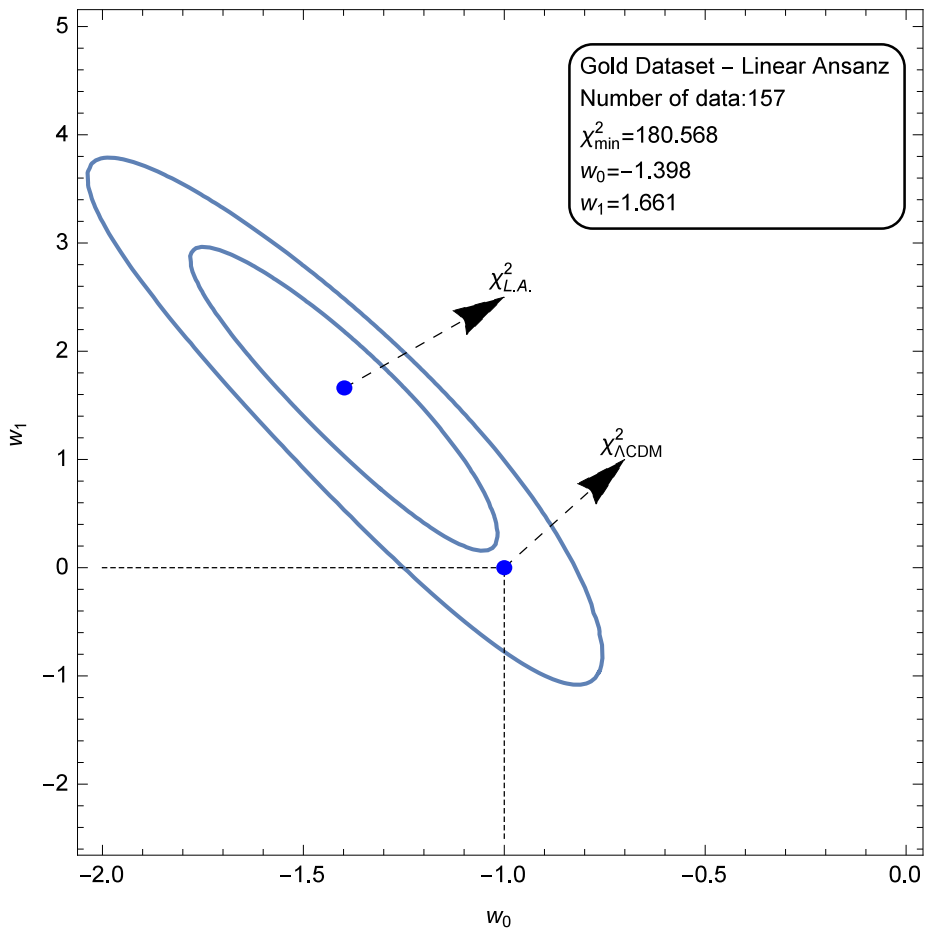

Figure 5.10: The 1σ and 2σ confidence contours level of Linear Ansanz. A prior $\Omega_{0m} = 0.309$ has been used

5.3.2 CPL Ansanz

Next we consider the Chevallier-Polarski-Linder (CPL) ansanz[128, 129] which is based on a linear expansion with respect to the scale factor around its present value $a(t_0) = 1$ and is of the form

$$w(z) = w_0 + w_1 \frac{z}{1+z} \tag{5.59}$$

where z is the redshift corresponding to the scale factor. The ansanz varies between w_0 at $z = 0$ and $w_0 + w_1$ at $z \to \infty$ with crossover at $z = 1$ where the two values contribute equally. The existence of such a crossover has the advantage that observations near it apply to a reduced parameter phase space, hence the remaining parameter estimates are more sensitive. The Hubble parameter corresponding to this ansanz is

$$H^2(z) = {H_0}^2 \left[\Omega_{0m}(1+z)^3 + (1-\Omega_{0m})\,(1+z)^{3(1+w_0+w_1)} e^{3w_1\left(\frac{1}{z+1}-1\right)}\right] \tag{5.60}$$

The best fit parameter values for this ansanz are $(w_0, w_1) = (-1.57 \pm 0.51, 3.25 \pm 2.74)$ giving $\chi^2 = 180.132$ at the minimum. The errors are also for this particular parametrization at the 1σ error level as it can be seen in the following contour plots[70]

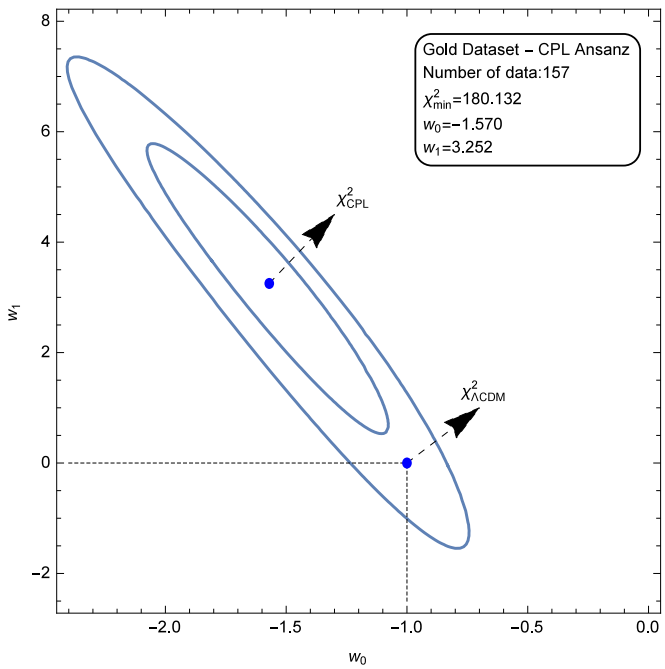

Figure 5.11: The 1σ and 2σ confidence contours level of CPL Ansanz. A prior $\Omega_{0m} = 0.309$ has been used

These parametrizations were chosen for their simplicity and for leading to fairly good fits to the data relatively to other parametrizations. Both of these ansanzs they share both of the properties referred above as it can be seen in Fig.5.12[70]

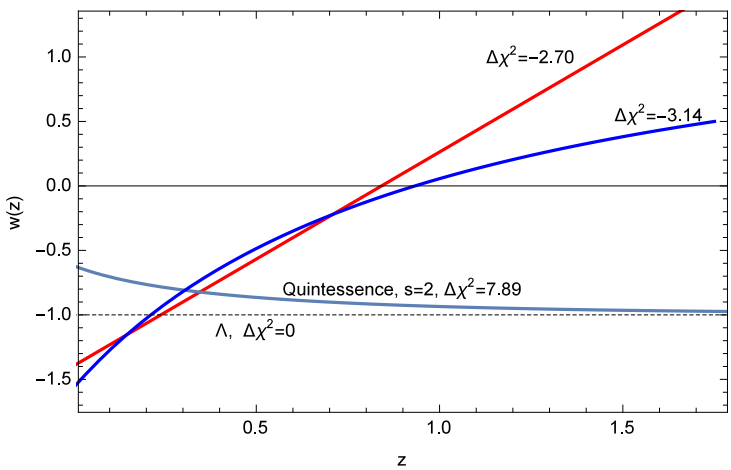

Figure 5.12: The evolution of w for the field theory models studied here superposed with two better fits obtained by arbitrary parametrization: L.A.(Red Line) and CPL Ansanz(Blue Line)

From the above analysis we see that the field theory models which do not cross the PDL have positive $\Delta\chi^2$ and therefore they provide worse fits than ΛCDM. In particular for the linear ansanz Eq.(5.52) we find $\Delta\chi^2 = -2.70734$ while for the smoother ansanz CPL of Eq.(5.59) we find $\Delta\chi^2 = -3.14334$. These differences mean that the point $(w_0, w_1) = (-1, 0)$ corresponding to the cosmological constant from the viewpoint of these parametrizations, lies in the 1σ region from the best fits obtained from these parametrizations. The ideal would be if the difference

$\Delta\chi^2 \geq 6.17 = \Delta\chi^2_{2\sigma}$ i.e. the point $(w_0, w_1) = (-1, 0)$ corresponding to the cosmological constant from the viewpoint of these parametrizations, to lie in the 2σ region from the best fits obtained from these parametrizations.

Model selection is the problem of distinguishing competing models, perhaps featuring different numbers of parameters. One could naively consider a model with many parameters which could give the desirable result, i.e. $\Delta\chi^2 \geq 6.17 = \Delta\chi^2_{2\sigma}$. The value of $\Delta\chi^2_{2\sigma}$ which corresponds to the 2σ region was calculated via[130]

$$P = \frac{1}{2\Gamma(n,2)} \int_0^{\frac{\Delta\chi^2_{2L}}{2}} \left(\frac{x}{2}\right)^{\frac{n}{2}-1} e^{-\frac{x}{2}} dx = 1 - \frac{\Gamma\left(\frac{n}{2}, \frac{\Delta\chi^2_{2L}}{2}\right)}{\Gamma\left(\frac{n}{2}\right)} \tag{5.61}$$

where n are the number of parameters of our model, $\Gamma(a)$ is the very well known Euler gamma function and $\Gamma(a, z)$ is the incomplete gamma function. For these parametrizations we set in Eq.(5.61) $n = 2$ and in order to obtain $P = 68\%$, i.e the 1σ error we set $\Delta\chi^2_{1L} = 2.3$. Similarly for the 2σ error the difference $\Delta\chi^2_{2L} = 6.17$.

There are many other parametrizations that have produced more desirable results[115]. Hence one should face the following question "How can we be sure that our model is correct?". It seems like a trick that we can induce some extra parameters and suddenly obtain the *"correct"* model. Fortunately the statistics literature contains two distinct sets of tools based on information theory such as the Akaike Information Criterion (AIC) and the Bayesian Information Criterion (BIC)[8]. These are measures of the relative quality of statistical models (parametrizations) for a given set of data which penalize models for the number of their parameters.

5.4 Information Criteria

In general, a model is a choice of parameters to be varied and a prior probability distribution on those parameters. The goal of model selection is to balance the quality of fit to observational data against the complexity, or predictiveness, of the model achieving that fit. This tension is achieved through model selection statistics, which attach a number to each model enabling a rank-ordered list to be drawn up. Typically, the best model is adopted and used for further inference such as permitted parameter ranges, though the statistics literature has also seen increasing interest in multi-model inference combining a number of adequate models.

Model selection is the problem of distinguishing competing models, perhaps featuring different numbers of parameters. One could naively consider a model with many parameters which could give the desirable result, i.e. $\Delta\chi^2 \geq \Delta\chi^2_{2\sigma}$. There are many other parametrizations that have produced more desirable results[94]. Hence one should face the following question "How can we be sure that our model is correct?". It seems like a trick that we can induce some extra parameters and suddenly obtain the *"correct"* model. Fortunately the statistics literature contains two distinct sets of tools those based on information theory such as like the Akaike Information Criterion (AIC)[131] and the Bayesian Information Criterion (BIC)[132]. These are measures of the relative quality of statistical models (parametrizations) for a given set of data which penalize models for the number of their parameters. Let us study these models separately

5.4.1 Akaike Information Criterion (AIC)

In order to understand the Akaike Information Criterion[131] we have to remember the "Kullback–Leibler Information(K-L)" because Akaike used this particular model in order to obtain his

[8]See Appendix C

criterion. Let us then begin without any issues of parameter estimation and deal with very simple expressions for the models f and g, assuming that they are completely known. Initially we will let both f and g be simple probability distributions, since this will allow an understanding of K-L information or distance between two models in a simple setting. However, we will soon switch to the concept that f is a notation for full reality or truth. We use g to denote an approximating model in terms of a probability distribution [133]

Kullback–Leibler Information

Kullback-Leibler information between models f and g is defined for continuous functions as the (usually multi-dimensional) integral

$$I(f,g) = \int f(x) log\left(\frac{f(x)}{g(x|\theta)}\right) dx$$

where log denotes the natural logarithm. The notation $I(f,g)$ denotes the "information lost when g is used to approximate f". As a heuristic interpretation, $I(f,g)$ is the distance from g to f .

We will use both interpretations throughout this section, since both seem useful. Of course, we seek an approximating model that loses as little information as possible. This is equivalent to minimizing $I(f,g)$, over g. Full reality f is considered to be given (fixed), and only g varies over a space of models indexed by θ. Similarly, Cover and Thomas[134] note that the K-L distance is a measure of the inefficiency of assuming that the distribution is g when the true distribution is f[133]

Kullback–Leibler Information(KL information)

The expression for the Kullback-Leibler information or distance in the case of discrete distributions such as the Poisson, binomial, or multinomial is

$$I(f,g) = \sum_{i=1}^{k} p_i log\left(\frac{p_i}{\pi_i}\right)$$

Here, there are k possible outcomes of the underlying random variable; the true probability of the i_{th} outcome is given by p_i, while the $\pi_1, \ldots, \pi_k$ constitute the approximating probability distribution (i.e., the approximating model). As in the continuous care the notation $I(f,g)$ denotes the information lost when g is used to approximate f or the distance from g to f.

In the following material we will generally think of K-L information in the continuous case and use the notation f and g for simplicity. The material above makes it obvious that both f and g (and their parameters) must be known to compute the K-L distance between these two models. However, if only relative distance is used, this requirement is diminished, since $I(f,g)$ can be written equivalently as

$$I(f,g) = \int f(x)\, log(f(x)) - \int f(x)\, log(g(x|\theta)) \tag{5.62}$$

Note that each of the two terms on the right of the above expression is a statistical expectation with respect to f (truth). Thus, the K-L distance (above) can be expressed as a difference between

two statistical expectations

$$I(f,g) = E_f\left[log(f(x))\right] - E_f\left[log(g(x|\theta))\right] \tag{5.63}$$

each with respect to the distribution f. This last expression provides easy insights into the derivation of AIC.

The first expectation $E_f\left[log(f(x))\right]$ is a constant that depends only on the unknown true distribution, and it is clearly not known (i.e., we do not know f in actual data analysis). Therefore, treating this unknown term as a constant, a measure of relative directed distance is possible. Clearly, if one computed the second expectation $E_f\left[log(g(x|\theta))\right]$ one could estimate $I(f,g)$ up to a constant C, namely $E_f\left[log(f(x))\right]$.

$$I(f,g) = C - E_f\left[log(g(x|\theta))\right] \Rightarrow I(f,g) - C = -E_f\left[log(g(x|\theta))\right]$$

The term $I(f,g) - C$ is a relative directed distance between f and g. Thus, $E_f\left[log(g(x|\theta))\right]$ becomes the quantity of interest for selecting a best model.

Akaike's [131] seminal paper proposed the use of the Kullback-Leibler information or distance as a fundamental basis for model selection. However, K-L distance cannot be computed without full knowledge of both f (full reality) and the parameters (θ) in each of the candidate models $g_i(x|\theta)$. Akaike found a rigorous way to estimate K-L information, based on the empirical log-likelihood function at its maximum point.

In data analysis the model parameters must be estimated, and there is usually substantial uncertainty in this estimation. Models based on estimated parameters, hence on $\hat{\theta}$ not θ, represent a major distinction from the case where model parameters would be known. This distinction affects how we must use K-L distance as a basis for model selection. Akalke showed that the critical issue for getting an applied K-L model selection criterion was to estimate[133]

$$E_y E_x\left[log\left(g(x|\hat{\theta}(y))\right)\right]$$

where x and y are independent random samples from the same distribution and both statistical expectations are taken with respect to truth f. This double expectation, both with respect to truth f, is the target of all model selection approaches, based on K-L information.

It is tempting to just estimate $E_y E_x\left[log\left(g(x|\hat{\theta}(y))\right)\right]$ by the maximized $Log\left(L(\theta)|data\right)$ for each model g_i . However, Akalke showed, in 1973[131], that the maximized log-likelihood is biased upward as an estimator of the model selection target. He also found that under certain conditions (these conditions are important, but quite technical) this bias is approximately equal to K, the number of estimable parameters in the approximating model. This is an asymptotic result of fundamental importance.

Thus, an approximately unbiased estimator of $E_y E_x\left[log\left(g(x|\hat{\theta}(y))\right)\right]$ for large samples and "good" models is $Log\left(L(\theta)|data\right) - K$. Akaike's finding of a relation between the relative expected K-L distance and the maximized log-likelihood has allowed major practical and theoretical advances in model selection and the analysis of complex data sets. The final form of the Akaike Information Criterion was obtained in its final form when in 1973 he multiplied $Log\left(L(\theta)|data\right) - K$ by -2 ("taking historical reasons into account") to obtain the final formula

$$AIC = -2Log\left(L(\theta)|data\right) + 2K \tag{5.64}$$

where the expression $-2Log\left(L(\theta)|data\right) = \chi^2$ [9], i.e the numerical value of the log-likelihood at its maximum point and k is the number of parameters of the model. This has become known as Akaike's information criterion or AIC.

[9] This particular equation holds true for gaussian distributed variables only.

Let us see how our parametrizations are penalised by the AIC. We will calculate the AIC for the ΛCDM, the Linear Ansanz and the CPL Ansanz. Of course the best model is the one which minimizes the AIC

$$\begin{aligned} AIC_{\Lambda CDM} &= 2k + \chi^2 = 2 \cdot 1 + 183.275 = 185.275 \\ AIC_{Linear} &= 2k + \chi^2 = 2 \cdot 2 + 180.568 = 184.568 \\ AIC_{CPL} &= 2k + \chi^2 = 2 \cdot 2 + 180.132 = 184.132 \\ \Delta_{AIC_{Linear}} &= -0.707 \\ \Delta_{AIC_{CPL}} &= -1.143 \end{aligned}$$

Thus we can see that the general parametrizations give a better result considering the AIC. Let us now see and the Bayesian Information Criterion.

5.4.2 Bayesian Information Criterion (BIC)

Another fundamental criterion in statistical mechanics is the Bayesian Information Criterion (BIC). The BIC was introduced by Schwarz in 1978[132] and is defined as

$$BIC = -2Log\left(L(\theta)|data\right) + klnN \tag{5.65}$$

where N is the number of data-points used in the fit. BIC arises from a Bayesian viewpoint with equal prior probability on each model and very vague priors on the parameters, given the model. The assumed purpose of the BIC-selected model was often simple prediction. The BIC assumes that the data-points are independent and identically distributed, which may or may not be valid depending on the dataset under consideration (e.g. it is unlikely to be good for cosmic microwave anisotropy data, but may well be for supernova luminosity-distance data).

Using the process above one can calculate

$$\begin{aligned} BIC_{\Lambda CDM} &= \chi^2 + klnN = 183.275 + 1 \cdot ln157 = 183.275 + 1 \cdot 5.06 = 188.331 \\ BIC_{Linear} &= \chi^2 + klnN = 180.568 + 5.06 = 185.624 \\ BIC_{CPL} &= \chi^2 + klnN = 180.132 + 5.06 = 185.302 \\ \Delta_{BIC_{Linear}} &= -2.707 \\ \Delta_{BIC_{CPL}} &= -3.029 \end{aligned}$$

As we can see from the above calculations considering the BIC, the general ansanzs give better fit and the two criteria agree in that. Unfortunately the fact that the difference of Δx^2 corresponding to the cosmological constant is not in the 2σ regions tells us that these particular parametrizations are not significantly better than the ΛCDM model.

5.5 Constraints on Scalar Tensor Quintessence Models

It should be pointed out that in the context of the Union2.1 and Gold datasets, parametrizations that allow for crossing of the PDL do not seem to have a significant advantage from the ΛCDM model since the χ^2 lies inside the 2σ confidence level. This indicates that either we must wait until further SnIa datasets are released or we should look for an alternative theory which describes the dark energy, i.e a model of the second class of models that we mentioned before. A representative model of this particular category is provided by scalar-tensor theories of gravity,

which theoretical equations were studied in detail in Chapter 4. These particular models have the additional advantage of providing a potential solution to the origin problem as the physical origin of the scalar field is the dynamical "Newton's constant" $F(\phi)$, which is minimally coupled to to the curvature scalar R.

5.5.1 Evolution of the ϕ Field and the Scale Factor

In this subsection we will study the cosmological dynamics of scalar tensor cosmological models. In order to do that, we will use the dynamical equation for the scale factor that we have already derived, i.e. Eq.(4.31) as well as Eq.(4.16). These equations along with the initial conditions represent a coupled system which can be solved numerically.

Subsequently we assume initial conditions deep in the matter era ($t \ll t_0$) when the scalar field is assumed frozen at $\phi(t_i) = \phi_i(\dot{\phi}(t_i) = 0)$. At that time we can ignore the $\phi-$terms of Eq.(4.31). Thus all the $\phi-$terms tend to zero, i.e.

$$\frac{\dot{\phi}^2}{3F} \to 0, \quad \frac{\bar{V}(\phi)}{3F} \to 0, \quad \bar{H}\frac{\dot{F}(\phi)}{2F(\phi)} \to 0, \quad \frac{\ddot{F}}{2F(\phi)} \to 0$$

Hence Eq.(4.31) can be written as

$$\frac{\ddot{a}}{a} = -\frac{\Omega_{0m}F_0}{2a^3F_i} \tag{5.66}$$

In the case of a matter dominated flat universe with dark energy, i.e. our case, in an FRW spacetime the *first (order) Friedmann equation* can be written as

$$\left(\frac{\dot{a}}{a}\right)^2 = \frac{\Omega_{0m}{F_0}^2}{{F_i}^2a^3} \Rightarrow \frac{\dot{a}}{a} = \frac{\sqrt{\Omega_{0m}}F_0}{a^{3/2}F_i} \Rightarrow \frac{da}{dt}\sqrt{a} = \sqrt{\Omega_{0m}}\frac{F_0}{F_i} \Rightarrow da\sqrt{a} = \sqrt{\Omega_{0m}}\frac{F_0}{F_i}dt \overset{\int}{\Rightarrow}$$
$$\overset{\int}{\Rightarrow} \frac{2}{3}a^{3/2} = \sqrt{\Omega_{0m}}\frac{F_0}{F_i}t \Rightarrow a^{3/2} = \frac{3F_0}{2F_i}\sqrt{\Omega_{0m}}t \Rightarrow a(t_i) = \left(\frac{3F_0}{2F_i}\sqrt{\Omega_{0m}}t\right)^{2/3} \Rightarrow a(t_i) = \left(\frac{9F_0}{4F_i}\Omega_{0m}\right)^{1/3} t^{2/3} \tag{5.67}$$

Taking the derivative of Eq.(5.67) it is straightforward to see

$$\dot{a}(t_i) = \frac{2}{3}\left(\frac{9F_0}{4F_i}\Omega_{0m}\right)^{1/3} t^{-1/3} \tag{5.68}$$

Of course when $F = 1$ Eq.(5.67) and Eq.(5.68) reduce to the usual ones in General Relativity as expected.

In order to solve the system of Eq.(4.31) and Eq.(4.16) with the above initial conditions we tune self-consistently the values of ϕ_i and $F_0 \equiv F(\phi(t_0)) = 1 - \lambda\phi_0$ so that the following consistency conditions are simultaneously satisfied at the present time

$$\begin{gathered} a(t_0) = 1 \\ H(t_0) = 1 \\ \Omega_{0\phi} = 0.7 \\ F(\phi(t_0)) \equiv 1 - \lambda\phi(t_0) = F_0 \end{gathered}$$

In practice we define t_0 as the present time, i.e the time that $a = 1$ and then tune ϕ_i and F_0 in Eq.(4.31) and in the initial conditions (5.67) and (5.68), so that the aforementioned consistency

conditions are simultaneously satisfied at the present time in the numerical solution. Therefore the coupled system that we solve numerically is the following

$$\frac{\ddot{a}}{a} = -\frac{\Omega_{0m} F_0}{2Fa^3} - \frac{\dot{\phi}^2}{3F} + \frac{\bar{V}}{3F} - \frac{\ddot{F}}{2F} - \bar{H}\frac{\dot{F}}{2F} \tag{5.69}$$

$$\ddot{\phi} + 3\frac{\dot{a}}{a}\dot{\phi} - 3\left(\frac{\ddot{a}}{a} + \frac{\dot{a}^2}{a^2}\right) F_\phi + V_\phi = 0 \tag{5.70}$$

$$\dot{\phi}(t_i) = 0 \tag{5.71}$$

$$a(t_i) = \left(\frac{9F_0}{4F_i}\Omega_{0m}\right)^{1/3} t^{2/3} \tag{5.72}$$

$$\dot{a}(t_i) = \frac{2}{3}\left(\frac{9F_0}{4F_i}\Omega_{0m}\right)^{1/3} t^{-1/3} \tag{5.73}$$

During this work a generic form of the potential $V(\phi) = -s\,\phi$ and the linear nonminimal coupling $F(\phi) = 1 - \lambda\,\phi$ is considered. This form, corresponds to a small value of vacuum energy expressed through the potential field $V(\phi)$ and also small deviations from GR expressed through the nonminimal coupling $F(\phi) = 1$. Solving the system numerically, one can obtain the following figure for the scale factor[70]

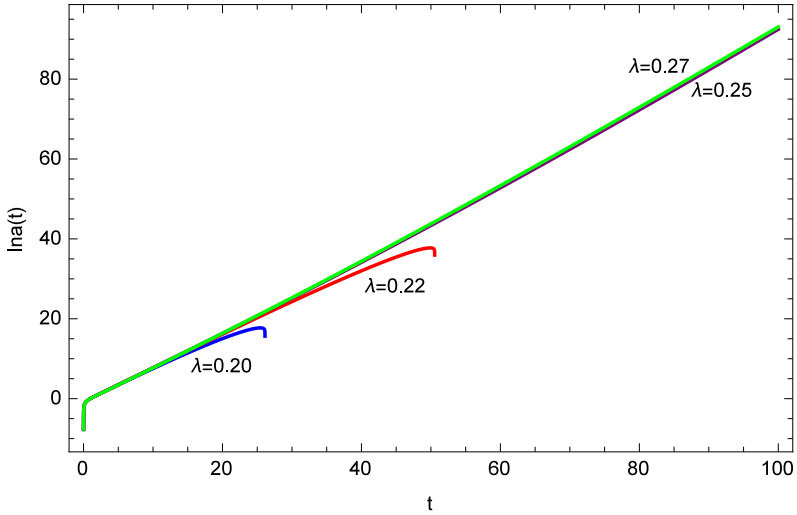

Figure 5.13: The collapse of the scale factor, in a logarithmic scale, for representative quintessence with linear potential, $s = 1$ and various values of slopes λ.

As we can see clearly from Fig.5.13 initially the universe expands with a late time acceleration but soon after the field potential develops to negative values, the scalar field gravitational interaction becomes strongly attractive and the scale factor collapses to a singularity. The curves stop when $F(\phi) \to 0$, i.e Eq.(5.69) is undefined. However, for values of λ larger than a critical value $\lambda_{crit.}$, the nonminimal coupling becomes important and the dynamics of the scalar field change at late times. Instead of rolling down the potential towards larger field values, it starts rolling up its potential towards smaller (negative) field values as dictated by its non-minimal coupling to the metric (lower curves in Fig.5.14), hence shifting away from the Big Crunch Doomsday. This is shown in Fig.5.14 where we present the time evolution of the scalar field for values of λ below and above the critical value which for $s = 1$ is approximately $\lambda_{crit.} \simeq 0.24$[70]

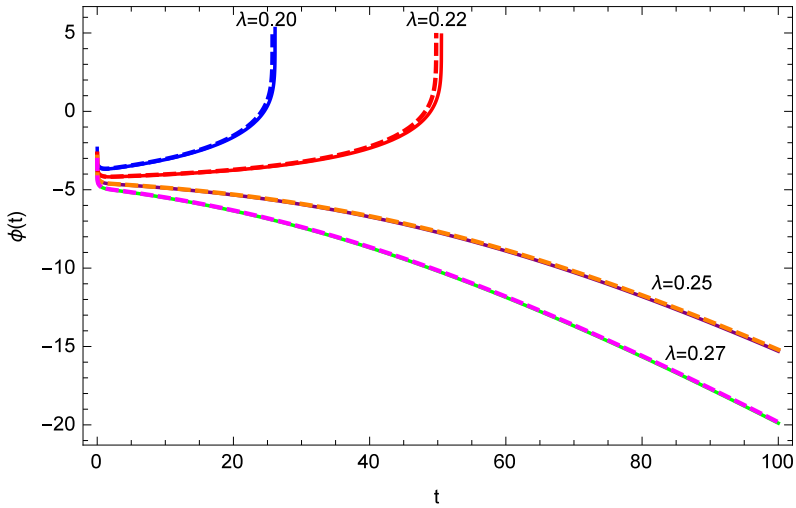

Figure 5.14: The evolution of the scalar field for $s = 1$ and various values of λ, above and below the critical values $\lambda_{crit.} \simeq 0.24$. The solid lines correspond to initial conditions $\dot{\phi}_i = 0$ while the dashed ones correspond to $\dot{\phi}_i = 15$

As we can see from Fig.5.14 the behaviour of the ϕ field is independent from the initial value that we use when we demand the consistency conditions to be satisfied, i.e obtaining a Universe with $H(z = 0) = 1$ and $\Omega_{0\phi} = 0.7$. Thus, it is possible to avoid Cosmic Doomsday[69, 124, 135, 136] with a carefully chosen set of (s, λ), which is a unique feature for models of this nature.

5.5.2 Equation of State

Next we will try some manipulations in order to derive the equation of state parameter w_{DE}. First we rewrite Eq.(4.29) and Eq.(4.30) in a more convenient form as follows

$$3F(\phi)\bar{H}^2 = \bar{\rho}_m + \frac{\dot{\phi}^2}{2} + \bar{V}(\phi) - 3\bar{H}\dot{F} \Rightarrow 3F(\phi)\bar{H}^2 = \frac{\rho_m}{{H_0}^2} + \frac{\dot{\phi}^2}{2} + \bar{V}(\phi) - 3\bar{H}\dot{F} \Rightarrow$$

$$\Rightarrow 3F(\phi)\bar{H}^2 + 3F_0\bar{H}^2 = \frac{\rho_m}{{H_0}^2} + \frac{\dot{\phi}^2}{2} + \bar{V}(\phi) - 3\bar{H}\dot{F} + 3F_0\bar{H}^2 \Rightarrow$$

$$3F_0\bar{H}^2 = \frac{\rho_m}{{H_0}^2} + \frac{\dot{\phi}^2}{2} + \bar{V}(\phi) - 3\bar{H}\dot{F} - 3(F - F_0)\bar{H}^2 \tag{5.74}$$

However in our model the Universe consists of matter and dark energy, thus $\rho_{total} = \rho_m + \rho_{DE}$. As a result, Eq.(5.74) can be written as

$$3F_0\bar{H}^2 = \bar{\rho}_m + \bar{\rho}_{DE} \Rightarrow \bar{\rho}_{DE} = \frac{\dot{\phi}^2}{2} + \bar{V}(\phi) - 3\bar{H}\dot{F} - 3(F - F_0)\bar{H}^2 \tag{5.75}$$

Similarly one can see that

$$-2F(\phi)\left(\frac{\ddot{a}}{a} - \frac{\dot{a}^2}{a^2}\right) = \bar{\rho}_m + \dot{\phi}^2 + \ddot{F} - \bar{H}\dot{F} \Rightarrow -2F(\phi)\frac{\ddot{a}}{a} + 2F(\phi)\frac{\dot{a}^2}{a^2} = \bar{\rho}_m + \dot{\phi}^2 + \ddot{F} - \bar{H}\dot{F} \Rightarrow$$

$$\Rightarrow -2F(\phi)\left(\dot{\bar{H}} + \bar{H}^2\right) + 2F(\phi)\bar{H}^2 = \bar{\rho}_m + \dot{\phi}^2 + \ddot{F} - \bar{H}\dot{F} \Rightarrow$$

$$\Rightarrow -2F(\phi)\dot{\bar{H}} - \cancel{2F(\phi)\bar{H}^2} + \cancel{2F(\phi)\bar{H}^2} = \bar{\rho}_m + \dot{\phi}^2 + \ddot{F} - \bar{H}\dot{F} \Rightarrow -2F(\phi)\dot{\bar{H}} = \bar{\rho}_m + \dot{\phi}^2 + \ddot{F} - \bar{H}\dot{F} \Rightarrow$$

$$\Rightarrow -2F(\phi)\dot{\bar{H}} - 2F_0\dot{\bar{H}} = \bar{\rho}_m + \dot{\phi}^2 + \ddot{F} - \bar{H}\dot{F} - 2F_0\dot{\bar{H}} \Rightarrow$$
$$\Rightarrow -2F_0\dot{\bar{H}} = \bar{\rho}_m + \dot{\phi}^2 + \ddot{F} - \bar{H}\dot{F} + 2(F - F_0)\dot{\bar{H}} + \bar{\rho}_{DE} - \bar{\rho}_{DE} \tag{5.76}$$

But $-2F_0\dot{\bar{H}} = \bar{\rho}_m + \bar{\rho}_{DE} + \bar{p}_{DE}$, hence

$$\bar{p}_{DE} = \dot{\phi}^2 + \ddot{F} - \bar{H}\dot{F} + 2(F - F_0)\dot{\bar{H}} - \frac{\dot{\phi}^2}{2} - \bar{V}(\phi) + 3\bar{H}\dot{F} + 3(F - F_0)\bar{H}^2 \Rightarrow$$
$$\Rightarrow \bar{p}_{DE} = \frac{\dot{\phi}^2}{2} + \ddot{F} - \bar{V}(\phi) + 2\bar{H}\dot{F} + (F - F_0)\left(2\dot{\bar{H}} + 3\bar{H}^2\right) \tag{5.77}$$

Now we are ready to obtain the equation of state parameter w_{DE}, as follows[69]

$$w_{DE} = \frac{\bar{p}_{DE}}{\bar{\rho}_{DE}} = \frac{\frac{1}{2}\dot{\phi}^2 - \bar{V} + \ddot{F} + 2\bar{H}\dot{F} - \left(2\dot{\bar{H}} + 3\bar{H}^2\right)(F_0 - F)}{\frac{1}{2}\dot{\phi}^2 + \bar{V} - 3\bar{H}^2(F - F_0) - 3\bar{H}\dot{F}}$$
$$= \frac{\left[\dot{\phi}^2 - \frac{1}{2}\phi^2\right] + \ddot{F} + \left[3\bar{H}\dot{F} - \bar{H}\dot{F}\right] - \bar{V} - 3\bar{H}^2(F_0 - F) - 2\dot{\bar{H}}(F_0 - F)}{\frac{1}{2}\dot{\phi}^2 + \bar{V} - 3\bar{H}^2(F - F_0) - 3\bar{H}\dot{F}} \Rightarrow$$
$$\Rightarrow w_{DE} = -1 + \frac{\dot{\phi}^2 + \ddot{F} - \bar{H}\dot{F} - 2\dot{\bar{H}}(F_0 - F)}{\frac{1}{2}\dot{\phi}^2 + \bar{V} - 3\bar{H}^2(F - F_0) - 3\bar{H}\dot{F}} \tag{5.78}$$

Let us now return to the usual energy conservation equation, in order to connect the w_{DE} with the observable Hubble parameter, for a pressureless fluid an integrate that equation

$$\frac{d\rho_m}{dt} + 3H\rho_m = 0 \Rightarrow \frac{d\rho_m}{\rho_m} = -3Hdt \overset{\int}{\Rightarrow} \rho_m = \rho_{0m}\left(\frac{a_0}{a(t)}\right)^3 \overset{a_0=1}{\Longrightarrow} \rho_m = \rho_{0m}\frac{1}{a^3} = \rho_{0m}(1+z)^3 \tag{5.79}$$

Using Eq.(4.27), Eq.(5.79) can be written as

$$\rho_m = \frac{\rho_{0m}}{3F_0{H_0}^2}3(1+z)^3{H_0}^2F_0 = 3\Omega_{0m}{H_0}^2(1+z)^3F_0$$

Consequently, the $\bar{\rho}_{DE}$ is defined via the following equation

$$3F_0\bar{H}^2 = \bar{\rho}_m + \bar{\rho}_{DE} = \bar{\rho}_{DE} + \frac{\rho_m}{{H_0}^2} = \bar{\rho}_{DE} + 3\Omega_{0m}(1+z)^3F_0 \Rightarrow \bar{\rho}_{DE} = 3F_0\bar{H}^2 - 3\Omega_{0m}(1+z)^3F_0 \tag{5.80}$$

Similarly for the pressure $\bar{p}_{DE}$

$$-2F_0\dot{\bar{H}} = \bar{\rho}_m + \bar{\rho}_{DE} + \bar{p}_{DE} \Rightarrow \bar{p}_{DE} = -2F_0\dot{\bar{H}} - 3F_0\bar{H}^2 \tag{5.81}$$

Now we are ready to compute w_{DE} rewriting the dark energy state parameter using Eq.(5.80) and Eq.(5.81) as follows

$$w_{DE} = \frac{\bar{p}_{DE}}{\bar{\rho}_{DE}} = \frac{-2F_0\dot{\bar{H}} - 3F_0\bar{H}^2}{3F_0\bar{H}^2 - 3\Omega_{0m}(1+z)^3F_0} = \frac{-2\dot{\bar{H}} - 3\bar{H}^2}{3\bar{H}^2 - 3\Omega_{0m}(1+z)^3} \tag{5.82}$$

Eq.(5.82) is quite similar to Eq.(3.14) from Ref.[69]. All we need to do is to rewrite the term $-2\dot{\bar{H}}$ as follows

$$\dot{\bar{H}} = \frac{d\bar{H}}{dt} = \frac{d\bar{H}}{dz}\frac{dz}{dt}$$
$$\bar{H} = \frac{\dot{a}}{a} = (z+1)\frac{d}{dt}\left(\frac{1}{z+1}\right) = -\frac{dz/dt}{z+1} \Rightarrow \frac{dz}{dt} = -\bar{H}(z+1) \text{ hence } \dot{\bar{H}} = -\frac{d\bar{H}}{dz}\bar{H}(z+1)$$

Also one can easily see that

$$\frac{d\bar{H}^2(z)}{dz} = 2\bar{H}(z)\frac{d\bar{H}}{dz} \Rightarrow \frac{d\bar{H}}{dz} = \frac{d\bar{H}^2(z)}{dz}\frac{1}{2\bar{H}(z)}$$

Hence

$$2\dot{\bar{H}} = -\cancel{2}\frac{d\bar{H}^2(z)}{dz}\frac{1}{\cancel{2}\cancel{\bar{H}(z)}}\cancel{\bar{H}(z)}(z+1) = -\frac{d\bar{H}^2(z)}{dz}(z+1) \tag{5.83}$$

Comparing Eq.(5.83) and (5.82) the equation of state parameter is given by[69]

$$w_{DE} = \frac{3\bar{H}^2(z) - (1+z)\frac{d\bar{H}^2(z)}{dz}}{3\bar{H}^2(z) - 3\Omega_{0m}(1+z)^3} \tag{5.84}$$

Let us now numerically[10] study equation Eq.(5.78) by solving the aforementioned dynamical system. At early times, for $\lambda < \lambda_{crit.}$, the w_{DE} reaches the value -1, when the potential energy dominates over the kinetic energy. However, when the potential becomes negative, the w_{DE} departs towards positive values, leading to infinite attractive gravity and a Big Crunch singularity at a finite future time. In contrast, if $\lambda > \lambda_{crit.}$ the w_{DE} remains stable in the value -1. This can be seen in the Fig.5.15 below[70]

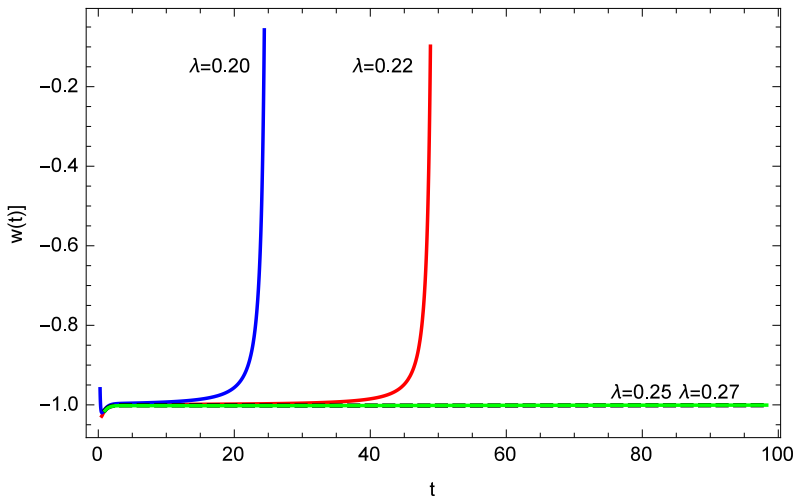

Figure 5.15: The evolution of the equation of state parameter for $s = 1$ and values of λ above and below the critical values $\lambda_{crit(s=1)} = 0.24$

We have repeated the above analysis for various values of s of the potential in order to obtain the λ_{crit} as a function of s. For small values of the slope s, the dynamics leading to a singularity can be reversed by increasing the value of the coupling parameter λ. The required value of λ for reversal of the doomsday dynamics, i.e. $\lambda_{crit.}$, increases almost linearly with s as shown in Fig.5.16[70]

[10] See Appendix C

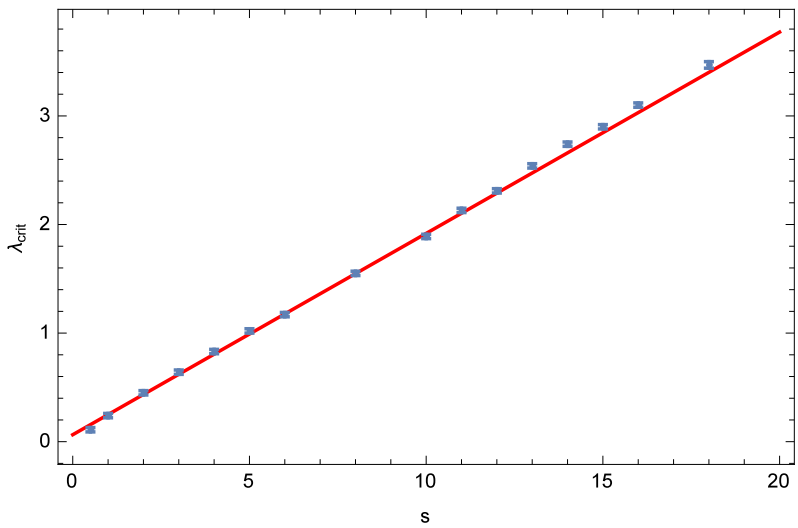

Figure 5.16: The critical value of λ for various values of the slope s of the linear potential. The dependence of $\lambda_{crit.}$ on s is approximately linear

Consequently the relation for the linear fit is $\lambda_{crit.} \simeq 0.064 + 0.185s$. The fact that λ and s are linearly related is very striking. A possible explanation for the linearity is that by fixing the ϕ_i in order to obtain our Universe we give specific energy in the ϕ field. Unfortunately an analytical derivation of the numerically derived values of $\lambda_{crit.}$ was impossible to be calculated and it is postponed for future analysis.

5.5.3 Rayleigh Equation

In order to understand our previous results, i.e the existence of the critical points of the λ parameter, we are obligated to study the system analytically. A possible approach could be obtained by deriving an effective evolution equation for the scalar field ϕ. For the derivation we will use the Equations of Motion starting from Eq.(4.16) which can be written in a more convenient form as follows

$$\ddot{\phi} + 3\frac{\dot{a}}{a}\dot{\phi} - 3\left(\frac{\ddot{a}}{a} + \frac{\dot{a}^2}{a^2}\right)F_\phi + V_\phi = 0 \Rightarrow \ddot{\phi} + 3\frac{\dot{a}}{a}\dot{\phi} - 3F_\phi\left(\dot{H} + H^2 + H^2\right) + V_\phi = 0 \Rightarrow$$

$$\ddot{\phi} + 3\frac{\dot{a}}{a}\dot{\phi} - 3F_\phi\left(\dot{H} + 2H^2\right) + V_\phi = 0 \Rightarrow \ddot{\phi} + 3\frac{\dot{a}}{a}\dot{\phi} - 3F_\phi\dot{H} - 6F_\phi H^2 + V_\phi = 0 \tag{5.85}$$

Also one should rewrite Eq.(4.11) and Eq.(4.14) as

$$3F(\phi)H^2 = \rho_m + \frac{\dot{\phi}^2}{2} + V(\phi) - 3H\dot{F} \xRightarrow{\times\frac{2}{F(\phi)}} 6H^2 = \frac{2\rho_m}{F} + \frac{\dot{\phi}^2}{F} + \frac{2V}{F} - 6H\frac{\dot{F}}{F} \tag{5.86}$$

$$-2F(\dot{H} + H^2 - H^2) = \rho_m + \dot{\phi}^2 + \ddot{F} - H\dot{F} \xRightarrow{\times\frac{3}{2F(\phi)}} -3\dot{H} = \frac{3\rho_m}{2F} + \frac{3\dot{\phi}^2}{2F} + \frac{3\ddot{F}}{2F} - \frac{3H\dot{F}}{2F} \tag{5.87}$$

Therefore Eq.(5.85), using Eq.(5.86) and Eq.(5.87), can be written as

$$\ddot{\phi} + 3\frac{\dot{a}}{a}\dot{\phi} + F_\phi\left(\frac{3\rho_m}{2F} + \frac{3\dot{\phi}^2}{2F} + \frac{3\ddot{F}}{2F} - \frac{3H\dot{F}}{2F}\right) - F_\phi\left(\frac{2\rho_m}{F} + \frac{\dot{\phi}^2}{F} + \frac{2V}{F} - 6H\frac{\dot{F}}{F}\right) + V_\phi = 0 \Rightarrow$$

$$\Rightarrow \ddot{\phi} + 3\frac{\dot{a}}{a}\dot{\phi} + F_\phi\left(\frac{3\rho_m}{2F} - \frac{4\rho_m}{2F} + \frac{3\dot{\phi}^2}{2F} - \frac{2\dot{\phi}^2}{2F} - \frac{3H\dot{F}}{2F} + \frac{12H\dot{F}}{2F} + \frac{3\ddot{F}}{2F} - \frac{2V}{F}\right) + V_\phi = 0 \Rightarrow$$

$$\Rightarrow \ddot{\phi} + 3\frac{\dot{a}}{a}\dot{\phi} + F_\phi\left(-\frac{\rho_m}{2F} + \frac{\dot{\phi}^2}{2F} + \frac{9H\dot{F}}{2F} + \frac{3\ddot{F}}{2F} - \frac{2V}{F}\right) + V_\phi = 0 \tag{5.88}$$

Let us now assume that $F(\phi) = 1 - \lambda \cdot \phi$ and $V = -s\phi$, as in the previous sections. Under this assumption, Eq.(5.88) can be written as

$$\ddot{\phi} + 3\frac{\dot{a}}{a}\dot{\phi} - \lambda \cdot \left(-\frac{\rho_m}{2F} + \frac{\dot{\phi}^2}{2F} + \frac{9H(-\lambda\dot{\phi})}{2F} + \frac{3(-\lambda\ddot{\phi})}{2F} - \frac{2(-s\phi)}{F}\right) - s = 0 \Rightarrow$$
$$\Rightarrow \ddot{\phi} + 3H\dot{\phi} + \frac{\lambda\rho_m}{2F} - \frac{\lambda\dot{\phi}^2}{2F} + \frac{9H\lambda^2\dot{\phi}}{2F} + \frac{3\lambda^2\ddot{\phi}}{2F} - \frac{2\lambda \cdot s\phi}{F} - s = 0 \Rightarrow$$
$$\ddot{\phi}\left(1 + \frac{3\lambda^2}{2F}\right) + 3H\dot{\phi}\left(1 + \frac{3\lambda^2}{2F}\right) - \frac{\lambda}{2F}\dot{\phi}^2 = s + \frac{2\lambda}{F}s\phi - \frac{\lambda}{2F}\rho_m \tag{5.89}$$

In order to be accurate we have to use the rescaled quantities, i.e. Eq.(5.89) should be written as $(H \to \bar{H}, \rho_m \to \bar{\rho}_m)$

$$\ddot{\phi}\left(1 + \frac{3\lambda^2}{2F}\right) + 3\bar{H}\dot{\phi}\left(1 + \frac{3\lambda^2}{2F}\right) - \frac{\lambda}{2F}\dot{\phi}^2 = s + \frac{2\lambda}{F}s\phi - \frac{\lambda}{2F}\bar{\rho}_m \Rightarrow$$
$$\Rightarrow \ddot{\phi}\left(1 + \frac{3\lambda^2}{2F}\right) + 3\bar{H}\dot{\phi}\left(1 + \frac{3\lambda^2}{2F}\right) - \frac{\lambda}{2F}\dot{\phi}^2 = s + \frac{2\lambda}{F}s\phi - \frac{\lambda}{2F}\frac{\rho_m}{{H_0}^2} \Rightarrow$$
$$\Rightarrow \ddot{\phi} + 3\bar{H}\dot{\phi}\left(1 + \frac{3\lambda^2}{2F}\right) - \frac{\lambda}{2F}\dot{\phi}^2 = s + \frac{2\lambda}{F}s\phi - \frac{\lambda\rho_{0m}}{2Fa^3{H_0}^2} \Rightarrow$$

$$\Rightarrow \ddot{\phi} + 3\bar{H}\dot{\phi}\left(1 + \frac{3\lambda^2}{2F}\right) - \frac{\lambda}{2F}\dot{\phi}^2 = s + \frac{2\lambda}{F}s\phi - \frac{3\lambda\rho_{0m}F_0}{3 \cdot 2F \cdot F_0 \cdot a^3{H_0}^2} \Rightarrow$$
$$\Rightarrow \ddot{\phi} + 3\bar{H}\dot{\phi}\left(1 + \frac{3\lambda^2}{2F}\right) - \frac{\lambda}{2F}\dot{\phi}^2 = s + \frac{2\lambda}{F}s\phi - \frac{3\Omega_{0m}F_0\lambda}{2Fa^3} \tag{5.90}$$

This is a Rayleigh equation[69] which has some similarities with the standard forced-damped oscillator. However, there are important differences like the presence of the non-linear term of the field derivative which complicate the analysis and do not allow the use of the sign of the "force" term as a qualitative simple indicator of the dynamics. Now, considering that $F > 0$ one can see that each term from Eq.(5.90) leads the ϕ field in different direction. If $\ddot{\phi} > 0$, then we end up in Big Crunch as the field rolls down the potential and the gravity becomes strongly attractive. On the contrary if $\ddot{\phi} < 0$, then we end up to eternal expansion avoiding the Big Crunch singularity, as the field moves up the potential and the gravity becomes repulsive as the positive potential energy of the field eventually dominates.

From Eq.(5.90), one can observe that, the s term drives the scalar field towards the Big Crunch singularity whereas the other two terms revert the field from Big Crunch. At first, when the scale factor is small, the term $\frac{3\Omega_{0m}F_0\lambda}{2Fa^3}$ dominates and gives an impulse to the ϕ field towards negative values but as the Universe reaches a deSitter expansion and the scale factor becomes larger this particular term vanishes. Now let us plot the "effective force" as a function of the field for various cases of (s, λ)[70]

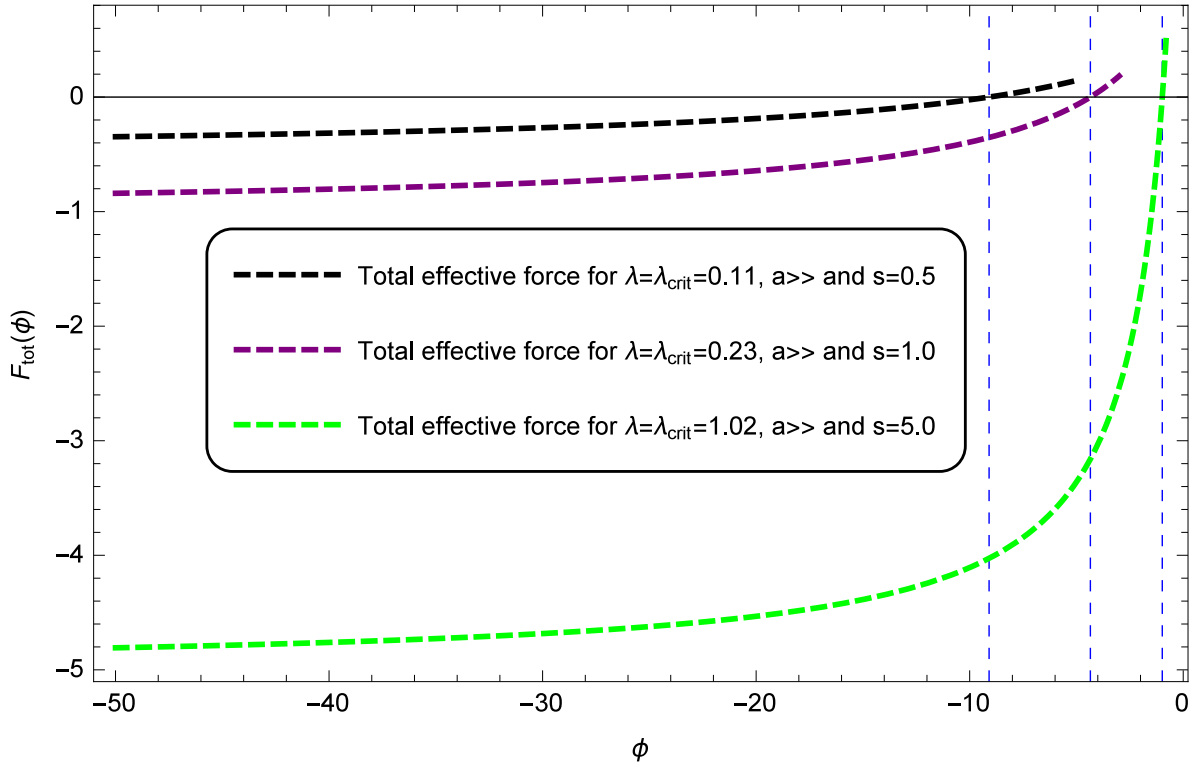

Figure 5.17: Total "effective force" as a function of the field ϕ for various cases of (s, λ)

From Fig.5.17 for various cases of (s, λ) one can observe the existence of some critical values of the ϕ field, i.e. $\phi_{crit.}$, for which the sign of $F_{tot.}(\phi)$ changes and from negative becomes positive. These particular values for some cases can be seen is Fig.5.17 as blue lines. If the impulse of the term which is proportional to a^{-3} is such that the ϕ field to reach the $\phi_{crit.}$ value then we avoid the Big Crunsh singularity. Otherwise the field will get eventually positive values thus we end up in the Big Crunch Doomsday. Finally, demanding that $F_{tot.}(\phi) = 0$ and considering the $\lambda_{crit.}$ that we have already calculated numerically (see [70]) one can construct the following table

s	$\lambda_{crit.}$	λ_{chosen}	$\phi_{crit.}$	ϕ_{min}
0.5	0.11	0.1099	-9.0909	-8.46744
1.0	0.23	0.2200	-4.3478	-4.17967
2.0	0.45	0.4490	-2.2222	-2.18038
3.0	0.63	0.6200	-1.5625	-1.54854
4.0	0.83	0.8290	-1.2048	-1.19371
5.0	1.02	1.0100	-0.9804	-0.97172
6.0	1.17	1.1699	-0.8547	-0.846719
8.0	1.55	1.5490	-0.6452	-0.637996
10.0	1.89	1.8899	-0.5263	-0.49351
11.0	2.13	2.1200	-0.4695	-0.468482
12.0	2.31	2.3000	-0.4329	-0.426898
13.0	2.54	2.5390	-0.3937	-0.387452
14.0	2.74	2.7300	-0.3650	-0.357725
15.0	2.90	2.8990	-0.3448	-0.331974
16.0	3.10	3.0900	-0.3226	-0.318037
18.0	3.47	3.4690	-0.2882	-0.285314

These particular values of $\phi_{crit.}$ correspond to the initial conditions which are fixed in order to obtain our Universe. If the initial condition are not fixed to such value of course the $\phi_{crit.}$ will be different.

In classical terms, the basic mechanism of our model could be presented as a ball rolling in a cliff. If the initial force given to the ball is suitable, then the ball will reach the peak of the cliff, i.e $\phi_{critical}$ and continue its movement across the other side. In the opposite scenario, where the ball will not manage to reach the $\phi_{critical}$ it will return in its initial position rolling in the opposite direction. This can be depicted on the following Fig.5.18

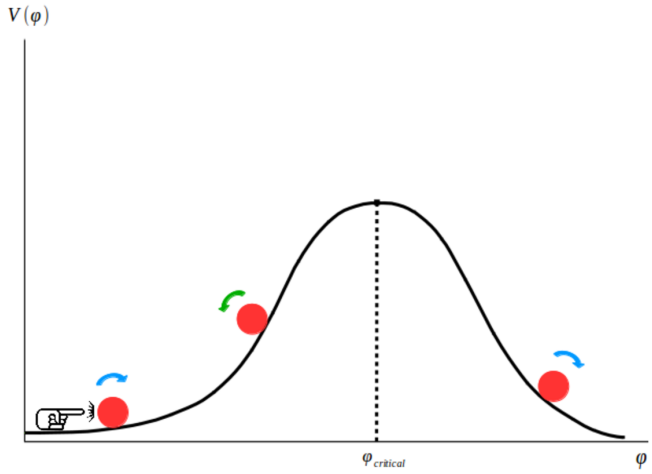

Figure 5.18: Classical analogous of the basic mechanism of the model

Finally an analytical derivation of the $\phi_{crit.}$, demanding $F(\phi)_{tot.} = 0$ in Eq.(5.90) and considering a linear non-minimal coupling $F(\phi) = 1 - \lambda\phi_{crit.}$, as follows

$$F(\phi)_{tot.} = 0 \Rightarrow s + \frac{2\lambda}{F} s\phi_{crit.} - \frac{3\Omega_{0m}F_0\lambda}{2Fa^3} = 0 \Rightarrow \phi_{crit.} = \frac{3F_0\,\lambda\,\Omega_{0m} - 2a^3\,s}{2a^3\lambda\,s} \tag{5.91}$$

This is a general method and the $\phi_{crit.}$ can be obtained for any form of V and F by deriving the corresponding Rayleigh equation. Let us now plot the $\phi_{crit.}$ as a function of λ for small and large values of the scale factor[70]

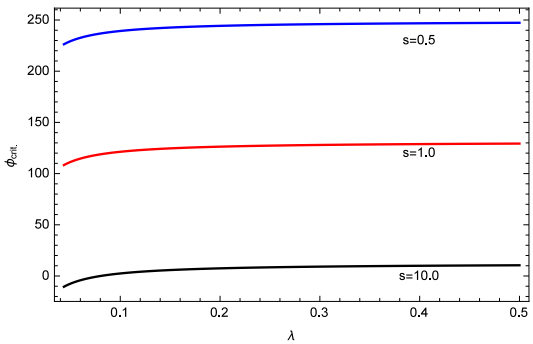

Figure 5.19: The evolution of $\phi_{crit.}$for the linear potential $V = -s \cdot \phi$ and small values of a

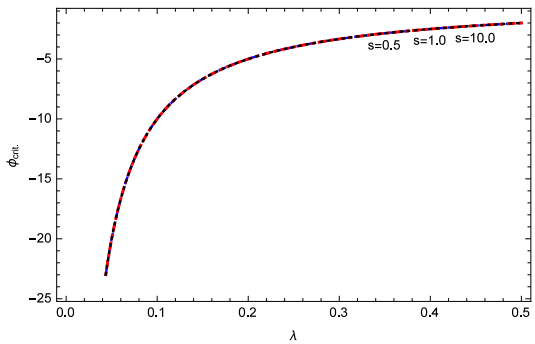

Figure 5.20: The evolution of $\phi_{crit.}$for the linear potential $V = -s \cdot \phi$ and large values of a

For large values of the scale factor the $\phi_{crit.}$ is the same for any value of s as it was expected from Eq.(5.91).

5.5.4 Fit to SnIa Data

Having solved the aforementioned system numerically, for linear potential let us examine if our model provides a better fit to the Union 2.1 Dataset than the quintessence models or the ΛCDM model. In order to do that we will obtain the minimum χ^2 function for various pairs of (s, λ) using the same procedure as in Subsubsection 5.2.2.1. It has to be mentioned that for the "χ^2 *function*" there is no analytical expression, therefore all the calculated results were obtained manually. So, one is able to derive the figure below[70]

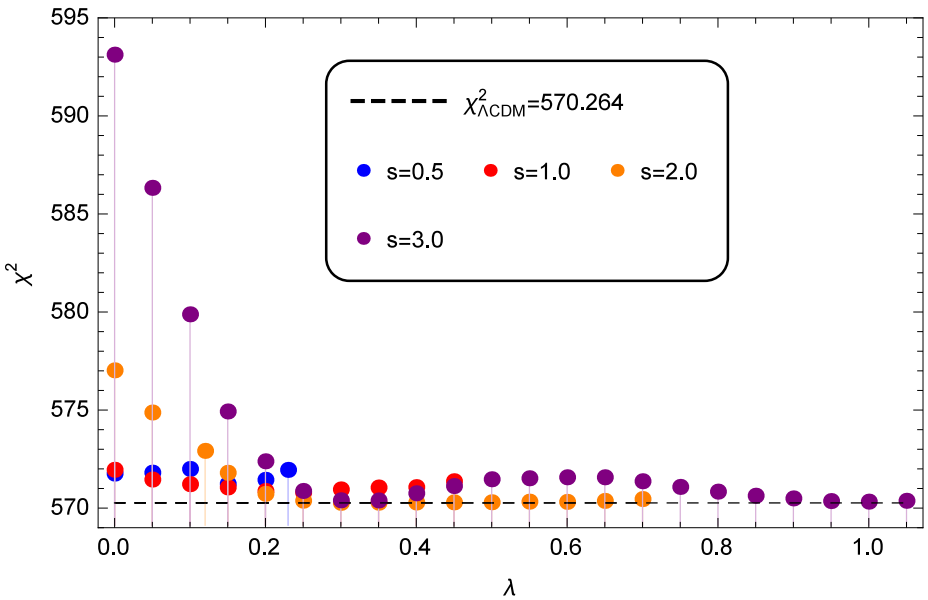

Figure 5.21: Fit to the Union 2.1 Dataset for various pairs of (s, λ)

From Fig.5.21 the lowest value appears to be for the pair $(s, \lambda) = (2.0, 0.3)$ where $\chi^2_{s=2.0,\lambda=0.3} = 570.269$. Even though the obtained value is almost to the ΛCDM model, unfortunately it provides marginally worse fit. More information about the best fit "χ^2 *function*" can be obtained through the 1σ and 2σ probability contours. Based on the numerically obtained values for the "χ^2 *function*" we construct the contours in the parameter space of s and λ as follows[70]

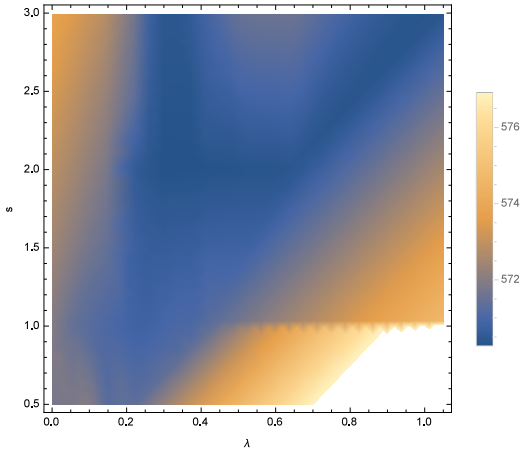

Figure 5.22: 1σ χ^2 contour for linear potential $V = -s \cdot \phi$

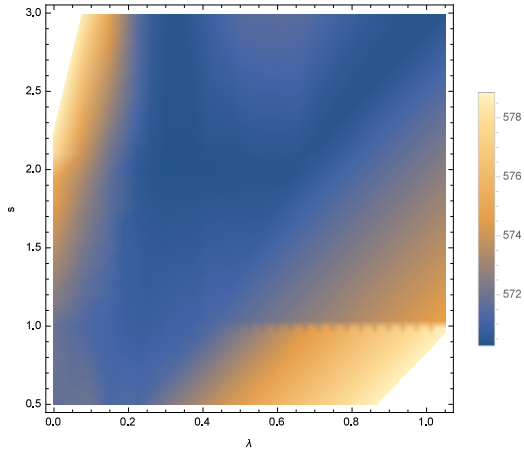

Figure 5.23: 2σ χ^2 contour for linear potential $V = -s \cdot \phi$

It has to be mentioned that in Fig.5.22 and Fig.5.23 one could observe a peculiar line for $s = 1.0$. This is due to the fact that for larger values of λ our code had some difficulties concerning the conditions to the present time to be satisfied. Based on Fig.5.22 and Fig.5.23 one could calculate the probability that the numerical χ^2 lies in the 1σ and 2σ confidence level from the χ^2 of the ΛCDM via the equation [126]

$$P(s, \lambda) = \mathcal{N} e^{-\chi^2(s,\lambda)/2} \tag{5.92}$$

5.5.5 Alternative Forms of Potential

Let us now focus on an alternative form of potential in order to see if the fit to the data is better than the linear potential. Of course the equations for modified gravity remain the same except the Rayeleight equation Eq.(5.90).

5.5.5.1 Dynamics for $V = s\,|\phi|^n$

Assuming the same initial conditions as before, we solve the new system of equations numerically, i.e Eq.(5.69)-(5.73) considering that $V(\phi) = s\,|\phi|^n$. From the numerical code one can see the same behaviour as that of the linear potential, i.e the existence of critical points. Therefore the figure for the scale factor is[70]

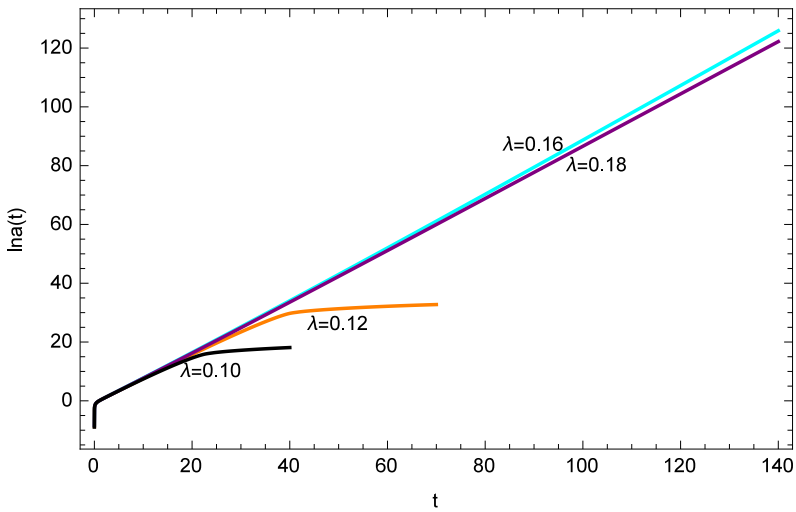

Figure 5.24: The scale factor, in a logarithmic scale, for representative quintessence with $V(\phi) = s\,|\phi|^n$, $s = 1$, $n = 0.8$ and various values of slopes λ.

The curves stop because once again $F(\phi) \to 0$. When the field rolls towards zero and achieve positive values instead of a Big Crunch Doomsday it oscillates around zero. When λ is larger than the critical value to the corresponding s the field shifts away from the singularity as in for the linear potential. This can be seen clearly in the figure below[70]

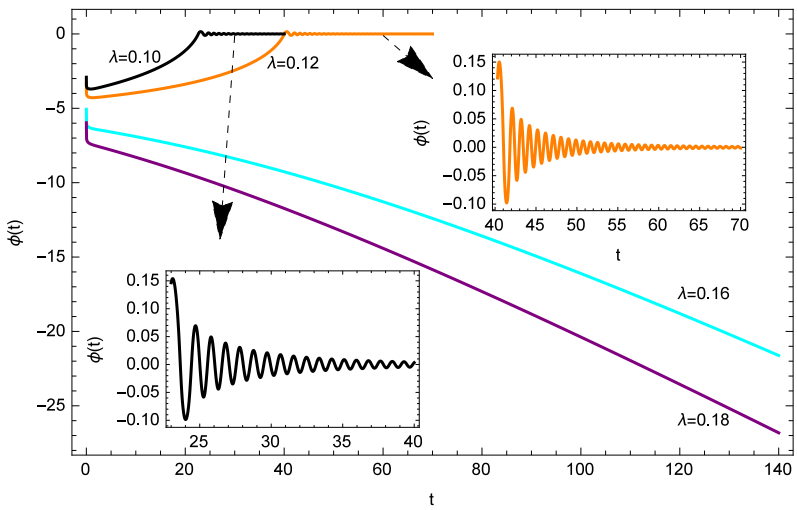

Figure 5.25: The evolution of the scalar field for $s = 1$, $n = 0.8$ and various values of λ above and below the critical values $\lambda_{crit} \simeq 0.15$.

Based on the existence of critical points for the linear potential, we consider the possibility for the existence of critical values for λ and for this particular choice of potential. Working as before for many pairs of (s, λ) we derived numerically the $\lambda_{critical}$ as a function of s (see [70]). Once again, as it was expected, the critical points increase almost linearly with s as it can be seen in Fig.5.26[70]

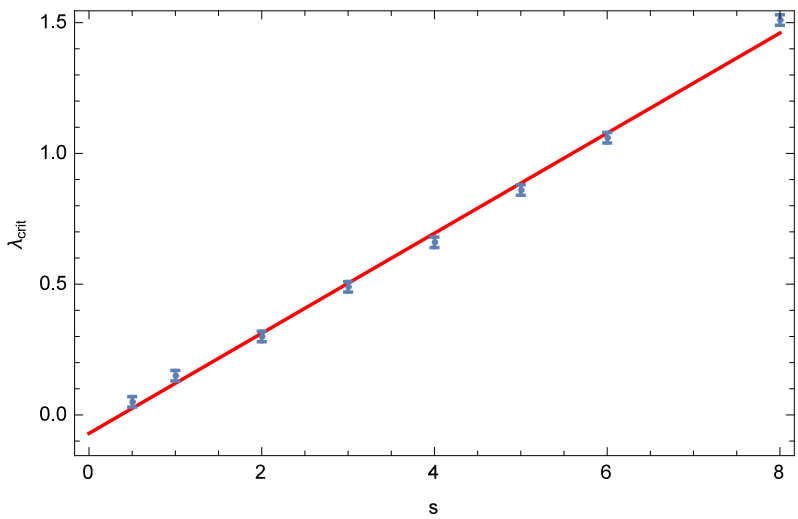

Figure 5.26: The critical values of λ for various slopes of s. The potential form is $V = s \cdot |\phi|^n$

The relation for the linear fit is $\lambda_{crit.} \simeq -0.071 + 0.191s$. The explanation for this linearity is possible the same as that for the linear potential.

Finally in order to understand the existence of the critical points we should study, once more, the effective evolution for the scalar field ϕ, i.e Rayleigh equation. For the derivation we will start from Eq.(5.88) and substitute that $F(\phi) = 1 - \lambda \cdot \phi$ and $V = s \cdot |\phi|^n$

$$\ddot{\phi} + 3\frac{\dot{a}}{a}\dot{\phi} + F_\phi \left(-\frac{\rho_m}{2F} + \frac{\dot{\phi}^2}{2F} + \frac{9H\dot{F}}{2F} + \frac{3\ddot{F}}{2F} - \frac{2V}{F} \right) + V_\phi = 0 \Rightarrow$$

$$\Rightarrow \ddot{\phi} + 3\frac{\dot{a}}{a}\dot{\phi} - (-\lambda) \left(\frac{\rho_m}{2F} - 3\frac{(-\lambda\,\ddot{\phi})}{2F} - 9H\frac{(-\lambda\phi)}{2F} - \frac{\dot{\phi}}{2F} + 2\frac{s|\phi|^n}{F} \right) + ns|\phi|^{n-1}\,\epsilon(\phi) = 0 \quad (5.93)$$

where $\epsilon(\phi) = \begin{cases} -1, & \text{for } \phi < 0 \\ 1, & \text{for } \phi > 0 \end{cases}$ is the sign function. With no loss of generality we may focus on the half period $\frac{T}{2}$ for which $\phi < 0 \Rightarrow \epsilon(\phi) = -1$. Hence Eq.(5.93) can be written as[11]

$$\ddot{\phi} + 3\frac{\dot{a}}{a}\dot{\phi} + \frac{\lambda\,\rho_m}{2F} + \frac{3\lambda^2\,\ddot{\phi}}{2F} + \frac{9H\lambda^2\dot{\phi}}{2F} - \frac{\lambda\dot{\phi}^2}{2F} - \frac{2\lambda s\phi^n}{F} - ns\phi^{n-1} = 0$$

Now collecting the terms, we obtain the following equation

$$\ddot{\phi}\left(1 + \frac{3\lambda^2}{2F}\right) + 3H\left(1 + \frac{3\lambda^2}{2F}\right)\dot{\phi} - \frac{\lambda\dot{\phi}^2}{2F} = -\frac{\lambda\rho_m}{2F} + \frac{2\lambda s\phi^n}{F} + ns\phi^{n-1} \quad (5.94)$$

Next, in order to be accurate we have to use the rescaled quantities with the present day Hubble parameter, i.e $H \to \bar{H}$ and $\rho_m \to \bar{\rho}_m$. Therefore Eq.(5.94) takes the form

$$\ddot{\phi}\left(1 + \frac{3\lambda^2}{2F}\right) + 3\bar{H}\left(1 + \frac{3\lambda^2}{2F}\right)\dot{\phi} - \frac{\lambda\dot{\phi}^2}{2F} = -\frac{\lambda\bar{\rho}_m}{2F} + \frac{2\lambda s\phi^n}{F} + ns\phi^{n-1} \Rightarrow$$

$$\ddot{\phi}\left(1 + \frac{3\lambda^2}{2F}\right) + 3\bar{H}\left(1 + \frac{3\lambda^2}{2F}\right)\dot{\phi} - \frac{\lambda\dot{\phi}^2}{2F} = -\frac{\lambda}{2F}\frac{\rho_m}{{H_0}^2} + \frac{2\lambda s\phi^n}{F} + ns\phi^{n-1} \Rightarrow$$

[11] During our calculations with no loss of generality we assume that the power n is odd. If n was even, then the last two terms would have the same sign but it would be positive.

$$\ddot{\phi}\left(1+\frac{3\lambda^2}{2F}\right)+3\bar{H}\left(1+\frac{3\lambda^2}{2F}\right)\dot{\phi}-\frac{\lambda\dot{\phi}^2}{2F}=-\frac{\lambda\rho_{0m}}{2Fa^3{H_0}^2}+\frac{2\lambda s\phi^n}{F}+ns\phi^{n-1}\Rightarrow$$
$$\ddot{\phi}\left(1+\frac{3\lambda^2}{2F}\right)+3\bar{H}\left(1+\frac{3\lambda^2}{2F}\right)\dot{\phi}-\frac{\lambda\dot{\phi}^2}{2F}=-\frac{3\lambda\Omega_{0m}F_0}{2Fa^3}+\frac{2\lambda s\phi^n}{F}+ns\phi^{n-1} \tag{5.95}$$

Eq.(5.95) is the Rayleigh equation for $V = s|\phi|^n$ and each term leads the ϕ field in different directions which justifies, as before, the existence of critical points. If $\ddot{\phi} > 0$, then the ϕ field will move down the potential towards zero leading to oscillation(blue arrows). If $\ddot{\phi} < 0$, then the field will move up to the potential and will revert into positive values shifting away from the oscillations(green arrow).

From Eq.(5.95) one can see that the term that is analogous to a^{-3} is negative hence it pushes the field ϕ towards negative values, shifting away from the oscillations and leading in a deSitter expansion. The other two terms, i.e. $\frac{2\lambda s\phi^n}{F}$ and $ns\phi^{n-1}$, are positive, therefore they lead the ϕ field in positive values, i.e. to oscillations. All this can be seen in the following figure

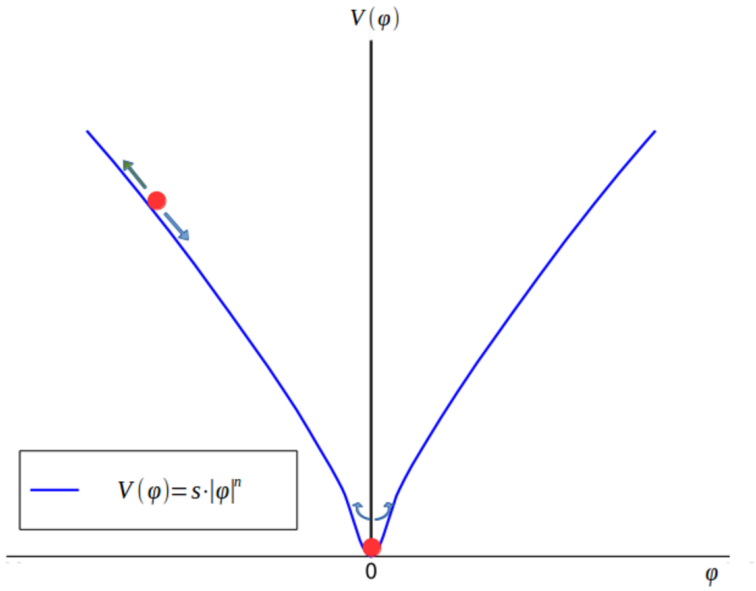

Figure 5.27: Basic mechanism for $V = s \cdot |\phi|^n$

5.5.5.2 Fit to SnIa Data

Let us examine if the fit of our model for $V = s\cdot|\phi|^n$ to the Union2.1 Dataset is better than the ΛCDM or the scalar tensor quintessence with linear potential. Following the same procedure as before we calculate manually the "χ^2 *function*" for various cases of (s, λ) up to the value $s = 4.0$. The fit can be seen below[70]

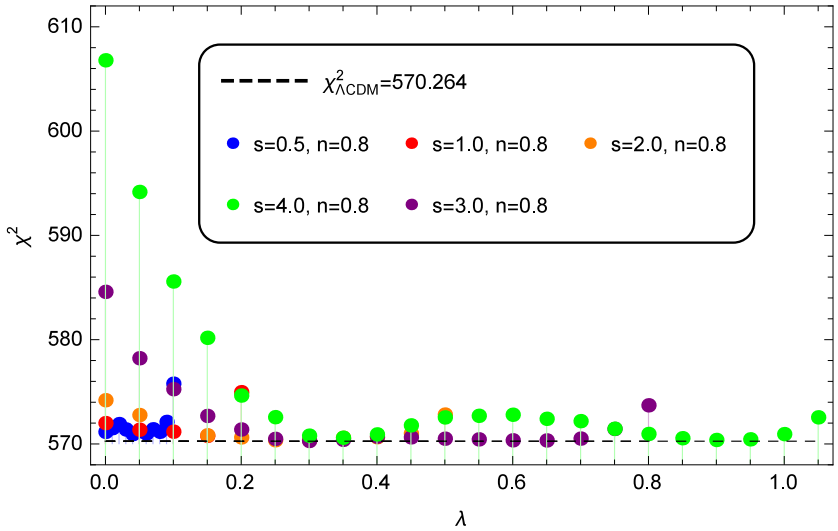

Figure 5.28: Fit to the Union 2.1 Dataset for various cases of (s, λ) and $V = s \cdot |\phi|^n$, with $n = 0.8$

From Fig.5.28 the lowest value for χ^2 appears to be $(s, \lambda) = (3.0, 0.3)$, where $\chi^2_{s=3.0,\lambda=0.3} = 570.287$. Unfortunately the fit for this particular choice of potential is worse not only from the one that emerges for linear potential, but also from the ΛCDM model.

Based on the numerically obtained values for the "χ^2 *function*" we are able construct the correspondng contours in the parameter space of s and λ as follows[70]

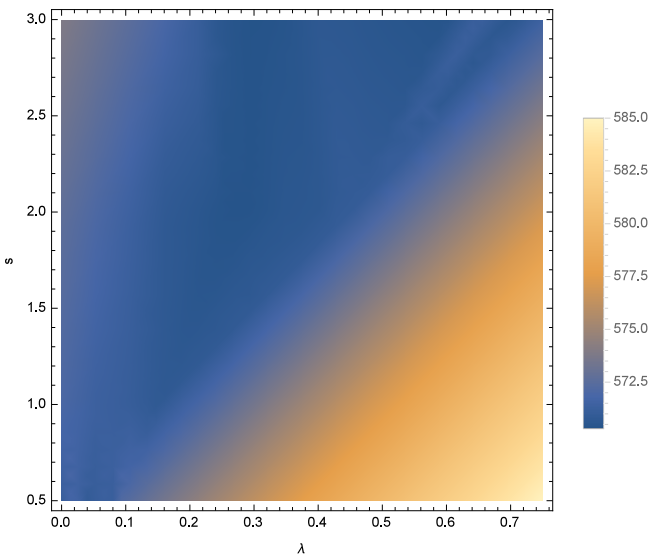

Figure 5.29: 1σ χ^2 contour for potential $V = s \cdot |\phi|^n$

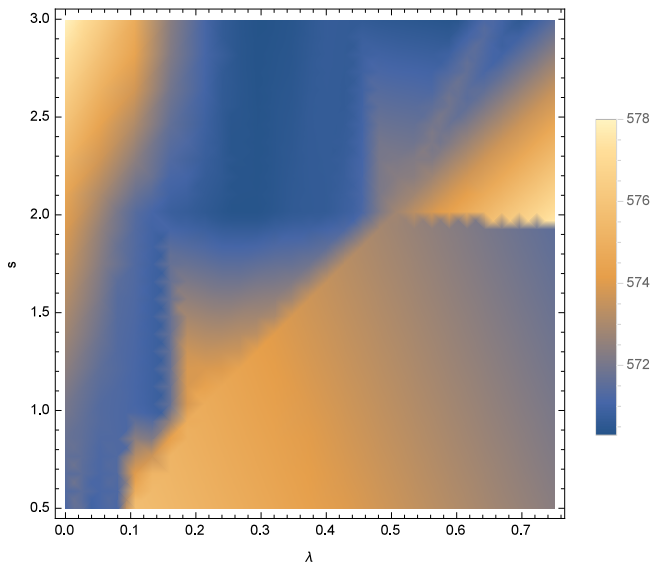

Figure 5.30: 2σ χ^2 contour for potential $V = s \cdot |\phi|^n$

Once again in Fig.5.30 one could observe peculiar lines for various pairs of s and λ. Once more this is due to the fact that for larger values of λ our code had some difficulties concerning the conditions to the present time to be satisfied and this difficulty is much more intense for this case of potential. Therefore for the 2σ contour we considered more pairs of (s, λ)

Chapter 6

Conclusions and Future Prospects

6.1 Conclusions

The purpose of this thesis was to study some of the most interesting possible models attempting to explain the observed accelerating expansion of the Universe. These possible explanations correspond to specific models in the context of GR, the *quintessence models*[87–90], and modified theories of gravity, the *scalar tensor quintessence models*[93–95]. For this purpose recent cosmological data have been used and studied extensively (supernovae type Ia datasets[116, 125]) as consistency tests to our models.

The simplest candidate model is none other than the cosmological constant that has negative pressure and it is known as the Λ CDM model[123, 137, 138]. Even though the ΛCDM model provides an excellent fit to the cosmological data to date and has the additional advantage of simplicity due to a single free parameter, it is somewhat problematic taking into account the fact that faces two major issues/problems that have not been answered yet

- The Cosmological Constant Problem: Observationally, the cosmological constant density is 120 orders of magnitude smaller than the energy density associated with the Planck scale. How could the cosmological constant have been so large during the inflation period and so small today?

- The Cosmic Coincidence Problem: Why is the energy density of dark energy dominant today?

These particular challenges led to many alternative theories in order to explain the accelerated expansion of the Universe.

One of the possible solutions is a scalar field minimally coupled to gravity called *quintessence*. The *quintessence* field has the following Lagrangian[92]

$$\mathscr{L}_{quin.} = \frac{1}{2}\dot{\phi}^2 - V(\phi)$$

This model was studied extensively as an alternative theory for DE and the dynamical equations Eq.(3.13) and Eq.(3.15) were proven.

Even though the *quintessence* field has dynnamical evolution and thus can solve coincidence problem[81], the origin of the scalar field is still a problem. So, as a possible solution scalar tensor quintessence model have been proposed, which have the additional advantage of providing

a potential solution to the origin problem as the physical origin of the scalar field is the dynamical "Newton's constant"[93–95]. For this kind of models[47, 96]

$$G_{eff} = \frac{1}{F(\phi)} \left(\frac{2F + 4\left(\frac{dF}{d\phi}\right)^2}{2F + 3\left(\frac{dF}{d\phi}\right)^2} \right)$$

The cosmological dynamics for general scalar tensor quintessence field was studied extensively. The dynamical equations for this kind of alternative model were obtained by varying the action with a general metric and then use FRW metric and by using the FRW metric directly in Einstein-Hilbert action and vary with respect to the scale factor. The second method that was used, is particular useful and can lead to dynamical equations for a wide range of cosmological models[66–69]. Of course the equations that we calculated were the same as it was expected[69]. Next we rescaled the dynamical equations using the present day Hubble parameter and obtain the density parameters for matter Eq.(4.27) and dark energy Eq.(4.28).

Finally the cosmological observational probes were presented, which can be categorised into geometrical and dynamical ones[104]. Considering the supernovae type Ia as standard candles astronomers could measure many useful quantities such as the luminosity distance. Using the luminosity distance one could define the apparent magnitude and the distance modulus of the SnIa. All these quantities have been calculated and published in datasets such as the Gold[116] and the Union2.1 dataset[125] that were used in our analysis as a consistency test to the models that we have studied theoretically.

For the quintessence models, solving the system numerically, we observed that it can mimic the basic mechanism of the cosmological constant however using the Gold and the Union2.1 datasets was deduced that they have serious problems to exceed the quality of fit of a cosmological constant. This led to the introduction of other dynamical parametrizations, such the Linear Ansanz[115] and the CPL Ansanz[128, 129], which have been tested with the information criteria AIC[131] and BIC[132], which are measures of the relative quality of statistical models (parametrizations) for a given set of data which penalize models for the number of their parameters. Even though they provide a better fit it is not significantly better than that of the ΛCDM model despite the additional number of parameters. It has to be mentioned that the CPL and Linear Ansanz do not correspond to any specific physical model. They are ad-hoc parametrizations of the evolution of the equation of state parameter.

Then a dynamical analysis of scalar tensor quintessence models was made. Solving the system of Eq.(5.69)-Eq.(5.73) numerically, considering a generic form of the potential $V(\phi) = -s\,\phi$ and $F(\phi) = 1 - \lambda\,\phi$ for the linear nonminimal coupling. From the numerical solution was deduced that when the λ becomes larger than a critical value, unique for every s, then the ϕ field instead of rolling down, it starts rolling up its potential towards negative field values and as a result it rolls away from the Big Crunch Singularity, something that is a unique feature for this particular category of models. This particular behaviour of the field can be explained considering the Rayleigh equation[69]

$$\ddot{\phi} + 3\bar{H}\dot{\phi}\left(1 + \frac{3\lambda^2}{2F}\right) - \frac{\lambda}{2F}\dot{\phi}^2 = s + \frac{2\lambda}{F}s\phi - \frac{3\Omega_{0m}F_0\lambda}{2Fa^3}$$

In the beginning the term proportional to the scale factor dominates and gives an initial impulse to the field towards negative values but as the Universe reaches a deSitter expansion and the scale factor becomes larger this particular term vanishes. If the impulse of the term which is proportional to a^{-3} is such that the ϕ field to reach a $\phi_{crit.}$ value then we avoid the Big Crunsh

singularity. Otherwise the field will get eventually positive values thus we end up in the Big Crunch Doomsday. When the term that is proportional to a^{-3} vanishes the term s leads the field to Big Crunch but the term $\frac{2\lambda}{F}s\phi$ leads the field to shift away from the singularity. When λ is small the dominant term is s leading the field to the singularity. However, as λ gets larger then the $\frac{2\lambda}{F}s\phi$ term eventually dominates over s and as a result the ϕ field evolves towards negative values (up its potential).

An analytical expression for the $\phi_{crit.}$ was obtained and we numerically calculated the values of $\phi_{crit.}$ up to the value of $s = 18$. Also we calculate a numerical approximation to the relation between $\lambda = f(s)$, which appears to be linear. The fact that these two parameters are linearly related is very striking and it could be due to the fact of fixing the initial conditions, and in particular, the initial value of the field in order to obtain our Universe, since when we run the code for different values there was no linearity. As a result for this fixing is the specific energy of the ϕ field which corresponds to value below or above $\phi_{crit.}$.

Also the χ^2 function[126] for various pairs of (s, λ) was calculated manually and the corresponding contour plots in the parameter space of s and λ were constructed, in order to see which pair of parameter is consistent with the Union2.1 Dataset[125]. In our analysis the range of the parameters that correspond to the 1σ confidence level contour are $0.5 \leq s \leq 3$ and $0 \leq \lambda \leq 1.05$. Finally we repeated the same analysis (analytical and numerical) for alternative potential and in particular of the form $V = s\,|\phi|^n$. For this kind of potential the same basic mechanism was observed, as before. When the field rolls towards zero and achieve positive values instead of a Big Crunch Doomsday it oscillates around zero. On the other hand if λ is larger than the critical value of λ to the corresponding s the field shifts away from the singularity and reaches a deSitter evolution as in for the linear potential. The corresponding 1σ range of parameters for this particular potential are $0.5 \leq s \leq 3$ and $0 \leq \lambda \leq 0.75$.

6.2 Future Prospects

The avoidance of Cosmic Doomsday is a very striking result because it is a unique feature for models of this nature. The Big Crunch is one of the scenarios predicted by many cosmological models in which the Universe may end[124, 135, 139]. This scenario is supported and from the *quintessence* model that we have already studied extensively in this thesis. However for the *scalar tensor quintessence* models considering a generic form of the potential $V(\phi) = -s\,\phi$ and for the linear nonminimal coupling $F(\phi) = 1 - \lambda\,\phi$ the Big Crunch that would occur in the context of General Relativity is avoided[69].

With that in mind we are planning to explore furthermore this model, numerically and analytically. An interesting extension of this study is the analytical derivation of the numerically derived values of $\lambda_{crit.}(s)$ which appears to be an approximately linear function and the possible dependence of linearity on the initial values. Also one could extend the Eq.(5.91) for general forms of the potential V and the nonminimal coupling F. Evolving this theory, one could investigate nonlinear coupling to gravity, e.g. $F(\phi) = 1 - \lambda\phi^2$, or couplings with a minimum in general, which will give a greater understanding of our results. For this kind of coupling to gravity we expect the same behaviour as in linear coupling, i.e the total effective force to get positive values.

Another interesting extension of this project is to derive a general form for the virial theorem derived in Brans-Dicke scalar oscillations. The virial theorem for Brans-Dicke scalar oscillations connecting the mean kinetic and potential energies was derived in Ref.[140]. However the action in Ref.[140] is similar to the one that we have studied in this thesis. This particular extension would be a very interesting extension. Finally another prospect to this work is to study the

physics of extreme cases, i.e. what happens when (in the future) F gets negative, what does it mean physically and when does it happen numerically. For $F < 0$ the graviton has negative mass[47] which leads to an unstable Universe which can lead to a metastable state.

Conclusively there is a wide field of research, most importantly theoretical, considering these theories of gravitation and their promising results.

Appendices

Chapter A

Analytical Calculations for Standard Cosmology

A.1 Riemann Tensor and Bianchi Identities

The Riemann tensor displays some very interesting algebraic identities. Starting from its definition[59]

$$R^a{}_{\beta\mu\nu} \equiv \Gamma^a{}_{\beta\nu,\mu} - \Gamma^a{}_{\beta\mu,\nu} + \Gamma^a{}_{\sigma\mu}\Gamma^\sigma{}_{\beta\nu} - \Gamma^a{}_{\sigma\nu}\Gamma^\sigma{}_{\beta\mu} \tag{A.1}$$

one could prove that (working on the local inertial frame, where at a given event the metric is the flat spacetime metric, i.e $\Gamma^a{}_{\mu\nu} = 0$)

$$R^a{}_{\beta\mu\nu} = \Gamma^a{}_{\beta\nu,\mu} - \Gamma^a{}_{\beta\mu,\nu} \tag{A.2}$$

Now, using the definition of the Christoffel's symbols, i.e Eq.(2.7) it is easily obtained that[1]

$$\Gamma^a{}_{\beta\nu,\mu} = \frac{1}{2}g^{a\delta}\left(g_{\delta\beta,\nu\mu} + g_{\delta\nu,\beta\mu} - g_{\beta\nu,\delta\mu}\right)$$
$$\Gamma^a{}_{\beta\nu,\mu} = \frac{1}{2}g^{a\delta}\left(g_{\delta\beta,\mu\nu} + g_{\delta\mu,\beta\nu} - g_{\beta\mu,\delta\nu}\right)$$

Since $g^{a\delta}{}_{,\mu} = 0$(see below) it is straightforward to show that the Riemann tensor takes the form

$$R^a{}_{\beta\mu\nu} = \frac{1}{2}g^{a\delta}\left(\cancel{g_{\delta\beta,\nu\mu}} + g_{\delta\nu,\beta\mu} - g_{\beta\nu,\delta\mu} - \cancel{g_{\delta\beta,\mu\nu}} - g_{\delta\mu,\beta\nu} + g_{\beta\mu,\delta\nu}\right) \Rightarrow$$
$$\Rightarrow R^a{}_{\beta\mu\nu} = \frac{1}{2}g^{a\delta}\left(g_{\delta\nu,\beta\mu} - g_{\beta\nu,\delta\mu} - g_{\delta\mu,\beta\nu} + g_{\beta\mu,\delta\nu}\right) \tag{A.3}$$

where we used the fact that partial derivatives always commute. Next, lowering the index a with the metric and setting $a = \lambda$ in Eq.(A.3) we get

$$R_{a\beta\mu\nu} \equiv g_{a\lambda}R^\lambda{}_{\beta\mu\nu} = \frac{1}{2}g_{a\lambda}g^{\lambda\delta}\left(g_{\delta\nu,\beta\mu} - g_{\beta\nu,\delta\mu} - g_{\delta\mu,\beta\nu} + g_{\beta\mu,\delta\nu}\right) = \frac{1}{2}\delta^\delta_a\left(g_{\delta\nu,\beta\mu} - g_{\beta\nu,\delta\mu} - g_{\delta\mu,\beta\nu} + g_{\beta\mu,\delta\nu}\right) \Rightarrow$$
$$\Rightarrow R_{a\beta\mu\nu} = \frac{1}{2}\left(g_{a\nu,\beta\mu} - g_{\beta\nu,a\mu} - g_{a\mu,\beta\nu} + g_{\beta\mu,a\nu}\right) \tag{A.4}$$

We can use this result to discover the symmetries of the Riemann Tensor. Using Eq.(A.4) it is straightforward to show that

$$R_{a\beta\mu\nu} = -R_{\beta a\mu\nu} = -R_{a\beta\nu\mu} = R_{\mu\nu a\beta}$$

[1]Here we have to mention that during this section of the appendix we use the notation $\Gamma^a{}_{\beta\nu,\mu}$ instead of $\Gamma^a_{\beta\nu,\mu}$. In reality the first is the right one but the blank in the indexes is skipped for simplicity.

i.e, that the Riemann tensor is antisymmetric on the final pair and second pair of indices, and symmetric on exchange of the two pairs.

Returning to the definition of Eq.(A.4) it is easy to prove that differentiating with respect to x^λ we get

$$R_{a\beta\mu\nu,\lambda} = \frac{1}{2}\left(g_{a\nu,\beta\mu\lambda} - g_{\beta\nu,a\mu\lambda} - g_{a\mu,\beta\nu\lambda} + g_{\beta\mu,a\nu\lambda}\right) \tag{A.5}$$

Using Eq.(A.5) and the fact that the partial derivatives commute it is straightforward to prove the Bianchi identity

$$R_{a\beta\mu\nu,\lambda} + R_{a\beta\lambda\mu,\nu} + R_{a\beta\nu\lambda,\mu} = 0$$

This equation is valid in a local inertial frame, therefore in a general one we get

$$R_{a\beta\mu\nu;\lambda} + R_{a\beta\lambda\mu;\nu} + R_{a\beta\nu\lambda;\mu} = 0 \tag{A.6}$$

This is a tensor equation, therefore valid in any coordinate system. It is called the Bianchi identity. By contracting both sides of the aforementioned equation with a pair o metric tensors, one can end up with

$$\begin{aligned} g^{\beta\nu}\, g^{a\mu}\left(R_{a\beta\mu\nu;\lambda} + R_{a\beta\lambda\mu;\nu} + R_{a\beta\nu\lambda;\mu}\right) = 0 \Rightarrow g^{\beta\nu}\left(R^{\mu}{}_{\beta\mu\nu;\lambda} - R^{\mu}{}_{\beta\mu\lambda;\nu} + R^{\mu}{}_{\beta\nu\lambda;\mu}\right) = 0 \Rightarrow \\ \Rightarrow R^{\nu}{}_{\nu;\lambda} - R^{\nu}{}_{\lambda;\nu} - R^{\nu\mu}{}_{\nu\lambda;\mu} = 0 \end{aligned} \tag{A.7}$$

The first term of Eq.(A.7) on the left contracts to yield a Ricci scalar, while the third term contracts to yield a mixed Ricci tensor namely

$$R_{;\lambda} - R^{\nu}{}_{\lambda;\nu} - R^{\mu}{}_{\lambda;\mu} = 0 \Rightarrow R_{;\lambda} = 2R^{\mu}{}_{\lambda;\mu} \tag{A.8}$$

where in the last term we changed the dummy index from μ to ν and combined them into a single term.

Alternatively one can see that Eq.(A.8) can be written as

$$\nabla_\mu R^{\mu}{}_{\lambda} = \frac{1}{2}\nabla_\lambda R \Rightarrow \nabla_\lambda R^{\lambda}{}_{\mu} = \frac{1}{2}\nabla_\mu R \Rightarrow \nabla_\lambda\left(R^{\lambda}{}_{\mu} - \frac{1}{2}\delta^{\lambda}{}_{\mu}R\right) = 0 \tag{A.9}$$

These are the twice-contracted Bianchi identities, often simply also called the Bianchi identities. Since the mixed metric tensor is equivalent to the Kronecker delta and since the covariant derivative of the metric tensor is zero (so it can be moved in and out of the scope of any derivative), then

$$\nabla_\lambda\left(R^{\lambda}{}_{\mu} - \frac{1}{2}g^{\lambda}_{\mu}R\right) = 0 \Rightarrow \nabla^\lambda\left(R_{\lambda\mu} - \frac{1}{2}g_{\lambda\mu}R\right) = 0 \Rightarrow \nabla^\mu G_{\mu\nu} = 0 \tag{A.10}$$

A.2 *Continuity Equation* for Friedmann Equations

In order to prove Eq.(2.27), we will need Eq.(2.24) and Eq.(2.26). Starting from Eq.(2.24)

$$\begin{aligned} \frac{\dot{a}^2}{a^2} = \frac{8\pi G}{3}\rho - \frac{k}{a^2} \Rightarrow \dot{a}^2 = \frac{8\pi G}{3}\rho a^2 - k \xRightarrow{\cdot \mathrm{d/dt}} \\ \Rightarrow 2\dot{a}\ddot{a} = \frac{8\pi G}{3}\left(\dot{\rho}a^2 + 2a\dot{a}\rho\right) \end{aligned}$$

By using the second Friedmann equation, i.e Eq.(2.26) we end up with

$$2\frac{\dot{a}}{a}\left[-\frac{4\pi G}{3}(\rho+p)\right] = \frac{8\pi G}{3}\left(\dot{\rho}+2\frac{\dot{a}}{a}\rho\right) \Rightarrow -\frac{\dot{a}}{a}(\rho+3p) = \dot{\rho}+2\frac{\dot{a}}{a}\rho \Rightarrow$$
$$\Rightarrow \dot{\rho}+3\frac{\dot{a}}{a}(\rho+p) = 0.$$

i.e Eq.(2.27). One could see that the *continuity equation* is not an independent equation because of the Bianch identities. The *Einstein tensor* satisfies the Bianchi identities[2], i.e $\nabla^\mu G_{\mu\nu} = 0 \Rightarrow \nabla_\nu G^{\mu\nu} = 0$. Therefore the same must be true for the *energy-momentum tensor* $\nabla_\nu T^{\mu\nu} = 0$ taking into account Eq.(2.40).

A.3 Variation of Ricci Scalar

We begin with the definition of Ricci Scalar

$$R = g^{\mu\nu}R_{\mu\nu} \Rightarrow \delta R = R_{\mu\nu}\delta g^{\mu\nu} + g^{\mu\nu}\delta R_{\mu\nu} \tag{A.11}$$

But the Riemann curvature tensor is defined as

$$R^\rho{}_{\sigma\mu\nu} = \partial_\mu\Gamma^\rho_{\nu\sigma} - \partial_\nu\Gamma^\rho_{\mu\sigma} + \Gamma^\rho_{\mu\lambda}\Gamma^\lambda_{\nu\sigma} - \Gamma^\rho_{\nu\lambda}\Gamma^\lambda_{\mu\sigma}$$
$$\delta R^\rho{}_{\sigma\mu\nu} = \partial_\mu\delta\Gamma^\rho_{\nu\sigma} - \partial_\nu\delta\Gamma^\rho_{\mu\sigma} + \delta\Gamma^\rho_{\mu\lambda}\Gamma^\lambda_{\nu\sigma} + \Gamma^\rho_{\mu\lambda}\delta\Gamma^\lambda_{\nu\sigma} - \delta\Gamma^\rho_{\nu\lambda}\Gamma^\lambda_{\mu\sigma} - \Gamma^\rho_{\nu\lambda}\delta\Gamma^\lambda_{\mu\sigma}$$

The covariant derivative of a tensor with mixed indices, in general, is[2]

$$\nabla_\lambda C^i_{jk} = \partial_\lambda C^i_{jk} + \Gamma^i_{\lambda m}C^m_{jk} - \Gamma^m_{\lambda j}C^i_{mk} - \Gamma^m_{\lambda k}C^i_{jm} \tag{A.12}$$

Hence we can calculate

$$\nabla_\lambda(\delta\Gamma^\rho_{\nu\mu}) = \partial_\lambda(\delta\Gamma^\rho_{\nu\mu}) + \Gamma^\rho_{\sigma\lambda}\delta\Gamma^\sigma_{\nu\mu} - \Gamma^\sigma_{\nu\lambda}\delta\Gamma^\rho_{\sigma\mu} - \Gamma^\sigma_{\mu\lambda}\delta\Gamma^\rho_{\nu\sigma} \tag{A.13}$$

We can now observe that the expression for the variation of Riemann curvature tensor is equal to the difference of two such terms

$$\nabla_\mu(\delta\Gamma^\rho_{\nu\sigma}) = \partial_\mu(\delta\Gamma^\rho_{\nu\sigma}) + \Gamma^\rho_{\kappa\mu}\delta\Gamma^\kappa_{\nu\sigma} - \Gamma^\kappa_{\nu\mu}\delta\Gamma^\rho_{\kappa\sigma} - \Gamma^\kappa_{\sigma\mu}\delta\Gamma^\rho_{\nu\kappa}$$
$$\nabla_\nu(\delta\Gamma^\rho_{\mu\sigma}) = \partial_\nu(\delta\Gamma^\rho_{\mu\sigma}) + \Gamma^\rho_{\kappa\nu}\delta\Gamma^\kappa_{\mu\sigma} - \Gamma^\kappa_{\mu\nu}\delta\Gamma^\rho_{\kappa\sigma} - \Gamma^\kappa_{\sigma\nu}\delta\Gamma^\rho_{\mu\kappa}$$

and by setting $\kappa = \lambda$ we obtain

$$\nabla_\mu(\delta\Gamma^\rho_{\nu\sigma}) - \nabla_\nu(\delta\Gamma^\rho_{\mu\sigma}) = \partial_\mu(\delta\Gamma^\rho_{\nu\sigma}) + \Gamma^\rho_{\lambda\mu}\delta\Gamma^\lambda_{\nu\sigma} - \cancel{\Gamma^\lambda_{\nu\mu}\delta\Gamma^\rho_{\lambda\sigma}} - \Gamma^\lambda_{\sigma\mu}\delta\Gamma^\rho_{\nu\lambda} - \partial_\nu(\delta\Gamma^\rho_{\mu\sigma}) -$$
$$- \Gamma^\rho_{\lambda\nu}\delta\Gamma^\lambda_{\mu\sigma} + \cancel{\Gamma^\lambda_{\mu\nu}\delta\Gamma^\rho_{\lambda\sigma}} + \Gamma^\lambda_{\sigma\nu}\delta\Gamma^\rho_{\mu\lambda} = \delta R^\rho{}_{\sigma\mu\nu} \tag{A.14}$$

We may now obtain the variation of the Ricci curvature tensor simply by contracting two indices of the variation of the Riemann tensor

$$\delta R^\rho{}_{\mu\sigma\nu} = \nabla_\sigma(\delta\Gamma^\rho_{\nu\mu}) - \nabla_\nu(\delta\Gamma^\rho_{\mu\sigma}) \xRightarrow{\text{contraction}} \delta R_{\mu\nu} = \nabla_\rho(\delta\Gamma^\rho_{\nu\mu}) - \nabla_\nu(\delta\Gamma^\rho_{\rho\mu})$$

Therefore, the variation of the Ricci scalar with respect to the inverse metric is given by

$$\delta R = R_{\mu\nu}\delta g^{\mu\nu} + \nabla_\sigma(g^{\mu\nu}\delta\Gamma^\sigma_{\mu\nu} - g^{\mu\sigma}\delta\Gamma^\rho_{\rho\mu}) \tag{A.15}$$

[2]The rule is that for each contravariant (upper) index in the tensor, there is a positive term with a Christoffel symbol, and for each covariant (lower) index, there is a negative term.

A.4 Proof of $\nabla_\sigma g^{\mu\nu} = 0$

In order to prove the requested equation we will use only the definition of the covariant derivative

$$\begin{aligned}\nabla_\sigma g_{\mu\nu} = g_{\mu\nu,\sigma} - \Gamma^\lambda_{\sigma\mu} g_{\lambda\nu} - \Gamma^\lambda_{\sigma\nu} g_{\mu\lambda} = g_{\mu\nu,\sigma} - \frac{1}{2} g_{\lambda\nu} g^{\lambda\rho} \left(g_{\sigma\rho,\mu} + g_{\mu\rho,\sigma} - g_{\sigma\mu,\rho}\right) - \frac{1}{2} g_{\mu\lambda} g^{\lambda\rho} \left(g_{\sigma\rho,\nu} + g_{\nu\rho,\sigma} - g_{\sigma\nu,\rho}\right) = \\ = g_{\mu\nu,\sigma} - \frac{1}{2}\delta^\rho_\nu \left(g_{\sigma\rho,\mu} + g_{\mu\rho,\sigma} - g_{\sigma\mu,\rho}\right) - \frac{1}{2}\delta^\rho_\mu \left(g_{\sigma\rho,\nu} + g_{\nu\rho,\sigma} - g_{\sigma\nu,\rho}\right) = \\ = g_{\mu\nu,\sigma} - \frac{1}{2}\left(\cancel{g_{\sigma\nu,\mu}} + g_{\mu\nu,\sigma} - \cancel{g_{\sigma\mu,\nu}}\right) - \frac{1}{2}\left(\cancel{g_{\sigma\mu,\nu}} + g_{\nu\mu,\sigma} - \cancel{g_{\sigma\nu,\mu}}\right) = g_{\mu\nu,\sigma} - \frac{1}{2}\left(g_{\mu\nu,\sigma} + g_{\nu\mu,\sigma}\right) = \\ = g_{\mu\nu,\sigma} - \frac{1}{2}\left(g_{\mu\nu,\sigma} + g_{\mu\nu,\sigma}\right) = g_{\mu\nu,\sigma} - \frac{\cancel{2}}{\cancel{2}} g_{\mu\nu,\sigma} = 0 \end{aligned} \tag{A.16}$$

Considering Eq.(A.16) one can easily obtain that

$$\nabla_\sigma g^{\mu\nu} = \nabla_\sigma g_{\kappa\lambda} g^{\kappa\mu} g^{\lambda\nu} = 0 \Rightarrow \nabla_\sigma g^{\mu\nu} = 0 \tag{A.17}$$

Similarly we get

$$g^{\mu\nu}_{;\rho} = g^{\mu}_{\nu;\rho} = g_{\mu\nu;\rho} = 0.$$

A.5 Variation of the Square Root of the Determinant of the Metric Tensor

Let us now compute the variation of the square root of the determinant of the metric tensor. We do tha calculation fully general for n-dimensional Riemannian spaces and then apply it for the pseudo-Rimanannian 4-dimensional space of General Relativity. Firstly, we write the determinant simply as

$$g \equiv det\left(g_{a\beta}\right) \tag{A.18}$$

We have that

$$\delta\left(\sqrt{g}\right) = \frac{1}{2\sqrt{g}}\delta g$$

Now, for any square $n \times n$ matrix A it hold that

$$det\left(A\right) = e^{Tr(A)} \tag{A.19}$$

Setting $A \to g_{a\beta}$ to (A.19), we arrive at

$$g = det\left(g_{a\beta}\right) = e^{Tr\left(g_{a\beta}\right)} \tag{A.20}$$

and under the variation $g_{a\beta} \to g_{a\beta} + \delta g_{a\beta}$ it follows that

$$det(g_{a\beta} + \delta g_{a\beta}) = e^{Tr\left(g_{a\beta} + \delta g_{a\beta}\right)} = e^{Tr\left(g_{a\beta}\right) + Tr\left(\delta g_{a\beta}\right)} = \underbrace{e^{Tr\left(g_{a\beta}\right)}}_{\equiv g} e^{Tr\left(\delta g_{a\beta}\right)} \tag{A.21}$$

where on going from the second to the third equality we employed the linearity of the trace. Since the variations δg are small, in the expansion of $e^{Tr(\delta g_{ab})}$ we can neglect second and higher order terms and we shall have

$$e^{Tr(\delta g_{ab})} \approx 1 + Tr(\delta g_{ab}) \tag{A.22}$$

and therefore

$$det(g_{a\beta} + \delta g_{a\beta}) \approx g\,(1 + Tr(\delta g_{a\beta})) \tag{A.23}$$

but, by the definition of the trace

$$Tr(\delta g_{a\beta}) = g^{a\beta}\delta g_{a\beta} \tag{A.24}$$

Hence Eq.(A.23) can be written as

$$det(g_{a\beta} + \delta g_{a\beta}) \approx g\left(1 + g^{a\beta}\delta g_{a\beta}\right) \tag{A.25}$$

Using the latter to the definition of the variation, we arrive at

$$\begin{aligned} \delta g = \delta\left(det(g_{a\beta})\right) = det(g_{a\beta} + \delta g_{a\beta}) - det(g_{a\beta}) \approx \\ \approx g\left(1 + g^{a\beta}\delta g_{a\beta}\right) - g = g g^{a\beta}\delta g_{a\beta} \Rightarrow \delta g = -g g_{a\beta}\delta g^{a\beta} \end{aligned} \tag{A.26}$$

Finally using (A.26) we are ready to prove (2.38) as follows

$$\begin{aligned} \delta\left(\sqrt{g}\right) = \frac{1}{2\sqrt{g}}\delta g = -\frac{1}{2}\frac{(\sqrt{g})^{\cancel{2}}}{\cancel{\sqrt{g}}} g_{a\beta}\delta g^{a\beta} = -\frac{1}{2}\sqrt{g} g_{a\beta}\delta g^{a\beta} \Rightarrow \\ \Rightarrow \delta\left(\sqrt{g}\right) = -\frac{1}{2}\sqrt{g} g_{a\beta}\delta g^{a\beta} \end{aligned} \tag{A.27}$$

Now, in order to get the expression for the 4-dimensional pseudo-Riemannian space of General Relativity, we simply replace $g \to -g$ and let the indices run from 0 to 3 (The usual Greek ones). We then have

$$\delta\left(\sqrt{-g}\right) = -\frac{1}{2}\sqrt{-g} g_{\mu\nu}\delta g^{\mu\nu} \tag{A.28}$$

where $\mu, \nu = 0, 1, 2, 3$ as usual.

A.6 Friedmann Equations for ΛCDM Model

In order to derive the Friedmann equations for the ΛCDM model, i.e. Eq.(2.56) (2.57), we will start from the Einstein field equations for the ΛCDM model calculating the (00) component and (11) component as follows

- <u>(00) component:</u>

$$\begin{aligned} G_{00} = 8\pi G T_{00} \Rightarrow R_{00} - \frac{1}{2}g_{00}R - \Lambda g_{00} = 8\pi G T_{00} \Rightarrow -3\frac{\ddot{a}}{a} - \frac{1}{2}\cdot 1 \cdot \left[-6\left(\frac{\ddot{a}}{a} + \frac{\dot{a}^2}{a^2} + \frac{k}{a^2}\right)\right] - \Lambda = \\ = 8\pi G T_{00} \Rightarrow -3\cancel{\frac{\ddot{a}}{a}} + 3\cancel{\frac{\ddot{a}}{a}} + 3\frac{\dot{a}^2}{a^2} + 3\frac{k}{a^2} - \Lambda = 8\pi G\rho \Rightarrow \left(\frac{\dot{a}}{a}\right)^2 + \frac{k}{a^2} = \frac{8\pi G}{3}\rho + \frac{\Lambda}{3} \Rightarrow \\ \Rightarrow \left(\frac{\dot{a}}{a}\right)^2 = \frac{8\pi G}{3}\rho + \frac{\Lambda}{3} - \frac{k}{a^2} \end{aligned} \tag{A.29}$$

For $\Lambda = 0$ Eq.(A.29) one can revert to Eq.(2.24) as it was expected.

- <u>(11) component:</u>

$$G_{11} = 8\pi G T_{11} \Rightarrow R_{11} - \frac{1}{2} g_{11} R - \Lambda g_{11} = 8\pi G T_{11} \Rightarrow$$

$$\Rightarrow \frac{a\ddot{a} + 2\dot{a}^2 + 2k}{1 - kr^2} - \frac{1}{2}\left(-\frac{a^2}{1 - kr^2}\right)\left[-6\left(\frac{\ddot{a}}{a} + \frac{\dot{a}^2}{a^2} + \frac{k}{a^2}\right)\right] - \Lambda\left(\frac{a^2}{1 - kr^2}\right) = 8\pi G p \frac{a^2}{1 - kr^2} \Rightarrow$$

$$\Rightarrow 2a\ddot{a} + \dot{a}^2 + k - \Lambda a^2 = -8\pi G p a^2 \xRightarrow{:a^2} 2\frac{\ddot{a}}{a} + \frac{\dot{a}^2}{a^2} + \frac{k}{a^2} - \Lambda = -8\pi G p \xRightarrow{Eq.(A.29)}$$

$$\Rightarrow 2\frac{\ddot{a}}{a} + \frac{8\pi G\rho}{3} - \cancel{\frac{k}{a^2}} + \frac{\Lambda}{3} + \cancel{\frac{k}{a^2}} - \Lambda = -8\pi G p \Rightarrow 2\frac{\ddot{a}}{a} + \frac{8\pi G\rho}{3} - \frac{2\Lambda}{3} = -8\pi G p \Rightarrow$$

$$\Rightarrow \frac{\ddot{a}}{a} = -\frac{4\pi G}{3}(\rho + 3p) + \frac{\Lambda}{3} \tag{A.30}$$

Once again for $\Lambda = 0$ Eq.(A.30) one can revert to Eq.(2.26).

Chapter B

Analytical Calculations for Modified Gravity

First let us take a look at the variations of the Christoffel symbols

$$\delta\Gamma^{\sigma}_{\alpha\beta} = \delta\Big[\frac{1}{2}g^{\sigma\gamma}(g_{\gamma\alpha,\beta} + g_{\gamma\beta,\alpha} - g_{\beta\alpha,\gamma})\Big] = \frac{1}{2}\delta g^{\sigma\gamma}(g_{\gamma\alpha,\beta} + g_{\gamma\beta,\alpha} - g_{\beta\alpha,\gamma}) + \\ + \frac{1}{2}g^{\sigma\gamma}(\delta g_{\gamma\alpha,\beta} + \delta g_{\gamma\beta,\alpha} - \delta g_{\beta\alpha,\gamma})$$

However,

$$\nabla_{\gamma}\delta g_{\alpha\beta} = \delta g_{\alpha\beta,\gamma} - \Gamma^{\sigma}_{\gamma\alpha}\delta g_{\sigma\beta} - \Gamma^{\sigma}_{\gamma\beta}\delta g_{\alpha\sigma} \tag{B.1}$$

therefore it is straightforward to show that

$$\delta\Gamma^{\sigma}_{\alpha\beta} = \frac{1}{2}\delta g^{\sigma\gamma}(g_{\gamma\alpha,\beta} + g_{\gamma\beta,\alpha} - g_{\beta\alpha,\gamma}) + \frac{1}{2}g^{\sigma\gamma}(\nabla_{\beta}\delta g_{\gamma\alpha} + \cancel{\Gamma^{\sigma}_{\beta\gamma}\delta g_{\sigma\alpha}} + \Gamma^{\sigma}_{\beta\alpha}\delta g_{\gamma\sigma} + \nabla_{a}\delta g_{\gamma\beta} + \cancel{\Gamma^{\sigma}_{\alpha\gamma}\delta g_{\sigma\beta}} + \\ + \Gamma^{\sigma}_{\alpha\beta}\delta g_{\gamma\sigma} - \nabla_{\gamma}\delta g_{\alpha\beta} - \cancel{\Gamma^{\sigma}_{\gamma\alpha}\delta g_{\sigma\beta}} - \cancel{\Gamma^{\sigma}_{\gamma\beta}\delta g_{\alpha\sigma}} = \frac{1}{2}\delta g^{\sigma\gamma}(g_{\gamma\alpha,\beta} + g_{\gamma\beta,\alpha} - g_{\beta\alpha,\gamma}) + \\ + \frac{1}{2}g^{\sigma\gamma}(\nabla_{a}\delta g_{\gamma\beta} + \nabla_{\beta}\delta g_{\gamma\alpha} - \nabla_{\gamma}\delta g_{\alpha\beta} + 2\Gamma^{\lambda}_{\beta\alpha}\delta g_{\gamma\lambda}) \tag{B.2}$$

Using the equations that we showed in Appendix A

$$\delta g_{\alpha\beta} = -g_{\alpha\mu}g_{\beta\nu}\delta g^{\mu\nu}$$
$$\delta g^{\alpha\beta} = -g^{\alpha\mu}g^{\beta\nu}\delta g_{\mu\nu}$$
$$g_{\gamma\alpha,\beta} = \cancelto{0}{g_{\gamma\alpha;\beta}} + \Gamma^{\lambda}_{\gamma\beta}g_{\lambda\alpha} + \Gamma^{\lambda}_{\alpha\beta}g_{\gamma\lambda}$$
$$g_{\gamma\beta,\alpha} = \cancelto{0}{g_{\gamma\beta;\alpha}} + \Gamma^{\lambda}_{\gamma\alpha}g_{\lambda\beta} + \Gamma^{\lambda}_{\beta\alpha}g_{\gamma\lambda}$$
$$g_{\beta\alpha,\gamma} = \cancelto{0}{g_{\beta\alpha;\gamma}} + \Gamma^{\lambda}_{\beta\gamma}g_{\lambda\alpha} + \Gamma^{\lambda}_{\alpha\gamma}g_{\beta\lambda}$$

we derive

$$\delta\Gamma^{\sigma}_{\beta\alpha} = \frac{2}{2}\delta g^{\sigma\nu}\Gamma^{\lambda}_{\alpha\beta}g_{\nu\lambda} - \delta g^{\mu\nu}\delta^{\sigma}_{\mu}g_{\lambda\nu}\Gamma^{\lambda}_{\beta\alpha} + \frac{1}{2}g^{\sigma\gamma}(\nabla_{a}\delta g_{\gamma\beta} + \nabla_{\beta}\delta g_{\gamma\alpha} - \nabla_{\gamma}\delta g_{\alpha\beta})$$
$$\delta\Gamma^{\sigma}_{\alpha\beta} = \frac{1}{2}g^{\sigma\gamma}(\nabla_{a}\delta g_{\gamma\beta} + \nabla_{\beta}\delta g_{\gamma\alpha} - \nabla_{\gamma}\delta g_{\alpha\beta}) = \frac{1}{2}g^{\sigma\gamma}\Big[\nabla_{\beta}(-g_{\gamma\mu}g_{\alpha\nu}\delta g^{\mu\nu}) + \nabla_{a}(-g_{\gamma\mu}g_{\beta\nu}\delta g^{\mu\nu}) - \\ -\nabla_{\gamma}(-g_{\beta\mu}g_{\alpha\nu}\delta g^{\mu\nu})\Big] = -\frac{1}{2}\delta^{\sigma}_{\mu}g_{\alpha\nu}\nabla_{\beta}(\delta g^{\mu\nu}) - \frac{1}{2}\delta^{\sigma}_{\mu}g_{\beta\nu}\nabla_{\alpha}(\delta g^{\mu\nu}) + \frac{1}{2}g_{\beta\mu}g_{\alpha\nu}\nabla^{\sigma}(\delta g^{\mu\nu}) \Rightarrow \\ \Rightarrow \delta\Gamma^{\sigma}_{\beta\alpha} = -\frac{1}{2}g_{\alpha\nu}\nabla_{\beta}(\delta g^{\sigma\nu}) - \frac{1}{2}g_{\beta\nu}\nabla_{\alpha}(\delta g^{\sigma\nu}) + \frac{1}{2}g_{\beta\mu}g_{\alpha\nu}\nabla^{\sigma}(\delta g^{\mu\nu}) \tag{B.3}$$

In the above calculations we used the fact that, in the local inertial frame $\nabla_a g_{\mu\nu} = 0$. Taking into consideration Eq.(B.3) we finally obtain

$$g^{\mu\nu}\delta\Gamma^{\sigma}_{\mu\nu} = -\frac{1}{2}(g^{\mu\nu}g_{\nu\alpha}\nabla_{\mu}\delta g^{\alpha\sigma} + g^{\mu\nu}g_{\mu\alpha}\nabla_{\nu}\delta g^{\alpha\sigma} - g^{\mu\nu}g_{\mu\alpha}g_{\nu\beta}\nabla^{\sigma}\delta g^{\alpha\beta}) \Rightarrow$$
$$\Rightarrow g^{\mu\nu}\delta\Gamma^{\sigma}_{\mu\nu} = -\nabla_a\delta g^{a\sigma} + \frac{1}{2}g_{a\beta}\nabla^{\sigma}\delta g^{a\beta}$$

i.e Eq.(4.4). In a similar way one can prove Eq.(4.5)

Chapter C

Mathematica Algorithms

One of the most powerful tools to a physicist is programming. It is really convenient for him because programming gives him the opportunity to solve and understand in great depth complicated concepts and phenomena. During this thesis we are unsing *Mathematica* so we can reproduce most of the figures shown in Chapter 5. In this appendix we are going to reproduce some of the figures and give detailed analysis concerning the commands we used so the whole algorithm is able to run and give us useful results.

C.1 Quintessence Models

C.1.1 Reproduction of Fig.5.4-Fig.??

Let us start with the reproduction of Fig.5.4, i.e the evolution of the scalar phield ϕ for quintessence models with linear potential of slope $s = 1$. First of all we put in *Mathematica* Eq.(3.13) and Eq.(3.15) along with the initial conditions and solve the system numerically using the command *NDSolve*. In what follows ϕ_i is referred to as $f0$, s is referred to as ss, Ω_{0m} is referred to as $om0m$ and t_i and t_0 are the initial and final time respectively

```
aa = a[t]; fi = f[t];

aad = D[aa, t];

aadd = D[aa, {t, 2}];

fid = D[fi, t];

fidd = D[fi, {t, 2}];

f0 = −0.8; ss = 1.0; ti = 0.000025; t0 = 3.79; om0m = 0.3;

eq1 = aadd/aa +  fid^2 + ssfi + om0m/(2aa^3) == 0;

eq2 = fidd  + 3 fid(aad/aa) − ss == 0;

condition1 = f[ti]==f0;

condition2 = f′[ti]==0;
```

```
condition3 = a[ti] == (9om0m/4)^(1/3) ti^(2/3);

condition4 = a'[ti] == (2/3)(9om0m/4)^(1/3) ti^(−1/3);

solution = NDSolve[{eq1, eq2, condition1, condition2, condition3, condition4},

{aa, fi}, {t, ti, t0}, MaxSteps → 100000000];
```

Then we plot Fig.5.4 using the command *Plot* as long as the command *Part* in order to fix the appropriate solution for the ϕ field. The other commands such as *PlotStyle, PlotRange, etc.* concern exclusively the configuration of the plot

```
fsol = Part[Evaluate[f[t]/.solution], 1];

asol = Part[Evaluate[a[t]/.solution], 1];

Plot[fsol, {t, ti, t0}, Frame → True, FrameLabel → {t, "ϕ(t)"}, Axes → False, PlotRange → All]
```

Now concerning the reproduction of Fig.5.5 and ?? we use once again the *Plot* command as follows

```
Plot[asol, {t, ti, t0}, Frame → True, FrameLabel → {t, "α(t)"}, Axes → False, PlotRange → {0, 5.}]

vfinal[t1_]:=fsol/.t->t1;

Plot[−ss ∗ vfinal[t], {t, ti, t0}, Frame → True, Axes → False, PlotRange → All, FrameLabel → {t, "V(ϕ(t))"
```

Following the same procedure and using different values for s one is able to derive Fig.5.6

C.1.2 Reproduction of Fig.5.7

In order to reproduce Fig.5.7 we have to construct the equation of state parameter for various slopes of s. Let us recreate the code for $s = 1$. We start our algorithm with the exact same analysis as the one we used in Appendix C.1 and using Eq.(3.9) we construct the equation of state parameter in the beginning as a fuction of t and afterwards as a function of redshift

```
tt = Part[FindRoot[as[t]==1, {t, 1}], 1, 2];

tas[a_?NumericQ]:=Part[FindRoot[as[t] == a, {t, 1}], 1, 2]; enf = 0.5dfsol^2 − ssfsol;

ppf = 0.5dfsol^2 + ssfsol;

wft[t1_]:=ppf/enf/.t->t1;

wfa[a_]:=wft[tas[a]];

wfz[z_]:=wfa[1/(z + 1)];

Plot[wfz[z], {z, 0, 2}, Frame → True, PlotRange → All, FrameLabel → {z, "w(z)"}]
```

Repeating the same procedure as before for various slopes of s we obtain Fig.5.7

C.1.3 Reproduction of Fig.5.8

In order to construct Fig.5.8 we begin setting the directory with the command *SetDirectory* where our data are and in particular the txt file with the Gold Dataset. Next we will use the *Do* command in order to pair our data with physical quantities and we construct the corresponding Hubble free luminosity distance i.e Eq.(5.23) for a Universe with matter and dark energy.

```
SetDirectory[NotebookDirectory[]];

data = ReadList["Union21.txt", {Word, Number, Number, Number, Number}];

ndat = Length[data];

Do[zz[i] = data[[i, 2]], {i, 1, ndat}]

Do[ld[i] = data[[i, 3]], {i, 1, ndat}]

Do[sld[i] = data[[i, 4]], {i, 1, ndat}]

f[z_, om_]:=1/Sqrt[om(1 + z)^3 + (1 − om)];

rr[zz_?NumericQ, om_?NumericQ]:=

NIntegrate[f[z, om], {z, 0, zz}, MaxRecursion → 20, AccuracyGoal → 10];
```

Afterwards we minimize the χ^2 *function* as it is described in the main part of my thesis and insert Eq.(5.47) therefore calculating the χ^2 *function* for the ΛCDM model

```
chi2fa[om_]:=Sum[(ld[i] − 5Log[10, rr[zz[i], om] ∗ (1 + zz[i])])^2/(sld[i]^2), {i, 1, ndat}];

chi2fb[om_]:=Sum[(ld[i] − 5Log[10, rr[zz[i], om] ∗ (1 + zz[i])])/(sld[i]^2), {i, 1, ndat}];

chi2fc = Sum[1/(sld[i]^2), {i, 1, ndat}];

chi2fm[om_]:=chi2fa[om] − chi2fb[om]^2/chi2fc + Log[chi2fc/(2Pi)];

chi2minimum = FindMinimum[chi2fm[om], {om, 0.25}, PrecisionGoal → 18];

chi2lcmd = chi2fm[0.277612];

Print ["x^2_ΛCMD=", chi2lcmd]
```

$x^2_{\Lambda\mathrm{CMD}} = 570.264$

Now we are ready to obtain the χ^2 *function* for various slopes of s. In this appendix we will show the procedure only for $s = 0.1$.

```
aa = a[t]; fi = f[t];

aad = D[aa, t];

aadd = D[aa, {t, 2}];

fid = D[fi, t];

fidd = D[fi, {t, 2}];

ti = 0.000025; t0 = 2.25; f0 = −7; om0m = 0.3; ss = 0.1;
```

```
eq1 = aadd/aa + fid^2 + ssfi + om0m/(2aa^3) == 0;
eq2 = fidd + 3 fid(aad/aa) − ss == 0;
condition1 = f[ti]==f0;
condition2 = f′[ti]==0;
condition3 = a[ti] == (9om0m/4)^(1/3) ti^(2/3);
condition4 = a′[ti] == (2/3)(9om0m/4)^(1/3) ti^(−1/3);
solution = NDSolve[{eq1, eq2, condition1, condition2, condition3,
condition4}, {aa, fi}, {t, ti, t0}, MaxSteps → 100000000];
fsol = Part[Evaluate[f[t]/.solution], 1];
asol = Part[Evaluate[a[t]/.solution], 1];
Plot[fsol, {t, ti, t0}, Frame → True, FrameLabel → {t, "ϕ(t)"}, Axes → False, PlotRange → All];
Plot[asol, {t, ti, t0}, Frame → True, FrameLabel → {t, "α(t)"}, Axes → False, PlotRange → All];
vfinal[t1_]:=fsol/.t->t1;
Plot[−ss ∗ vfinal[t], {t, ti, t0}, Frame → True, PlotRange → All, FrameLabel → {t, "V(ϕ(t))"}];
dfsol = D[fsol, t];
enf = 0.5dfsol^2 − ssfsol;
as[t1_]:=asol/.t->t1;
tt = Part[FindRoot[as[t]==1, {t, 1}, AccuracyGoal → Infinity,
PrecisionGoal → 8, MaxIterations → 1000], 1, 2];
tas[a_?NumericQ]:=Part[FindRoot[Normal[as[t]] == a, {t, 1}, AccuracyGoal → Infinity,
PrecisionGoal → 8, MaxIterations → 1000], 1, 2];
hht[t1_?NumericQ]:=D[asol, t]/asol/.t->t1;
hha[a_?NumericQ]:=hht[tas[a]];
hhz[z_?NumericQ]:=hha[1/(z + 1)];
enf = 0.5dfsol^2 − ssfsol;
ppf = 0.5dfsol^2 + ssfsol;
wft[t1_]:=ppf/enf/.t->t1;
wfa[a_]:=wft[tas[a]];
wfz[z_]:=wfa[1/(z + 1)];
```

```
Clear[chi2fa, chi2fb, chi2fc, chi2fm]

f[z_]:=1/hhz[z];

rr[zz_?NumericQ]:=NIntegrate[f[z], {z, 0, zz}];

chi2fa = Sum[(ld[i] − 5Log[10, rr[zz[i]] ∗ (1 + zz[i])])^2/(sld[i]^2), {i, 1, ndat}];

chi2fb = Sum[(ld[i] − 5Log[10, rr[zz[i]] ∗ (1 + zz[i])])/(sld[i]^2), {i, 1, ndat}];

chi2fc = Sum[1/(sld[i]^2), {i, 1, ndat}];

chi2fm = chi2fa − chi2fb^2/chi2fc + Log[chi2fc/(2Pi)];

Print ["x^2_{s=0.1}=", chi2fm]

chi2difference = chi2fm − chi2lcmd;

Print ["Δχ^2_{s=0.1}=", chi2difference]
```

$x^2_{s=0.1} = 571.603$
$\Delta\chi^2_{s=0.1} = 1.33995$

Changing the value for s we derive the differences of $\Delta\chi's$ and construct Fig.5.8. Following the same procedure we are able to construct the corresponding Fig.5.9 for the Union 2.1 Dataset.

C.2 Scalar Tensor Quintessence Models

C.2.1 Reproduction of Fig.5.13 and Fig.5.14

For the reproduction of Fig.5.13 we will use the same procedure and commands as in Appendix C.1. However for the Scalar Tensor Quintessence Model the system that we have to solve is different. In particular the system that we have to solve numerically is Eq.(5.69)-Eq.(5.73). In what follows s is referred to as ss, λ is denotes as l, F_0 is $ff0$ and ϕ_i is referred to as fi

```
aa = a[t]; fi = f[t];

aad = D[aa, t];

aadd = D[aa, {t, 2}];

fid = D[fi, t];

fidd = D[fi, {t, 2}];

ff = 1 − l ∗ fi;

om0m = 0.3;

h = aad/aa;

ss = 1; ti = 0.00001; t0 = 26.11658597437683; l = 0.2; ff0 = 1.74; fii = −2.36;

dv = ss;
```

```
eq1 = aadd/aa == −om0m ∗ ff0/(2aa^3 ∗ ff) − −(1/(3ff))fid^2+
+(1/(3ff)) ∗ V − h ∗ D[ff, t]/(2ff) − D[ff, {t, 2}]/(2ff)/.V → −ss ∗ fi;
eq2 = fidd + 3(aad/aa) ∗ fid − dv − 3 ∗ D[ff, fi] ∗ (aadd/aa + aad^2/aa^2) == 0;
condition1 = f[ti] == fii;
condition2 = f′[ti] == 0;
condition3 = a[ti] == (9om0mff0/(4(1 − l ∗ fii)))^(1/3) ti^(2/3);
condition4 = a′[ti] == (2/3)(9om0mff0/(4(1 − l ∗ fii)))^(1/3) ti^(−1/3);
solution = NDSolve[{eq1, eq2, condition1, condition2, condition3, condition4}, {aa, fi}, {t, ti, t0}];
asol = Part[Evaluate[a[t]/.solution], 1];
fsol = Part[Evaluate[f[t]/.solution], 1];
dasol = D[asol, t];
ddasol = D[asol, {t, 2}];
Plot[fsol, {t, ti, t0}, PlotStyle → Blue, Frame → True, PlotRange → All, FrameLabel → {t, "ϕ(t)"}]
Plot[1 − l ∗ fsol, {t, ti, t0}, PlotStyle → Blue, Frame → True, PlotRange → All, FrameLabel → {t, "F(t)"}]
Plot[asol, {t, ti, t0}, PlotStyle → Blue, Frame → True, PlotRange → All, FrameLabel → {t, "a(t)"}]
Plot[Log[asol], {t, ti, t0}, PlotStyle → Blue, Frame → True, PlotRange → All, FrameLabel → {t, "lna(t)"}]
```

For values above $\lambda_{crit.}$ the dynamics for the ϕ field and the scale factor one can reproduce the Fig.5.13 and Fig.5.14

C.2.2 Reproduction of Fig.5.16

For the reproduction of Fig.5.16 all we have to do is obtain the $\lambda_{crit.}$ for every slope s. This can be calculated easily based on the different behaviour of the scalar field ϕ. Let us then run the following commands for $s = 1.0$

```
aa = a[t]; fi = f[t];
aad = D[aa, t];
aadd = D[aa, {t, 2}];
fid = D[fi, t];
fidd = D[fi, {t, 2}];
l = 0.1; fii = −6.3; ti = 0.00001; t0 = 76.27280353; ff0 = 1.70; ss = 0.5;
ff = 1 − l ∗ fi;
om0m = 0.3;
```

```
h = aad/aa;
dv = ss;
eq1 =
aadd/aa == −om0m ∗ ff0/(2aa^3 ∗ ff) − (1/(3ff))fid^2 + (1/(3ff)) ∗ V − h ∗ D[ff, t]/(2ff)−
D[ff, {t, 2}]/(2ff)/.V → −ss ∗ fi;
eq2 = fidd + 3(aad/aa) ∗ fid − dv − 3 ∗ D[ff, fi] ∗ (aadd/aa + aad^2/aa^2) == 0;
condition1 = f[ti] == fii;
condition2 = f′[ti] == 0;
condition3 = a[ti] == (9om0mff0/(4(1 − l ∗ fii)))^(1/3) ti^(2/3);
condition4 = a′[ti] == (2/3)(9om0mff0/(4(1 − l ∗ fii)))^(1/3) ti^(−1/3);
solution = NDSolve[{eq1, eq2, condition1, condition2, condition3, condition4}, {aa, fi},
{t, ti, t0}, MaxSteps → 10000000];
asol = Part[Evaluate[a[t]/.solution], 1];
fsol = Part[Evaluate[f[t]/.solution], 1];
dasol = D[asol, t];
ddasol = D[asol, {t, 2}];
Plot[fsol, {t, ti, t0}, PlotStyle → Blue, Frame → True, PlotRange → All, FrameLabel → {t, "ϕ(t)"}]
```

For these particular code the ϕ field behaves as follows

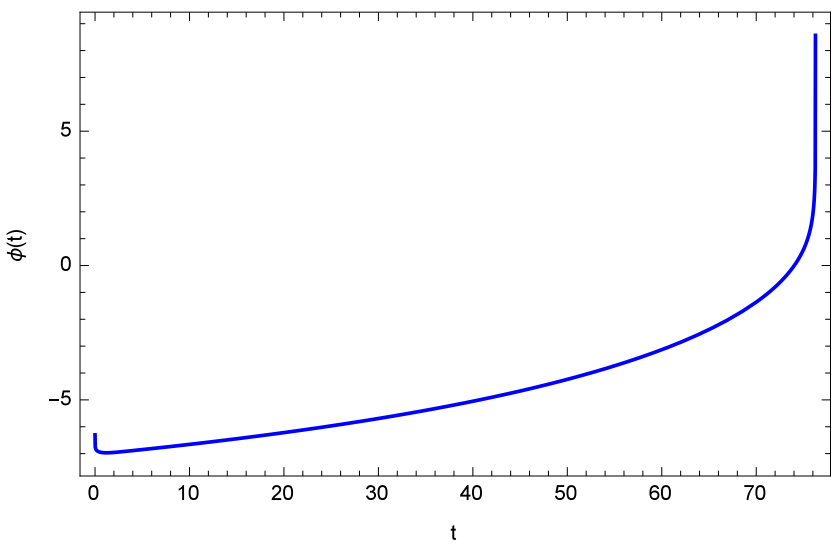

Figure C.1: Evolution of the scalar field for $s = 1$ and $\lambda = 0.10 < 0.11 = \lambda_{crit}$

Increasing now the value of $\lambda = 0.12$ the behaviour of the field changes and reverts from the

Big Crunch as it can be seen in the figure below

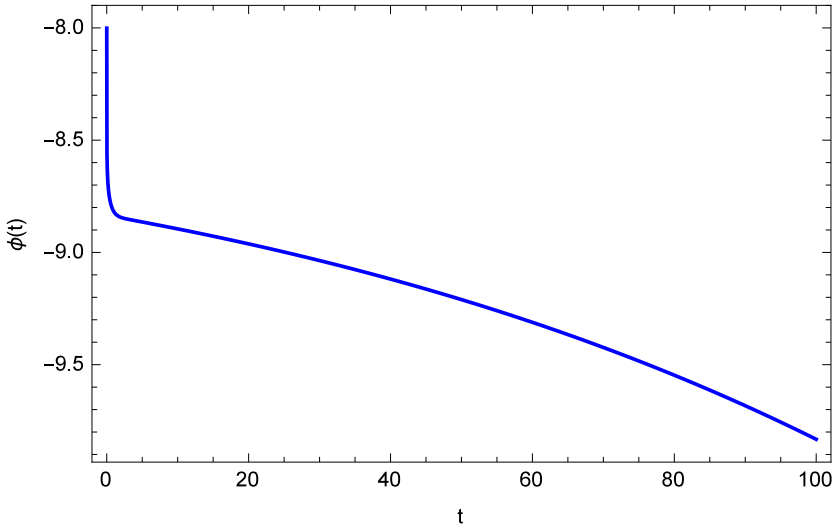

Figure C.2: Evolution of the scalar field for $s = 1$ and $\lambda = 0.12 > 0.11 = \lambda_{crit}$

Therefore for $s = 1$ the $\lambda_{crit} \simeq 0.11$. Repeating the same procedure for many slopes of s one can derive Fig.5.16 with the use of the *Show* command.

C.2.3 Reproduction of Fig.5.22 and Fig.5.23

In this final subsection we will reproduce Fig.5.22 and Fig.5.23, i.e the 1σ and 2σ probability contours for the linear potential. Unfortunately for this particular model there is no analytical expression for the "χ^2 *function*" thus we calculate χ^2's numerically following the same procedure as in Appendix C.1.3. Here we are showing as an example the algorithm for $s = 2.0$ and $\lambda = 0.3$ for the Union2.1 Dataset

```
Clear[a, aa, aad, aadd, fi, fid, fidd, eq1, eq2, condition1, condition2, condition3, condition4, fsol,
asol, tas, f, rr, hht, hha, chi2fa, chi2fb, chi2fc]
aa = a[t]; fi = f[t];
aad = D[aa, t];
aadd = D[aa, {t, 2}];
fid = D[fi, t];
fidd = D[fi, {t, 2}];
l = 0.3; fii = −0.58; ti = 0.001; t0 = 6.038484752612276; ff0 = 1.46; ss = 2.0;
ff = 1 − l ∗ fi;
om0m = 0.3;
h = aad/aa;
dv = ss;
```

```
eq1 =
aadd/aa == −om0m ∗ ff0/(2aa^3 ∗ ff) − (1/(3ff))fid^2 + (1/(3ff)) ∗ V − h ∗ D[ff, t]/(2ff)−
D[ff, {t, 2}]/(2ff)/.V → −ss ∗ fi;
eq2 = fidd + 3(aad/aa) ∗ fid − dv − 3 ∗ D[ff, fi] ∗ (aadd/aa + aad^2/aa^2) == 0;
condition1 = f[ti] == fii;
condition2 = f′[ti] == 0;
condition3 = a[ti] == (9om0mff0/(4(1 − l ∗ fii)))^(1/3) ti^(2/3);
condition4 = a′[ti] == (2/3)(9om0mff0/(4(1 − l ∗ fii)))^(1/3) ti^(−1/3);
solution = NDSolve[{eq1, eq2, condition1, condition2, condition3, condition4}, {aa, fi},
asol = Part[Evaluate[a[t]/.solution], 1];
fsol = Part[Evaluate[f[t]/.solution], 1];
dasol = D[asol, t];
ddasol = D[asol, {t, 2}];
as[t1_]:=asol/.t->t1;
tt = Part[FindRoot[as[t]==1, {t, 0.1}], 1, 2];
tas[a_]:=Part[FindRoot[as[t] == a, {t, 0.1}], 1, 2];
hht[t1_]:=D[asol, t]/asol/.t->t1;
hha[a_]:=hht[tas[a]];
hhz[z_]:=hha[1/(z + 1)];
dfsol = D[fsol, t];
ddfsol = D[fsol, {t, 2}];
dasol = D[asol, t];
Ht = dasol/asol;
dHt = D[Ht, t];
enf = (0.5dfsol^2 − ssfsol)/(3(1 − l ∗ fsol)hht[t]^2) + l ∗ dfsol/((1 − l ∗ fsol)hht[t])/.t → tt;
fff = (1 − l ∗ fsol)/.t → tt;
ppnew = dfsol^2 − l ∗ ddfsol + Ht ∗ l ∗ dfsol − 2 ∗ dHt ∗ (ff0 − (1 − l ∗ fsol));
rrnew = (0.5dfsol^2 − ssfsol) − 3 ∗ (Ht^2) ∗ (1 − l ∗ fsol − ff0) + 3 ∗ Ht ∗ l ∗ dfsol;
wwt = −1 + (ppnew/rrnew);
```

```
wwt/.t → t0;
f[z_]:=1/hhz[z]
ddz = 0.0001;
imax = 1200; zmax = 2; dz = zmax/imax;
ttable = Table[{0, 0}, {i, 1, imax}];
Do[ttable[[i]] = {idz, f[idz]}, {i, 1, imax}]
Plot[f[z], {z, 0, 2}, Frame → True, PlotStyle → Red, PlotRange → All];
ListPlot[ttable, PlotStyle → {Thick, Blue, PointSize[0.008]}, Frame → True, FrameLabel → {z, "w(z)"}];
f = Interpolation[ttable];
rr[zz_]:=NIntegrate[f[z], {z, 0, zz}];
chi2fa:=Sum[(ld[i] − 5Log[10, rr[zz[i]] * (1 + zz[i])])^2/(sld[i]^2), {i, 1, ndat}]
chi2fb:=Sum[(ld[i] − 5Log[10, rr[zz[i]] * (1 + zz[i])])/(sld[i]^2), {i, 1, ndat}]
chi2fc:=Sum[1/(sld[i]^2), {i, 1, ndat}]
chi2fm = chi2fa − chi2fb^2/chi2fc + Log[chi2fc/(2Pi)];
chi2difference = chi2fm2030 − chi2lcmd;
Print ["χ²_{s=2.0,λ=0.30}=", chi2fm]
Print ["Δχ²_{s=2.0,λ=0.30}=", chi2difference]
```

$\chi^2_{s=2.0,\lambda=0.30} = 570.269$
$\Delta\chi^2_{s=2.0,\lambda=0.30} = 0.00506429$

Now selecting various pairs of (s, λ) one is able to obtain every point from Fig.5.21. When we have obtained all the values that we want to include in our contours we use the *Interpolation* command as follows

```
h = Interpolation[{{{0.5, 0}, 571.759}, {{0.5, 0.05}, 571.808}, {{0.5, 0.10}, 571.996}, {{0.5, 0.15}, 571.239},
{{0.5, 0.2}, 571.442}, {{0.5, 0.22}, 571.302}, {{1.0, 0}, 571.954}, {{1, 0.05}, 571.456},
{{1, 0.1}, 571.219}, {{1, 0.15}, 571.054}, {{1, 0.2}, 570.872}, {{1., 0.25}, 570.788},
{{1., 0.3}, 570.953}, {{1, 0.35}, 571.050}, {{1., 0.4}, 571.069}, {{1, 0.42}, 571.303},
{{2, 0.15}, 571.801}, {{2, 0.2}, 570.728}, {{2, 0.25}, 570.379}, {{2, 0.3}, 570.269}, {{2, 0.35}, 570.276},
{{2, 0.4}, 570.276}, {{2, 0.5}, 570.297}, {{2, 0.55}, 570.329}, {{2, 0.6}, 570.318}, {{2, 0.65}, 570.367},
{{3, 0.2}, 572.387}, {{3, 0.25}, 570.874}, {{3, 0.3}, 570.398}, {{3, 0.35}, 570.390}, {{3, 0.4}, 570.756},
{{3, 0.45}, 571.124}, {{3, 0.5}, 571.471}, {{3, 0.55}, 571.552}, {{3, 0.6}, 571.572}, {{3, 0.65}, 571.571},
```

```
{{3, 0.7}, 571.369}, {{3, 0.75}, 571.081}, {{3, 0.8}, 570.840}, {{3, 0.85}, 570.631}, {{3, 0.9}, 570.494},
{{3, 0.95}, 570.358}, {{3, 1.}, 570.329}, {{3, 1.05}, 570.372}}, InterpolationOrder → 1];
```

Finally we use the *ContourPlot* and *DensityPlot* commands in order to derive Fig.5.22 as it can be seen below

```
ContourPlot[h[s, l], {l, 0., 1.05}, {s, 0.5, 3}, ContourShading → None];
DensityPlot[h[s, l], {l, 0., 1.05}, {s, 0.5, 3}, FrameLabel → {"λ", s}, WorkingPrecision → 5020,
PlotLegends → Automatic]
```

All the figures that were constructed for the potential of the form $V = s|\phi|^n$ are based on the same algorithms and commands. In Ref.[70] one can find analytically all the constructed figures along with the mathematica algorithms that have been used.

References

[1]G. F.R. E. Stephen W. Hawking, *The large scale structure of space-time*, Cambridge Monographs on Mathematical Physics (Cambridge University Press, 1975).

[2]S. Weinberg, *Gravitation and cosmology: principles and applications of the general theory of relativity* (Wiley, 1972).

[3]E. R. Harrison, "Comments on the big-bang", Nature **228**, 258–260 (1970).

[4]F. Zwicky, "On the Masses of Nebulae and of Clusters of Nebulae", apj **86**, 217 (1937).

[5]D. N. Spergel et al., "Wilkinson Microwave Anisotropy Probe (WMAP) three year results: implications for cosmology", Astrophys. J. Suppl. **170**, 377 (2007).

[6]W. J. G. de Blok and A. Bosma, "High-resolution rotation curves of low surface brightness galaxies", Astron. Astrophys. **385**, 816 (2002).

[7]F. Hoyle, "A New Model for the Expanding Universe", mnras **108**, 372 (1948).

[8]H. Bondi and T. Gold, "The Steady-State Theory of the Expanding Universe", mnras **108**, 252 (1948).

[9]C. O'Raifeartaigh and S. Mitton, "A new perspective on steady-state cosmology: from Einstein to Hoyle", in (2015).

[10]K. Helge, *Cosmology and controversy: the historical development of two theories of the universe*, 1st ed. (Princeton University Press, 1996).

[11]M. Livio, "Lost in translation: mystery of the missing text solved", Nature **479**, 171–173 (2011).

[12]G. Lemaître, "Expansion of the universe, A homogeneous universe of constant mass and increasing radius accounting for the radial velocity of extra-galactic nebulae", mnras **91**, 483–490 (1931).

[13]R. A. Alpher, H. Bethe, and G. Gamow, "The origin of chemical elements", Phys. Rev. **73**, 803–804 (1948).

[14]A. A. Penzias and R. Wilson, "A Measurement of Excess Antenna Temperature at 4080 Mc/s.", apj **142**, 419–421 (1965).

[15]A. H. Guth, "Inflationary universe: a possible solution to the horizon and flatness problems", Phys. Rev. D **23**, 347–356 (1981).

[16]G. Lazarides and C. Panagiotakopoulos, "Smooth hybrid inflation", Phys. Rev. D **52**, R559–R563 (1995).

[17]B. F. Williams et al., "Imaging and demography of the host galaxies of high-redshift type ia supernovae", Astron. J. **126**, 2608 (2003).

[18]M. Hicken, W. M. Wood-Vasey, S. Blondin, P. Challis, S. Jha, P. L. Kelly, A. Rest, and R. P. Kirshner, "Improved Dark Energy Constraints from ˜100 New CfA Supernova Type Ia Light Curves", apj **700**, 1097–1140 (2009).

[19]S. Nesseris and L. Perivolaropoulos, "Testing Lambda CDM with the Growth Function delta(a): Current Constraints", Phys. Rev. **D77**, 023504 (2008).

[20]D. Polarski and R. Gannouji, "On the growth of linear perturbations", Phys. Lett. **B660**, 439–443 (2008).

[21]K. Garrett and G. Duda, "Dark Matter: A Primer", Adv. Astron. **2011**, 968283 (2011).

[22]M. S. Turner and M. J. White, "CDM models with a smooth component", Phys. Rev. **D56**, R4439 (1997).

[23]V. Sahni, "Dark matter and dark energy", Lect. Notes Phys. **653**, [,141(2004)], 141–180 (2004).

[24]R. D. Peccei and H. R. Quinn, "Conservation in the presence of pseudoparticles", Phys. Rev. Lett. **38**, 1440–1443 (1977).

[25]K. A. Olive, "TASI lectures on dark matter", in Particle physics and cosmology: The quest for physics beyond the standard model(s). Proceedings, Theoretical Advanced Study Institute, TASI 2002, Boulder, USA, June 3-28, 2002 (2003), pp. 797–851.

[26]F. D. Steffen, "Dark Matter Candidates - Axions, Neutralinos, Gravitinos, and Axinos", Eur. Phys. J. **C59**, 557–588 (2009).

[27]C. Alcock et al., "The MACHO project: Microlensing results from 5.7 years of LMC observations", Astrophys. J. **542**, 281–307 (2000).

[28]H. E. S. Velten, R. F. vom Marttens, and W. Zimdahl, "Aspects of the cosmological "coincidence problem"", Eur. Phys. J. **C74**, 3160 (2014).

[29]J.-H. He and B. Wang, "Effects of the interaction between dark energy and dark matter on cosmological parameters", JCAP **0806**, 010 (2008).

[30]N. Arkani-Hamed, L. J. Hall, C. F. Kolda, and H. Murayama, "A New perspective on cosmic coincidence problems", Phys. Rev. Lett. **85**, 4434–4437 (2000).

[31]E. Bianchi and C. Rovelli, "Why all these prejudices against a constant?", (2010).

[32]B. Carter, "Anthropic principle in cosmology", in Current issues in cosmology. Proceedings, Colloquium on 'Cosmology: Facts and problems', Paris, France, June 8-11, 2004 (2006), pp. 173–179.

[33]J. A. W. John D. Barrow Frank J. Tipler, *The anthropic cosmological principle*, 1st ed., Oxford Paperbacks (Oxford University Press, USA, 1988).

[34]S. Weinberg, *Gravitation and cosmology: principles and applications of the general theory of relativity*, First Edition (Wiley, 1972).

[35]M. M. 'Cirkovi'c, "Anthropic fluctuations vs. weak anthropic principle", Foundations of Science **7**, 453–463 (2002).

[36]B. Carter, "Large number coincidences and the anthropic principle in cosmology", in Confrontation of cosmological theories with observational data, Vol. 63, edited by M. S. Longair, IAU Symposium (1974), pp. 291–298.

[37]B. Carter, "Anthropic interpretation of quantum theory", Int. J. Theor. Phys. **43**, 721–730 (2004).

[38]J. Garriga, A. D. Linde, and A. Vilenkin, "Dark energy equation of state and anthropic selection", Phys. Rev. **D69**, 063521 (2004).

[39]J. Garriga and A. Vilenkin, "Testable anthropic predictions for dark energy", Phys. Rev. **D67**, 043503 (2003).

[40]N. Arkani-Hamed, S. Dimopoulos, and G. R. Dvali, "The Hierarchy problem and new dimensions at a millimeter", Phys. Lett. **B429**, 263–272 (1998).

[41]I. Antoniadis, N. Arkani-Hamed, S. Dimopoulos, and G. R. Dvali, "New dimensions at a millimeter to a Fermi and superstrings at a TeV", Phys. Lett. **B436**, 257–263 (1998).

[42]T. Kaluza, "On the Problem of Unity in Physics", Sitzungsber. Preuss. Akad. Wiss. Berlin (Math. Phys.) **1921**, 966–972 (1921).

[43]D. Huterer and M. S. Turner, "Prospects for probing the dark energy via supernova distance measurements", Phys. Rev. **D60**, 081301 (1999).

[44]S. Carloni, P. K. S. Dunsby, S. Capozziello, and A. Troisi, "Cosmological dynamics of R**n gravity", Class. Quant. Grav. **22**, 4839–4868 (2005).

[45]S. Nojiri and S. D. Odintsov, "Unifying phantom inflation with late-time acceleration: Scalar phantom-non-phantom transition model and generalized holographic dark energy", Gen. Rel. Grav. **38**, 1285–1304 (2006).

[46]G. Allemandi, A. Borowiec, and M. Francaviglia, "Accelerated cosmological models in Ricci squared gravity", Phys. Rev. **D70**, 103503 (2004).

[47]G. Esposito-Farese and D. Polarski, "Scalar tensor gravity in an accelerating universe", Phys. Rev. **D63**, 063504 (2001).

[48]B. Boisseau, G. Esposito-Farese, D. Polarski, and A. A. Starobinsky, "Reconstruction of a scalar tensor theory of gravity in an accelerating universe", Phys. Rev. Lett. **85**, 2236 (2000).

[49]C. Armendariz-Picon, V. F. Mukhanov, and P. J. Steinhardt, "Essentials of k essence", Phys. Rev. **D63**, 103510 (2001).

[50]A. Yu. Kamenshchik, U. Moschella, and V. Pasquier, "An Alternative to quintessence", Phys. Lett. **B511**, 265–268 (2001).

[51]M. C. Bento, O. Bertolami, and A. A. Sen, "Generalized Chaplygin gas, accelerated expansion and dark energy matter unification", Phys. Rev. **D66**, 043507 (2002).

[52]N. Bilic, G. B. Tupper, and R. D. Viollier, "Unification of dark matter and dark energy: The Inhomogeneous Chaplygin gas", Phys. Lett. **B535**, 17–21 (2002).

[53]P. Kanti, *Lecture notes for the course of cosmology* (2014).

[54]H. Weyl, *Gruppentheorie und quantenmechanik* (Hirzel Leipzig, 1923).

[55]M. Farasat Shamir, A. Jhangeer, and A. A. Bhatti, "Exact Solutions of Bianchi Types I and V Models in $f(R,T)$ Gravity", (2012).

[56]W. J. Misner C.W. Thorne K.S., *Gravitation* (Freeman, 1973).

[57]H. Bondi, "Spherically symmetrical models in general relativity", Monthly Notices of the Royal Astronomical Society **107**, 410–425 (1947).

[58]M. Ross, *Introduction to cosmology* (Wiley, 2003).

[59]B. Schutz, *A first course in general relativity* (Cambridge University Press, 2009).

[60]J. Sylvester, "Xix. a demonstration of the theorem that every homogeneous quadratic polynomial is reducible by real orthogonal substitutions to the form of a sum of positive and negative squares", Philosophical Magazine Series 4 **4**, 138–142 (1852).

[61]S. Carroll, *Spacetime and geometry. an introduction to general relativity* (AW, 2004).

[62]S. Capozziello, R. de Ritis, C. Rubano, and P. Scudellaro, "Nöther symmetries in cosmology", La Rivista del Nuovo Cimento (1978-1999) **19**, 1–114 (1996).

[63]S. Capozziello, R. de Ritis, and A. A. Marino, "Some aspects of the cosmological conformal equivalence between 'Jordan frame' and 'Einstein frame'", Class. Quant. Grav. **14**, 3243–3258 (1997).

[64]R. P. Feynman, *Feynman lectures on gravitation, addison-wesley* (Addison-Wesley, 1995).

[65]D. Iosifidis, *Modified gravity and cosmology (master thesis)* (2013).

[66]S. Nojiri and S. D. Odintsov, "Where new gravitational physics comes from: M Theory?", Phys. Lett. **B576**, 5–11 (2003).

[67]B. Boisseau, G. Esposito-Farese, D. Polarski, and A. A. Starobinsky, "Reconstruction of a scalar tensor theory of gravity in an accelerating universe", Phys. Rev. Lett. **85**, 2236 (2000).

[68]S. Tsujikawa, "Matter density perturbations and effective gravitational constant in modified gravity models of dark energy", Phys. Rev. **D76**, 023514 (2007).

[69]A. Lykkas and L. Perivolaropoulos, "Scalar-Tensor Quintessence with a linear potential: Avoiding the Big Crunch cosmic doomsday", Phys. Rev. **D93**, 043513 (2016).

[70]L. Kazantzidis, All of the numerical calculations in this thesis are included in the following "`Dropbox folder link`" (June 2017).

[71]A. Einstein, "Kosmologische Betrachtungen zur allgemeinen Relativitätstheorie", Sitzungsberichte der Königlich Preußischen Akademie der Wissenschaften, 142–152 (1917).

[72]A. S. Eddington, "On the Instability of Einstein's Spherical World", MNRAS **9**, 668–678 (1930).

[73]E.Hubble, "A relation between distance and radial velocity among extra-galactic nebulae", PNAS, Proceedings of the National Academy of Sciences **15**, 168–173 (1929).

[74]D. Spergel et al., "Wilkinson Microwave Anisotropy Probe (WMAP) three year results: implications for cosmology", Astrophys.J.Suppl. **170**, 377 (2007).

[75]G. Miknaitis, G. Pignata, A. Rest, W. Wood-Vasey, S. Blondin, et al., "The ESSENCE Supernova Survey: Survey Optimization, Observations, and Supernova Photometry", Astrophys.J. **666**, 674–693 (2007).

[76]S. Perlmutter et al., "Measurements of Omega and Lambda from 42 high redshift supernovae", Astrophys. J. **517**, 565–586 (1999).

[77]A. G. Riess et al., "Observational evidence from supernovae for an accelerating universe and a cosmological constant", Astron. J. **116**, 1009–1038 (1998).

[78]J. L. Tonry et al., "Cosmological results from high-z supernovae", Astrophys. J. **594**, 1–24 (2003).

[79]R. Rakhi and K. Indulekha, "Dark Energy and Tracker Solution: A Review", (2009).

[80]E. J. Copeland, M. Sami, and S. Tsujikawa, "Dynamics of dark energy", Int. J. Mod. Phys. **D15**, 1753–1936 (2006).

[81]I. Zlatev, L.-M. Wang, and P. J. Steinhardt, "Quintessence, cosmic coincidence, and the cosmological constant", Phys. Rev. Lett. **82**, 896–899 (1999).

[82]T. Clifton, P. G. Ferreira, A. Padilla, and C. Skordis, "Modified Gravity and Cosmology", Phys. Rept. **513**, 1–189 (2012).

[83]M. H. Goroff and A. Sagnotti, "The Ultraviolet Behavior of Einstein Gravity", Nucl. Phys. **B266**, 709–736 (1986).

[84]G. 't Hooft and M. J. G. Veltman, "One loop divergencies in the theory of gravitation", Ann. Inst. H. Poincare Phys. Theor. **A20**, 69–94 (1974).

[85]H. Gies, B. Knorr, S. Lippoldt, and F. Saueressig, "Gravitational Two-Loop Counterterm Is Asymptotically Safe", Phys. Rev. Lett. **116**, 211302 (2016).

[86]L. J. Dixon, "Ultraviolet Behavior of $\mathcal{N} = 8$ Supergravity", Subnucl. Ser. **47**, 1–39 (2011).

[87]E. Jennings, C. M. Baugh, R. E. Angulo, and S. Pascoli, "Simulations of quintessential cold dark matter: beyond the cosmological constant", mnras **401**, 2181–2201 (2010).

[88]P. G. Ferreira and M. Joyce, "Cosmology with a primordial scaling field", Phys. Rev. D **58**, 023503 (1998).

[89]B. Ratra and P. J. E. Peebles, "Cosmological consequences of a rolling homogeneous scalar field", Phys. Rev. D **37**, 3406–3427 (1988).

[90]C. Wetterich, "Cosmology and the fate of dilatation symmetry", Nuclear Physics B **302**, 668 –696 (1988).

[91]O. M. Pimentel, G. A. González, and F. D. Lora-Clavijo, "The Energy-Momentum Tensor for a Dissipative Fluid in General Relativity", Gen. Rel. Grav. **48**, 124 (2016).

[92]L. Perivolaropoulos, "Constraints on linear negative potentials in quintessence and phantom models from recent supernova data", Phys. Rev. **D71**, 063503 (2005).

[93]S. Capozziello, R. de Ritis, and A. A. Marino, "Some aspects of the cosmological conformal equivalence between 'Jordan frame' and 'Einstein frame'", Class. Quant. Grav. **14**, 3243–3258 (1997).

[94]S. Capozziello, S. Nesseris, and L. Perivolaropoulos, "Reconstruction of the Scalar-Tensor Lagrangian from a LCDM Background and Noether Symmetry", JCAP **0712**, 009 (2007).

[95]R. de Ritis, A. A. Marino, C. Rubano, and P. Scudellaro, "Tracker fields from nonminimally coupled theory", Phys. Rev. **D62**, 043506 (2000).

[96]S. Nesseris and L. Perivolaropoulos, "Evolving newton's constant, extended gravity theories and snia data analysis", Phys. Rev. **D73**, 103511 (2006).

[97]E. Poisson and C. M. Will, "Gravitational waves from inspiraling compact binaries: Parameter estimation using second postNewtonian wave forms", Phys. Rev. **D52**, 848–855 (1995).

[98]P. D. Scharre and C. M. Will, "Testing scalar tensor gravity using space gravitational wave interferometers", Phys. Rev. **D65**, 042002 (2002).

[99]A. Friedland, H. Murayama, and M. Perelstein, "Domain walls as dark energy", Phys. Rev. **D67**, 043519 (2003).

[100]M. Li, "A Model of holographic dark energy", Phys. Lett. **B603**, 1 (2004).

[101]Q.-G. Huang and Y.-G. Gong, "Supernova constraints on a holographic dark energy model", JCAP **0408**, 006 (2004).

[102]S. M. Carroll, I. Sawicki, A. Silvestri, and M. Trodden, "Modified-Source Gravity and Cosmological Structure Formation", New J. Phys. **8**, 323 (2006).

[103]R. Maartens, "Brane world gravity", Living Rev. Rel. **7**, 7 (2004).

[104]E. Bertschinger, "On the Growth of Perturbations as a Test of Dark Energy", Astrophys. J. **648**, 797–806 (2006).

[105]D. J. Eisenstein et al., "Detection of the Baryon Acoustic Peak in the Large-Scale Correlation Function of SDSS Luminous Red Galaxies", Astrophys. J. **633**, 560–574 (2005).

[106]E. V. Linder, "Cosmic growth history and expansion history", Phys. Rev. **D72**, 043529 (2005).

[107]S. Nesseris, G. Pantazis, and L. Perivolaropoulos, "Tension and constraints on modified gravity parametrizations of $G_{\rm eff}(z)$ from growth rate and Planck data", (2017).

[108]P. Leandros, *Introduction to cosmology course* (2014).

[109]C. H. L. Hans Albrecht Bethe G. E. Brown, *Formation and evolution of black holes in the galaxy: selected papers with commentary*, World Scientific Series in 20th Century Physics (World Scientific Pub Co Inc, 2003).

[110]R. A. Daly and E. J. Guerra, "Quintessence, cosmology, and FRIIb radio galaxies", Astron. J. **124**, 1831 (2002).

[111]D. Hooper and S. Dodelson, "What can gamma ray bursts teach us about dark energy?", Astropart. Phys. **27**, 113–118 (2007).

[112]L. Perivolaropoulos, "Accelerating universe: observational status and theoretical implications", AIP Conf. Proc. **848**, [,698(2006)], 698–712 (2006).

[113]B. Ryden, *Introduction to cosmology* (Addison-Wesley, 2003).

[114]S. Dodelson, *Modern cosmology*, 1st ed. (Academic Press, 2003).

[115]S. Nesseris and L. Perivolaropoulos, "A Comparison of cosmological models using recent supernova data", Phys. Rev. **D70**, 043531 (2004).

[116]A. G. Riess et al., "Type Ia supernova discoveries at z ¿ 1 from the Hubble Space Telescope: Evidence for past deceleration and constraints on dark energy evolution", Astrophys. J. **607**, 665–687 (2004).

[117]P. M. Garnavich et al., "Constraints on cosmological models from Hubble Space Telescope observations of high z supernovae", Astrophys. J. **493**, L53–57 (1998).

[118]H. Wei, R.-G. Cai, and D.-F. Zeng, "Hessence: A New view of quintom dark energy", Class. Quant. Grav. **22**, 3189–3202 (2005).

[119]A. J. Conley et al., "Measurement of Omega(m), Omega(lambda) from a blind analysis of Type Ia supernovae with CMAGIC: Using color information to verify the acceleration of the Universe", Astrophys. J. **644**, 1–20 (2006).

[120]D. N. Spergel et al., "First year Wilkinson Microwave Anisotropy Probe (WMAP) observations: Determination of cosmological parameters", Astrophys. J. Suppl. **148**, 175–194 (2003).

[121]M. Tegmark et al., "Cosmological parameters from SDSS and WMAP", Phys. Rev. **D69**, 103501 (2004).

[122]U. Seljak et al., "Cosmological parameter analysis including SDSS Ly-alpha forest and galaxy bias: Constraints on the primordial spectrum of fluctuations, neutrino mass, and dark energy", Phys. Rev. **D71**, 103515 (2005).

[123]P. J. E. Peebles and B. Ratra, "The Cosmological constant and dark energy", Rev. Mod. Phys. **75**, 559–606 (2003).

[124]J. Garriga, L. Pogosian, and T. Vachaspati, "Forecasting cosmic doomsday from CMB / LSS cross - correlations", Phys. Rev. **D69**, 063511 (2004).

[125]N. Suzuki, D. Rubin, C. Lidman, G. Aldering, R. Amanullah, K. Barbary, L. F. Barrientos, J. Botyanszki, M. Brodwin, N. Connolly, K. S. Dawson, A. Dey, M. Doi, M. Donahue, S. Deustua, P. Eisenhardt, E. Ellingson, L. Faccioli, V. Fadeyev, H. K. Fakhouri, A. S. Fruchter, D. G. Gilbank, M. D. Gladders, G. Goldhaber, A. H. Gonzalez, A. Goobar, A. Gude, T. Hattori, H. Hoekstra, E. Hsiao, X. Huang, Y. Ihara, M. J. Jee, D. Johnston, N. Kashikawa, B. Koester, K. Konishi, M. Kowalski, E. V. Linder, L. Lubin, J. Melbourne, J. Meyers, T. Morokuma, F. Munshi, C. Mullis, T. Oda, N. Panagia, S. Perlmutter, M. Postman, T. Pritchard, J. Rhodes, P. Ripoche, P. Rosati, D. J. Schlegel, A. Spadafora, S. A. Stanford, V. Stanishev, D. Stern, M. Strovink, N. Takanashi, K. Tokita, M. Wagner, L. Wang, N. Yasuda, H. K. C. Yee, and T. S. C. Project, "The hubble space telescope cluster supernova survey. v. improving the dark-energy constraints above z¿1 and building an early-type-hosted supernova sample", The Astrophysical Journal **746**, 85 (2012).

[126]W. H. Press, B. P. Flannery, S. A. Teukolsky, and W. T. Vetterling, *Numerical recipes in c: the art of scientific computing*, 2nd ed. (Cambridge University Press, 1992).

[127]S. Nesseris and L. Perivolaropoulos, "Comparison of the legacy and gold snia dataset constraints on dark energy models", Phys. Rev. **D72**, 123519 (2005).

[128]M. Chevallier and D. Polarski, "Accelerating universes with scaling dark matter", Int. J. Mod. Phys. **D10**, 213–224 (2001).

[129]E. V. Linder, "Exploring the expansion history of the universe", Phys. Rev. Lett. **90**, 091301 (2003).

[130]R. Lazkoz, S. Nesseris, and L. Perivolaropoulos, "Exploring Cosmological Expansion Parametrizations with the Gold SnIa Dataset", JCAP **0511**, 010 (2005).

[131]H. Akaike, "A new look at the statistical model identification", Automatic Control, IEEE Transactions on **19**, 716–723 (1974).

[132]G. Schwarz, "Estimating the Dimension of a Model", The Annals of Statistics **6**, 461–464 (1978).

[133]D. A. Kenneth P. Burnham, *Model selection and multimodel inference: a practical information-theoretic approach*, 2nd ed (Springer, 2002).

[134]J. A. T. Thomas M. Cover, *Elements of information theory*, 99th, Wiley series in telecommunications (Wiley, 1991).

[135]R. Kallosh, J. Kratochvil, A. D. Linde, E. V. Linder, and M. Shmakova, "Observational bounds on cosmic doomsday", JCAP **0310**, 015 (2003).

[136]Y. Wang, J. M. Kratochvil, A. D. Linde, and M. Shmakova, "Current observational constraints on cosmic doomsday", JCAP **0412**, 006 (2004).

[137]T. Padmanabhan, "Cosmological constant: The Weight of the vacuum", Phys. Rept. **380**, 235–320 (2003).

[138]S. M. Carroll, "The Cosmological constant", Living Rev. Rel. **4**, 1 (2001).

[139]G. N. Felder, A. V. Frolov, L. Kofman, and A. D. Linde, "Cosmology with negative potentials", Phys. Rev. **D66**, 023507 (2002).

[140] L. Perivolaropoulos, "Equation of state of oscillating Brans-Dicke scalar and extra dimensions", Phys. Rev. **D67**, 123516 (2003).